Electrochemistry

International Edition: DOI: 10.1002/anie.201410823
German Edition: DOI: 10.1002/ange.201410823

The Chemistry of Redox-Flow Batteries

Jens Noack, Nataliya Roznyatovskaya, Tatjana Herr, and Peter Fischer*

Keywords:
electrochemistry · electrode reactions · electrolytes · energy storage · redox-flow batteries

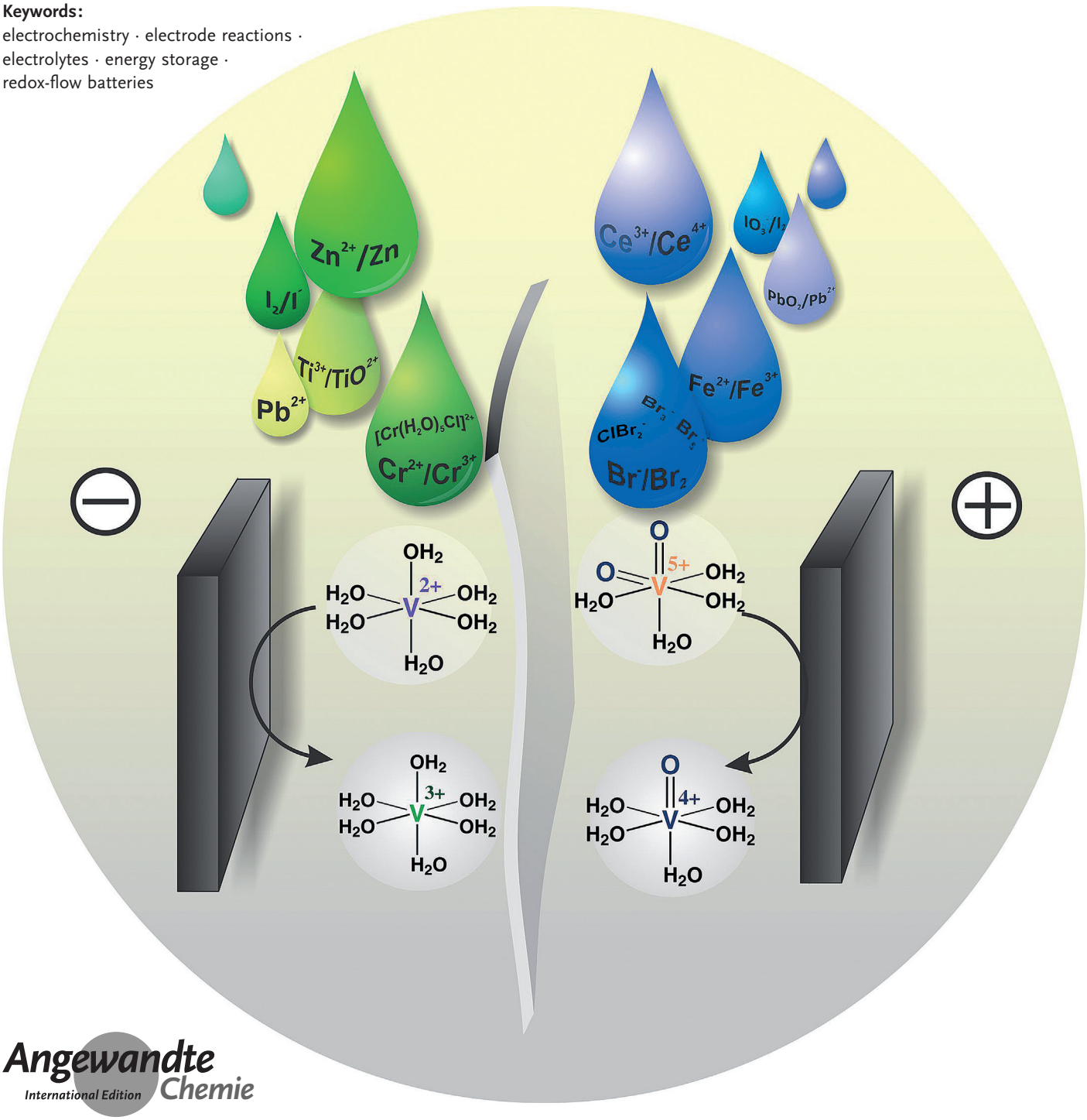

The development of various redox-flow batteries for the storage of fluctuating renewable energy has intensified in recent years because of their peculiar ability to be scaled separately in terms of energy and power, and therefore potentially to reduce the costs of energy storage. This has resulted in a considerable increase in the number of publications on redox-flow batteries. This was a motivation to present a comprehensive and critical overview of the features of this type of batteries, focusing mainly on the chemistry of electrolytes and introducing a thorough systematic classification to reveal their potential for future development.

From the Contents

1. Introduction

The growing contribution of fluctuating renewable energy sources to the electrical grid has resulted in energy storage becoming increasingly important to be able to ensure a reliable supply to consumers at all times.[1,2] The required storage time, which can range from a few milliseconds to months, is determined by the relevant application in the grid:

milliseconds to seconds	quality of supply
seconds to minutes	frequency stabilization
minutes to hours	peak load displacement
hours to weeks	long-term storage
months	seasonal storage

There are several different appropriate storage technologies for each applications.[3] Physical storage devices such as capacitors or fly wheels are appropriate for short-term storage; pumped-storage power plants, compressed air reservoirs, or batteries for medium time ranges; and secondary energy carriers such as hydrogen or methane (power to gas) for the longer term.[4] Currently the most popular battery technology is the lead-acid battery. Lead-acid batteries have relatively low investment costs. However, they also have a limited capacity for charging/discharging cycles, and need to be replaced once that has been exhausted. Other types of battery, such as nickel–cadmium, nickel–metal hydride and lithium-ion batteries have higher energy densities and higher numbers of cycles, but also carry higher costs. The most important requirements for a decentralized storage system for renewable energy to provide an alternative to fossil fuels are low costs for the stored energy and an optimized energy system.[5] This is the reason why the focus—in contrast to most other electrochemical energy storage devices—is not on high energy and power densities or on simple and compact systems, but rather on reliable and long-lasting storage devices, with low throughput costs for storage times of a few hours. As they offer independent scaling of energy and power, modular construction, replaceability of defective components, as well as cost-efficient media for storing energy, redox-flow batteries (RFBs) have the potential to meet this need. Redox-flow batteries are devices for the storage of electrochemical energy, in which the redox-active substances are flowing media and the redox reactions take place in an energy converter akin to a fuel cell. However, in contrast to fuel cells, the reactions can be electrochemically reversed. RFBs are, therefore, unique in that, depending on the process control and direction of electrical current, they can take the place of nearly every type of electrochemical energy converter and energy-storage device (Figure 1).

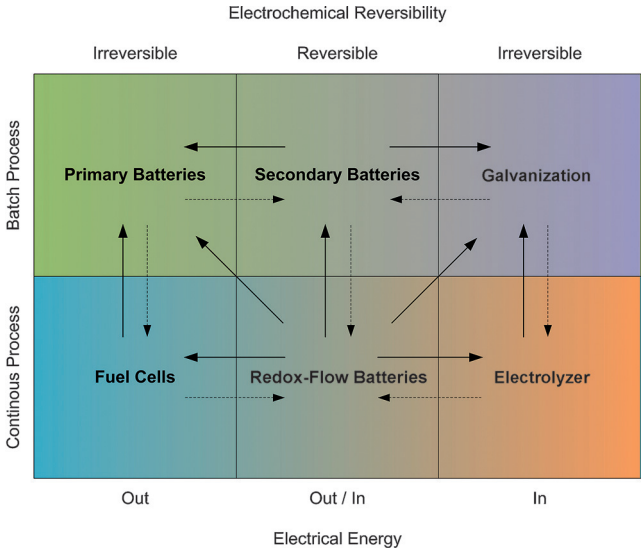

Figure 1. Position of redox-flow batteries in relation to other electrochemical energy storage devices and energy converters.[6]

As a result of the low costs and high availability of fossil fuels, RFBs had a niche existence in the 20th century, since renewable energy sources were at that time still expensive and only small amounts of it were available. Therefore, there was

[*] Dipl.-Ing. (FH) J. Noack, Dr. N. Roznyatovskaya, T. Herr, Dr. P. Fischer
Redox Flow Batteries Project Group
Fraunhofer Institute for Chemical Technology
Applied Electrochemistry
Joseph-von-Fraunhofer-Strasse 7, 76327 Pfinztal (Germany)
E-mail: Jens.Noack@ict.fraunhofer.de

no any need for the electrochemical storage of renewable energy. The intensity of the research, development, and commercialization of RFBs has increased noticeably in the last 10 years. The reason for this is, above all, the reconfiguration of the energy grid with an ever larger share of renewable energy, at the same time as costs of fossil fuels are increasing and prices for photovoltaic and wind energy are falling.

The development of redox-flow batteries goes back to a patent granted to Kangro in 1949.[7] In that patent, the author described the possibility of storing electrical energy in liquids through redox reactions of dissolved redox couples at electrodes, amongst other things for use as an energy buffer for fluctuating electricity producers such as wind turbines and tidal power plants. The first claim describes a system in which the substances dissolved in fluids are transferred in oxidized or reduced forms, as they pass through half-cells into separate tanks. They can be passed back through, to reverse the reaction. The second claim merits particular attention, according to which "*a single substance, which can appear in three or more valence states, is used as an electrochemically active substance in solution*", thereby allowing problems with diffusion, efficiency, and energy density to be minimized. This type of RFB was demonstrated on the basis of $Cr^{III}/Cr^{II}//Cr^{VI}/Cr^{III}$ (Cr-RFB; see Section 3.2.2.3) and it was only in the 1980s that the vanadium redox-flow battery (VRFB) was developed as a further example. As well as the Cr system, Kangro also named the two systems $Fe^{III}/Fe^{II}//Cr^{VI}/Cr^{III}$ and $Ti^{IV}/Ti^{III}//Cl_2/Cl^-$.

In the following years, further limitations were identified through the work of Pieper,[8] who undertook theoretical considerations of many elements in various oxidation states (Zn^{II}, Zn^{IV}, Pb^{II}, Pb^{IV}, As^{III}, As^{V}, Sb^{III}, Sb^{V}, Cu^{I}, Cu^{II}, Au^{I}, Au^{III}, Hg^{I}, Hg^{II}, Ga^{II}, Ga^{III}, Tl^{I}, Tl^{III}, Ce^{III}, Ce^{IV}, Ti^{III}, Ti^{IV}, V^{II}, V^{III}, V^{IV}, V^{V}, Cr^{II}, Cr^{III}, Cr^{VI}, Mo^{III}, Mo^{V}, Mo^{VI}, Mn^{II}, Mn^{III}, Mn^{IV}, Fe^{II}, Fe^{III}, Co^{II}, Co^{III}). A system using the redox couples V^{II}, V^{III}, V^{IV}, and V^{V} was not pursued further, as previous studies had resulted in hydrogen generation during the reduction of V^{IV} at platinum electrodes. Furthermore, the high price of vanadium at the time meant that its use as a medium for storing energy was not feasible. A system of Ti^{IV}/Ti^{III} as anolyte and Fe^{III}/Fe^{II} as catholyte was investigated in much closer detail (see Section 3.2.5.6). Kangro and Pieper concluded in 1962 that a Ti/Fe accumulator of this sort can be used for the storage of wind energy under a high storage/power relationship in an economically competitive way compared to lead– and nickel–iron batteries.[9]

During the 1970s, with the background of the first oil crisis, the National Aeronautic and Aerospace Administration in America (NASA) was active in the development of cost-effective electrochemical energy storage for storing renewable energies. Thaller et al.[115,116] examined various redox couples for their suitability for storing energy. Their focus was particularly on cost-effective materials. This finally resulted in the concept of redox-flow batteries with the redox couples Cr^{2+}/Cr^{3+} and Fe^{2+}/Fe^{3+} in hydrochloric solutions (see Section 3.2.2.1).

During the 1980s, Skyllas-Kazacos et al.[17] developed the vanadium redox-flow battery, which today is the RFB system that has been most thoroughly investigated. To date, a great number of electrodes, electrolyte compositions, membranes, models, and systems have been investigated (see Section 3.2.3.1).[10–15]

Jens Noack studied chemical and environmental engineering at the Hochschule für Technik und Wirtschaft in Dresden. Since 2007 he has worked at the Fraunhofer Institut für Chemische Technologie in the Department of Applied Electrochemistry, mainly on the development of redox-flow batteries. From 2009 until 2011 he was acting group leader of the newly formed redox-flow battery group. Since 2011 he has been carrying out PhD research at the Karlsruhe Institut für Technologie (KIT). He also works at the Fraunhofer ICT as Project Leader and Senior Development Engineer. His research is concerned with energy storage and conversion systems.

Peter Fischer studied physical chemistry at the Heinrich-Heine-University in Düsseldorf, Germany, where he developed analytical instruments for PEM fuel cells, such as locally resolved micro- Raman probes for the detection of gases in PEM fuel cells. Since 2011 he has been group leader of the Redox-Flow Battery Group at the Applied Electrochemistry Department at Fraunhofer Institute for Chemical Technology (ICT). He is responsible for the project RedoxWind, which involves installing a 2MW/20 MWh redox-flow battery at the Fraunhofer ICT.

Nataliya Roznyatovskaya studied chemistry at the Moscow State Lomonosov University and completed her PhD in 2005 on the mechanisms of the electrochemical reduction of binuclear metal–ligand complexes. After postdoctoral research at the University of Regensburg, she became scientific Associate in the Department of Applied Electrochemistry at the Fraunhofer ICT. Her research focuses on the electrochemical investigation of electrolytes for electrochemical storage and conversion.

Tatjana Herr received her degree in chemistry (2008) and master in chemistry (2010) from the Technical University of Braunschweig. She is currently a PhD candidate at the Fraunhofer Institute for Chemical Technology and Karlsruhe Institute of Technology, where she is working on non-aqueous vanadium redox-flow batteries, with a focus on electrolytes and increasing their energy density.

At the beginning of the 21st century, many new battery systems such as Zn/Ce, Pb, V-ClBr, and V-Cl^-/SO_4^{2-} were developed and investigated, alongside the commercialization of Fe/Cr-, Zn/Br-, and V-RFBs. Newer systems with aprotic, non-aqueous RFBs have only emerged in the last ten years (see Section 3.5).[16] Several reviews of RFBs have been published in the last three years alone. These reviews often focus on historical, commercial, or technical aspects,[17,18] or on materials, operational parameters, and constructional peculiarities.[15,19] In this Review, we draw a clear distinction between redox-flow batteries and other energy-storage technologies to provide a critical overview of the relevant chemical aspects of the various technologies and, in particular, the chemical properties of the various redox couples and their combinations.

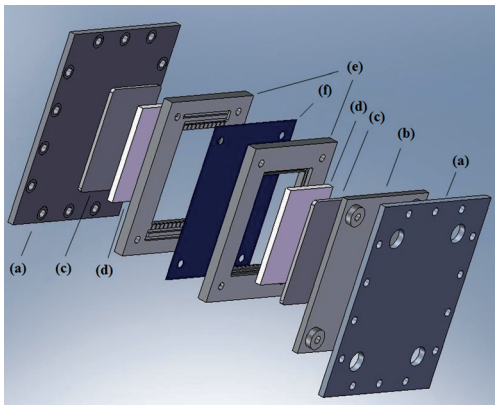

Figure 3. Exemplary structure of a redox-flow battery cell: a) end plate, b) isolation plate, c) graphite plate, d) graphite felt, e) flow frames, f) membrane.

2. General Structure of a Redox-Flow Battery

As with all other types of accumulators, in redox-flow batteries substances react in reversible reactions on electrodes through energy conversion in an electrochemical cell. The particular qualities of RFBs are characterized by the fact that the redox-active substances are always in flowing media (fluids, gases, suspensions etc.) and thereby allow an almost complete separation of the scaling of energy and power.[20] RFBs share this characteristic with fuel cells, although those utilize reactions that cannot be electrochemically reversed. In this way, the general structure of the electrochemical cells and cell stacks of the redox-flow batteries are, in principle, similar to those of fuel cells; however, they vary considerably in the detail, depending on the redox couples utilized. Figure 2

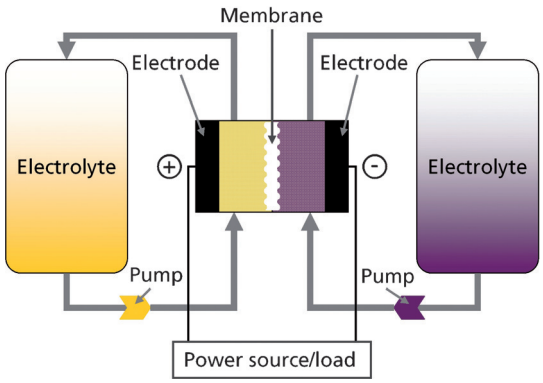

Figure 2. Redox-flow batteries with electrolytes as the media for energy storage.

shows schematically the general structure for the use of liquid media.

The electrochemical cells are divided by a membrane into two half-cells, through which the relevant solutions are pumped in circulation. The discharging process is observed, in keeping with battery convention,[21] and the positive electrode is always referred to as the cathode and the negative one is referred to as the anode. The associated energy storage is referred to as the catholyte and anolyte. In the case of RFBs, both single cells and systems of connected single cells are regarded as batteries. Batteries in which not all the redox-active material exists in a flowing form in a maximum of one half-cell, as is the case with, for example, Zn-based batteries, are referred to as hybrid RFBs.

Figure 3 shows the construction of an RFB cell. The end plates ensure the mechanical stability of the structure, the isolation plate provides electrical isolation between the half-cells, and the graphite plates close off the half-cells. The flow frames allow the distribution of the electrolyte, the graphite felts act as electrodes with a large surface area, and the membrane ensures the material separation of the two half-cells. In principle, a structure resembling a fuel cell with flow fields from structured graphite plates and diffusion electrodes could also be used. These structures are complicated to use, particularly as cell stacks, on account of the conductive electrolyte, since contact between the electrolyte and the electrode can only take place inside the cell to avoid overpotential. Cells without membranes are based on co-laminar fluid flows, of which Goulet and Kjeang provide an overview.[22]

The complete system of cells, fluid technology, pumps, heat management (where necessary), actuators, sensors, battery management systems etc. makes up the redox-flow battery. The complete battery system as well as the design of cells and cell stacks varies considerably depending on the battery chemistry used.

Important parameters of batteries that come up frequently are the overall current efficiency, cell efficiency, and energy density. The overall current efficiency (CE) is the product of the relevant current efficiency of the forward and backward reactions. It is principally a measure of secondary reactions. The energy efficiency (EE) is the ratio of the energy extracted and introduced and can be differentiated according to the system boundary, for example, into half-cell, cell, and battery efficiency. Often the energy efficiency of cells is given without any consideration of the peripherals. The question of energy density is similarly diffuse, as it is often given as the maximum storable energy at open-circuit voltage, which is related to the electrolyte solution under normal conditions.

When examining single cells, energy density values are also mostly related to the electrolyte solutions, in any event with an actual voltage curve in the discharging process, although this value lays some way below the maximum value. With other battery systems, comparable values are only obtained when the energy density of the complete battery structure is determined and defined inclusive of all components, which is the case almost only with commercial RFBs.

2.1. Electrodes

Alongside other components, electrodes are central in determining the capacity and the long-term stability of the RFB. They should possess a high electrochemical stability with simultaneously high reaction kinetics of the redox couple, as well as high electrical conductivity and mechanical stability at low cost. Through the use of redox couples with negative or strongly positive standard electrode potentials in aqueous media, carbon-based materials are most commonly considered as a consequence of their inert character and high levels of hydrogen and oxygen overvoltage, despite the fact that they have a low level of electrical conductivity and mechanical stability.[14] The actual electrode is made out of a material with a high specific surface area, such as graphite felt, in which the electrolyte is mostly conducted through the electrode. A graphite or bipolar plate provides the electrical contact between the half-cells and a polymer filling prevents electromigration from the electrolyte solution out of the half cell. The kinetics of the reactions and the surface area of the electrode materials can be increased by various types of pretreatment. The electrode surface can be oxidized chemically, electrochemically, or thermally, for example, to influence the redox reactions sensitive to the chemical state of the electrode surface.[23–26] Further procedures include chemical doping[27,28] and the addition of nanomaterials.[29–31]

Cell design with structured graphite composite plates use carbon paper or graphite fleece as diffusion electrodes, as in fuel cells.[27,32,33] In this way, clear increases in power density could be aimed for in some cases.[32]

Dimensionally stable anodes (dsas) composed of titanium and a metal coating proved to also be suitable. For example, vanadium[36] and cerium[34,35] had a good reversibility at platinized titanium, as well as vanadium at IrO_2-covered Ti. The disadvantages compared to carbon-based electrodes are, however, the high price and the fast kinetics of oxygen evolution.[36] Metal electrodes often have the disadvantage that they are not chemically stable in the solution or that they, similar to Pb and Ti, become passive through oxidation.

Chakrabati et al.[10] and Parasuraman et al.[14] provide an overview of the development of the electrode materials for redox-flow batteries.

2.2. Separators

Separators were introduced into RFBs to prevent any mixing of the electrolyte solutions, and thereby stop an uncontrolled reaction between the half-cells. The majority of publications that have appeared to date that exclusively deal with the development and optimization of separators for RFBs are concerned with vanadium redox-flow batteries.[11] Other flow batteries generally use separator materials that have already been developed for fuel cells, electrolyzers, or water treatment.

In principle, the separators can be classified into four groups: 1) mesoporous separators, 2) ionic exchange membranes, 3) hybrid membranes, and 4) solid ionic conductors.

1. The porous separators currently used are generally flexible polymer systems. For porous solid objects, distinctions are drawn according to the pore size (PS) between nanoporous ($PS < 1$ nm), microporous ($1 < PS < 2$ nm), mesoporous ($2\text{ nm} < PS < 50$ nm), and macroporous materials ($PS > 50$ nm). In contrast, the divisions for the filtration membranes for membrane separators are taken to be nanofiltration membranes ($PS < 5$ nm), ultrafiltration membranes ($5 < PS < 100$ nm), and microfiltration membranes ($100\text{ nm} < PS < 10\ \mu m$). Conventional battery separators of stretched polyolefin films are generally in the realm of microfiltration membranes. The passing of redox-active ions through the pores means that the efficiency of an RFB drops, which means that these separators cannot be used without further modification. The use of commercial separators for lead batteries (Daramic) without pretreatment has previously, therefore, only been recommended for iron–vanadium redox-flow batteries.[37] A frequent variation is the retroactive modification of the Daramic separators with cross-linked polymers[38] or filler. Filling the pores in this way should prevent the passing of larger ions, without limiting the conductivity of the protons. To achieve a high level of selectivity, the pores of microfiltration membranes are frequently postmodified by filling with solutions of ion exchangers, known as ionomer solutions.[39–42]

Microfiltration or ultrafiltration membranes can also be produced according to the phase-inversion methods developed by Loeb and Sourirajan.[43] These methods can produce asymmetrical membranes, in which the pore radius is shrunk to the thickness of a membrane. Examples of these are membranes based on polyacrylonitrile (PAN),[44] polyethersulfone mixed with sulfonated polyether ether ketone (PES/SPEEK),[45] and polyvinylidene fluoride (PVDF).[46] The pores can also be filled and covered with inorganic fillers such as methyl orthosilicates to increase the selectivity and wetting of the pores.[47]

2. Ionic exchange membranes are generally formed from a base polymer, known as the "polymer backbone", to which acidic or basic side chains are introduced. The polar functional groups of organic acids or bases bind water or dipolar solvent molecules, which leads to a swelling of the polymer. If the swelling is completely successful, ionic charges can be exchanged through a network of solvent molecules. The bonded ionic groups in the polymer form a charged stationary phase, which provides, by means of an electrostatic shield, a largely selective transfer of cations or anions through the membrane. Ionic exchange membranes can be divided into three groups according to the charge of their stationary phase: a) cationic ion-exchange membranes, b) anionic ion-exchange membranes, and c) amphoteric ion-exchange membranes.

a) Cationic ion-exchange membranes can be divided into subgroups of fluorinated and nonfluorinated membranes depending on their base polymer.

Fluorinated cationic exchange membranes are characterized by a high chemical stability towards oxidants and reductants. They are stable in moderately concentrated acids and alkalis. The standard materials for fluorinated exchange membranes are perfluorosulfonic acids (PFSAs). The main example of this sort of exchange material is NAFION, manufactured by the company DuPont. This membrane material, which was developed for chlorine-alkali electrolysis, is often regarded as a form of standard material for cationic exchange membranes. In NAFION, the sulfonic acid groups are bound to the polymer backbone by fully fluorinated polypropylene glycol ether. The number of fluoropropyl ether groups determine both the chemical stability of the polymer and also its swelling behavior. These days various firms offer PFSA membranes with various side-chain lengths.

PFSA membranes can be produced in two different ways. They can be extracted from solution ("solution casting") or be obtained through extrusion of the fluorosulfonic acid precursor and subsequent alkali hydrolysis. The casting of membranes from a solution offers the advantage over the extrusion method that conductive domains form as inverse micelles in the solution, which lead to ionic channels. For information about the theory of ionic conductivity in PFSA exchange membranes, see also Yeager and Steck.[48]

"Solution casting" offers the capability to scrape membranes out of aqueous or alcoholic PFSA solutions on a polymer carrier. There is also the capability for mixing solutions with various other polymers and cross-linkers to achieve the appropriate properties in one membrane. Development goals for modified membranes from solution are high ionic conductivity, limited expansion during swelling, higher selectivity, more limited electro-osmotic mobility, and low permeability to large cations, also called permselectivity.

A disadvantage of PFSA membranes is an accumulation or deposition of vanadium species on the surface area and internally within the membrane. This phenomenon is called "fouling".[49]

Nonfluorinated cation exchangers are generally formed from sulfonated polyether ether ketone (SPEEK).[50] A further method of obtaining nonfluorinated membranes is the postmodification of polyphenylene sulfone[51] (PPS, PS, PES) or polyimides by sulfonation.[52,53] However, membranes from aromatic, nonfluorinated polymers frequently do not have a sufficient chemical stability to vanadium electrolyte solutions[54,55] and tend to form cracks.

b) Anionic exchange membranes have a higher permselectivity than cationic exchange membranes, which results in a higher current efficiency of the RFB. As cationic groups, triethylamine groups are generally inserted into a base polymer by chloromethylation. Base polymers include poly(vinylbenzylstyrene) copolymer cross-linked with adipic acid,[56] poly(fluorenyl ether),[57] or poly(aryl ether ketone phtalazinone) (PAEKP).[58–62]

c) Amphoteric ion-exchange membranes have both cationic and anionic groups. These membranes are generally obtained by the radiation-graft copolymerization of prefabricated films or powdered PVDF[63–66] or ETFE[67] with the help of gamma rays. Cationic groups are inserted using grafted polystyrene or α-methylstyrene and subsequently sulfonated with chlorosulfuric acid. Anionic groups are obtained by copolymerization of dimethylaminoethyl methacrylate or trimethylaminoethyl methacrylate.

3. Composite membranes comprise inorganic substances which are inserted into the polymer matrix during solution casting following the sol–gel process. The aim is to reduce the size of the pores in these membranes and thereby increase the permselectivity of the membranes. Examples of such membrane systems are silicates in NAFION[68–70] or partially fluorinated SPEEK,[71] zirconium phosphate in partially fluorinated SPEEK,[72] and polytungstate in sulfonated polyphenylene sulfide (PPS).[73]

4. Solid-state conductors are rarely used in an RFB, since ion-conducting crystals, ceramics, or glasses usually only have sufficient conductivity at temperatures over 300 °C. The conductivity of these systems is generally up to one or two orders of magnitude lower than the ionic exchange membranes. For RFBs, their use in lithium-RFBs is only suggested in a few systems. Lithium-conducting glasses were use in these cases.[74]

Some hybrid flow batteries with solid metal electrodes or gas diffusion electrodes[75] can theoretically also be used without separators. However, to avoid short circuits caused by dendritically deposited metal or the flooding of the gas diffusion electrodes, hybrid RFBs generally still include porous separators or membranes. Theoretically, any flow battery could also be used without separators. In order to do so, the electrolyte liquids of anolyte and catholyte in the cells must be exactly co-laminar and without any turbulence (Figure 4). At the low flow rate in the RFB, this condition

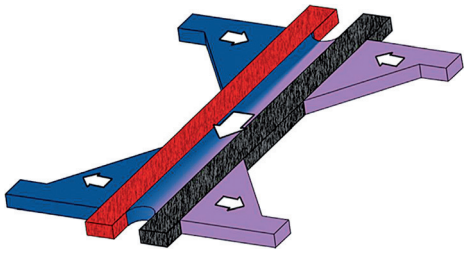

Figure 4. Co-laminar redox-flow battery with porous electrodes.[22]

can be simply implemented in a flow-through reactor. RFBs without membranes are mostly employed as laminar microflow reactors.[76,77] Porous flow electrodes in such structures may not come into any contact with the boundary layer, however, since that would result in the electrolytes becoming mixed. Goulet and Kjeang,[22] in their review about co-laminar flow reactors, describe RFB microreactors that can also be used reversibly with porous flow electrodes.

3. Battery Chemistry

3.1. General Aspects

The working principle of redox-flow batteries in the discharge mode can be generally represented as a chemical reaction of two redox couples that results from the combination of two corresponding half-reactions as follows:

$$\text{Anode}: \quad A^{x} \rightleftharpoons A^{x+z} + z\,e^{-} \qquad \phi_A$$
$$\text{Cathode}: \quad C^{y} + z\,e^{-} \rightleftharpoons C^{y-z} \qquad \phi_C$$
$$\text{Cell}: \quad A^{x} + C^{y} \rightleftharpoons A^{x+z} + C^{y-z} \qquad \phi_{Cell} = \phi_C - \phi_A$$

The two redox couples A^x/A^{x+z} and C^{y-z}/C^y are used for the positive and negative electrode reactions. The electrolyte-specific performance and energy density of RFBs are defined by the difference in the redox potentials of the redox pairs ϕ_{Cell}, known as the cell voltage, and by other parameters such as:

1) The standard potentials of half-cell reactions which thermodynamically enable a high cell voltage, but at the same time thermodynamically or kinetically prevent side reactions.
2) The stability and solubility of the ions in the oxidation states involved.
3) The rapid and reversible electrode reactions.
4) The availability of raw materials, their affordability, and influence on the environment.

In real batteries, compromises need to be found when selecting suitable electrolytes, because the various requirements are independent of each other and often contradictory. The combination of strong oxidizing and strong reducing redox couples with high cell voltages is beneficial from the point of view of higher energy densities, but this cannot be the only selection criterion, because it would lead to, for example, an increased tendency towards side reactions, high costs of suitable chemically stable materials, or the solubility and reaction kinetics can be limited. It is shown by the example of an aqueous electrolyte in Figure 5 that the pH-dependent stability of the electrolyte as well as the stability of each redox species (Pourbaix diagram) and other components of the electrolyte need to be taken into account. Table 1 provides an overview of combinations of redox pairs, which correspond to published types of batteries. As can be seen, most battery electrolytes are acidic, because many metal ions, except for zinc, precipitate as insoluble hydroxides at high pH values and are, therefore, unsuitable for use in RFB electrolytes.

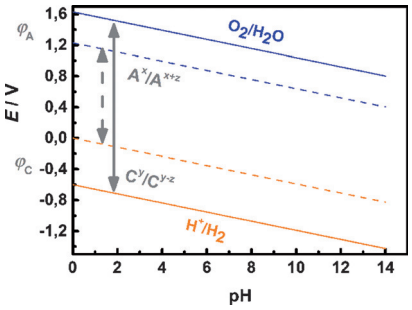

Figure 5. Standard potential (*E* versus NHE) versus the pH value for hydrogen and oxygen evolution reactions (dashed lines), with overpotentials at carbon-based electrodes (solid lines) in aqueous media and area of optimal potentials for anodic and cathodic couples for stable battery electrolytes.[6]

The atomic or molecular weight of the redox-active chemical substances or compounds used as electrolyte components and the number of electrons transferred in their half-cell reactions in addition to their standard redox

Table 1: Selected examples of inorganic redox couples for RFBs. The colors of the cells correspond to the pH value of the electrolytes; red—acidic, blue—basic, orange—neutral. Stage of development: A—half-cell study, B—prototype tested, C—technology has been commercialized.

Cathode / Anode	E^0 [V]	MnO_2/Mn_2O_3 0.15	$Fe(CN)_6^{3-}/Fe(CN)_6^{4-}$ 0.36	Cu^+/Cu 0.52	Fe^{3+}/Fe^{2+} 0.77	VO_2^+/VO^{2+} 0.99	$ClBr_2^-/Br^-$ 1.04	Br_2/Br^- [a] 1.09	NpO_2^+/NpO_2^{2+} 1.14	IO_3^-/I_2 1.2	O_2/O^{2-} 1.23	$HCrO_4^-/Cr^{3+}$ 1.35	Cl_2/Cl^- 1.36	PbO_2/Pb^{2+} 1.46	Mn^{3+}/Mn^{2+} 1.54	Ce^{4+}/Ce^{3+} 1.72
$Zn(OH)_4^{2-}/Zn$	-1.22	B	B													
Zn^{2+}/Zn	-0.76					B	B	C					B			B
Fe^{2+}/Fe	-0.45				A											
S/S_2^{2-}	-0.43							C								
Cr^{3+}/Cr^{2+}	-0.41				C			A				B				
Cd^{2+}/Cd	-0.40				B											
V^{3+}/V^{2+}	-0.26				B	C	B				B				B	B
Pb^{2+}/Pb	-0.13													B		
H^+/H_2	0				B	B		B					B			
TiO^{2+}/Ti^{3+}	0.04				A		A						A			
Cu^{2+}/Cu^+	0.15			B												
Np^{4+}/Np^{3+}	0.15								B							
Cu^{2+}/Cu	0.34													B		
I_2/I^-	0.54									A						

[a] Or Br_3^-/Br^- 1.06 V (based on formation of polybromide), the potentials can vary according to the composition of the electrolytes because of complex formation.

potentials and solubility need to be taken into account to reach a high energy density. The common evaluation parameter is the gravimetric and volumetric energy density. However, the difference between theoretically calculated and practically attainable energy densities may be several orders of magnitude, especially when the reaction is slow. For example, the theoretical energy density of Zn/Br RFBs is 570 $Wh\,kg^{-1}$, but only approximately 70 $Wh\,kg^{-1}$ has been achieved in practice.[21] In addition to the charged redox-active species, their counterions and possibly ions of the supporting electrolyte, that is, protons usually not being represented in the general reaction equations, are important to maintain the mass and charge balance. This balance is related to the changes in the composition of the each half-cell electrolyte and its physicochemical properties (pH value, ionic strength, conductivity, viscosity etc.) during the battery operation, that is, changing of its state of charge.

For each state of charge, the solubility and stability of the redox-active species should remain high enough to enable stable battery performance. As a consequence of the high solubility and conductivity of inorganic substances in aqueous media, a variety of batteries with this type of electrolyte dominate. Metal complexes with organic ligands are more soluble and stable in organic solvents. The use of these solutions as electrolytes can provide potentially higher cell voltages than aqueous electrolytes, but their specific electrical conductivity and the solubility of the redox-active species are still low. Chemical elements with at least three oxidation states can be considered as species for both half-cells, whereby in the best case all three compounds are soluble. In this case, the diffusion of redox-active species into another half-cell compartment (so called cross-over) is minimized and is limited to electro-osmotic effects. The electrolyte, which consists of a mixture of cathodic and anodic redox compounds of different elements, is often characterized by a lower solubility of the corresponding salts and, therefore, a lower energy density compared to the battery, where by virtue of their different chemical nature, the catholytes and anolytes are separated.

Electrode reactions can be accompanied by a phase change, which occurs for example during the formation of metal deposits or gaseous products. As shown in Figure 6, RFBs can be classified according to the aggregate state of the reactants and products of the half-cell reactions. This classification remains arbitrary, however, because of a variety of electrolyte-specific phenomena during battery operation. Much more laborious technical solutions are required for the operation of batteries with multiphase systems compared to the classical single-phase liquid batteries. This is especially relevant to provide a uniform metal deposition or continuous gas feed and storage, as well as circulating the suspensions.

All half-cell reactions proceed at the interface between the electrode and the electrolyte, where the kinetics of electron transfer is determined directly by the type of electrochemical reaction. In general, electrode reactions can be divided into two groups:

1) Outer-sphere reactions, where the charge tunnels through the solvation shell of the redox-active species. The kinetics of these reactions is independent of the state of the electrode surface, that is, oxygen/carbon ratio, specific

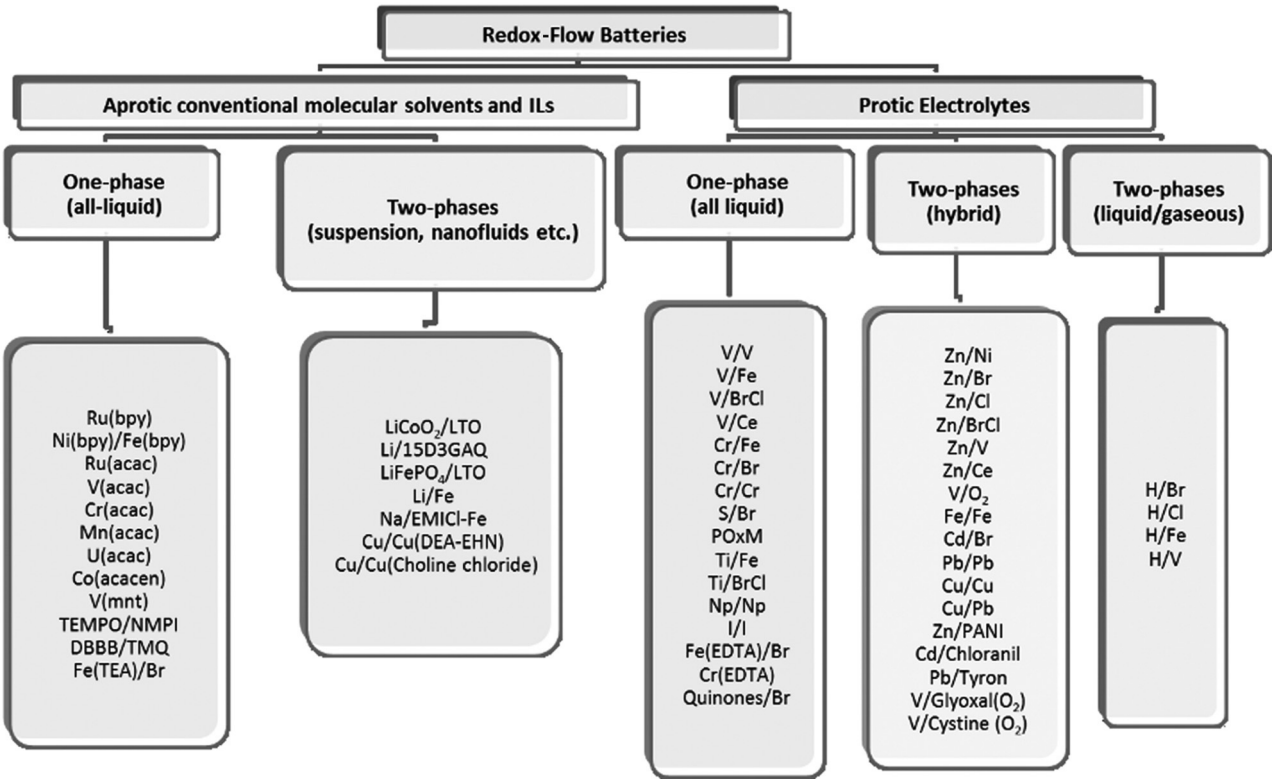

Figure 6. Redox-flow batteries classified according to electrolyte system and aggregate state.[6]

adsorption to surface groups, or monolayer coverage. This mechanism could be beneficial for RFBs, however it is more relevant mostly for ligand-stabilized metal ions, which have a high molar mass and low solubility that result finally in a low energy density of the electrolyte.

2) Inner-sphere reactions, which involve specific interactions of the electrode surface. For these reactions, the kinetics of the redox couples is highly dependent on the state of the electrode surface, and can be, for example, catalyzed by surface carbonyl groups (Fe^{3+}/Fe^{2+}, V^{3+}/V^{2+}), or is sensitive to non-oxide-catalyzed adsorption of a monolayer ($[Fe(CN)_6]^{4-}/[Fe(CN)_6]^{3-}$). In this mechanism, special care should be taken with electrode pretreatment and its durability, as reaction rates can vary by several orders of magnitude compared to the outer-sphere pathway.

We consider further the chemical aspects of the various electrolyte redox species and processes associated with half cells or battery performance. Half-cells with metal deposition are very similar to conventional primary or secondary batteries from a chemical or an electrochemical point of view, and are only differentiated by their combination with a redox couple presenting another half-cell electrolyte. For this reason, we consider in more detail mainly the redox couples used and investigated mostly for RFB electrolytes.

3.2. Inorganic Redox Couples/Protic Electrolytes

3.2.1. Zn^{2+}/Zn

Zinc deposition proceeds in aqueous solutions despite its high negative standard electrode potential because the hydrogen evolution reaction is kinetically inhibited and results in a high hydrogen overpotential.[78] Zinc-based RFBs are hybrid RFBs because of the phase transition, in which capacity is limited by the amount of zinc deposited in the anode compartment. Deposition does not proceed uniformly because of current-density differences and incomplete zinc dissolution. This leads to a risk of dendrite formation, thus causing short circuiting of cells. However, as a consequence of its price, availability, high negative electrode potential, two-electron transfer, and intensive research for over two hundred years on zinc-related electrochemistry and hence available information, zinc remains an interesting element for RFBs.

3.2.1.1. $Zn^{2+}/Zn//Br_2/Br^-$

The zinc/bromine system goes back to Charles Bradley[79] in 1885, and next to the Zn/Cl_2 system it is the oldest RFB hybrid system. In this system, a $ZnBr_2$ solution is used, the conductivity of which can be enhanced by the addition of salts such as KBr and KCl.[80] The zinc ions in the electrolyte are in the form of $[ZnCl_3]^-$, $[ZnCl_4]^{2-}$, $[ZnBr_3]^-$, or generally as $[(ZnX_2)_2(\mu\text{-}X)_2]^{2-}$.[82] Zinc is generally deposited on a carbon anode, which can lead to dendrite growth and consequent losses in efficiency or complete failure.[81] The negative half-cell often has a spacer component to ensure that there is enough space for zinc deposition between the electrode and the membrane.

$$\begin{aligned}
&\text{Anode :} && Zn^{2+} + 2\,e^- \rightleftharpoons Zn && \varphi^0_A = -0.76\,V\\
&\text{Cathode :} && 2\,Br^- \rightleftharpoons Br_2 + 2\,e^- && \varphi^0_C = +1.06\,V\\
&\text{Cell :} && Zn^{2+} + 2\,Br^- \rightleftharpoons Zn + Br_2 && \phi_Z = 1.82\,V
\end{aligned}$$

The solubility of bromine in water is only 0.43 mol L^{-1} at 20 °C. However, the presence of bromide and chloride ions allows significantly higher concentrations to be achieved as a result of the formation of polyhalides (Br_3^-, Br_5^-, $ClBr_2^-$).[82] Bromine undergoes base-assisted hydrolysis in water. Therefore, the electrolytes for Zn/Br RFBs are strongly acidic, with halides and complexing agents added to conserve bromine. The elementary bromine produced during charging is kept in equilibrium with polybromide ions in solution. High self-discharge currents occur because of the diffusion of polybromide ions through the membrane to the anode and of their reaction with zinc. Either organic solvents such as propionitrile[83,84] or quarternary ammonium bromides can be used[85,86] to limit the diffusion. Nowadays, *N*,*N*-methylethylpyrrolidinium (MEP) or *N*,*N*-methylethylmorpholinium (MEM) or their mixtures are mostly used.[87–89] The presence of the quarternary ammonium bromides (QBr) results in the stabilization of the existing polybromide complexes by interaction with the large organic cation to form a hydrophobic organic phase separated from the aqueous solution. The amount of active bromine in the aqueous phase is significantly lowered (ca. 0.01 mol L^{-1}), but bromine from both phases is reduced during discharge (Figure 7). The existence of a series of complex polybromides

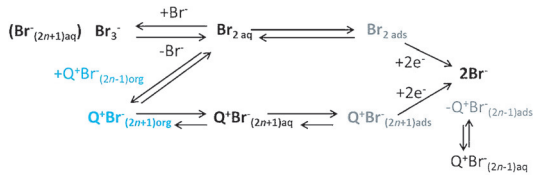

Figure 7. Complex formation equilibria between aqueous and organic phases in a bromine half-cell and reaction paths of discharge from the results of Fabjan and Hirss.[97] Q stands for MEM/MEP, $n = 1$–5.

which participate in a variety of complex equilibria with each other is assumed. The use of ion-selective membranes can keep the bromine-rich fluid stream away from the zinc deposition to minimize self-discharge and short-circuiting by zinc dendrites.[90]

The Br_2/Br^- redox reactions with strong chemisorption of bromide ions or radicals are multistep and electrochemically reversible at platinum electrodes; they can be classified as inner-sphere reactions.[91,92] The rates of the Br_2/Br^- redox reactions are more than two orders of magnitude smaller at carbon electrodes, which are usually used in battery systems, than at platinum electrodes.[93,94] It is assumed that the bromide oxidation proceeds according to a Volmer–Heyrovsky mechanism, that is, discharge (V) followed by associative desorption (H):

$$Br^- \rightleftharpoons Br_{ads} + e^- \quad (V)$$
$$Br_{ads} + Br^- \rightleftharpoons Br_2 + e^- \quad (H)$$

However, assumptions regarding the rate-determining step are controversial, and the exact role played by the state of the carbon-based electrode surfaces in the reaction has not yet been clarified. Initial ideas regarding catalytic effects were based on glassy carbon modified with carbon nanotubes[95] and with graphene oxide/polymer composite electrodes.[96]

Although complexing agents (QBr) have been used for over 40 years for bromine complexation, the electrochemical properties of Br_2/Br^- have only recently been studied. In addition to the storage of bromine, QBr promotes the specific adsorption of bromide at the carbon/polymer composite electrode, thus accelerating the Br_2/Br^- reaction.[98] The relatively high solubility of the redox pair and a two-electron transfer enable maximum energy density, depending on the source, of theoretically up to 570 $Wh\,kg^{-1}$, whereas approximately 70 $Wh\,kg^{-1}$ can be achieved in practice.[99,21]

3.2.1.2. $Zn^{2+}/Zn//Cl_2/Cl^-$

As an alternative to zinc/bromine RFBs, a significantly more reactive chlorine/chloride cathode couple can be used. In this case, the chlorine produced during charging is dissolved in a separate container at 10 °C with water as chlorhydrate $Cl_2{\cdot}H_2O$ and is released again during discharge by heating.[100] This can result in an energy efficiency of up to 65 %. The higher standard potential of Cl_2/Cl^- results in the open-circuit voltage being approximately 300 mV higher, at 2.16 V.

$$\text{Anode}: \quad Zn^{2+} + 2\,e^- \rightleftharpoons Zn \qquad \varphi^0_A = -0.76\,V$$
$$\text{Cathode}: \quad 2\,Cl^- \rightleftharpoons Cl_2 + 2\,e^- \qquad \varphi^0_C = +1.40\,V$$
$$Cl_2 + x\,H_2O \rightleftharpoons Cl_2 \cdot x\,H_2O$$
$$\text{Cell}: \quad Zn^{2+} + 2\,Cl^- \rightleftharpoons Zn + Cl_2 \qquad \varphi^0_Z = 1.80\,V$$

Besides the corrosion and toxicity, the high cathode potential, that is, strong oxidative behavior, requires the application of inert, for example, titanium-based, electrode materials, at which the Cl_2/Cl^- reaction is rather slow.

3.2.1.3. $Zn^{2+}/Zn//ClBr_2^-/Br^-$

To combine the advantages of higher redox potential, that is, reactivity, of chlorine and the higher kinetics of bromine-based Zn-RFBs, Zhang et. al used an electrolyte based on 2 M Cl^- and 2 M Br^- to investigate a zinc/polyhalide RFB.[101]

$$\text{Anode}: \quad Zn^{2+} + 2\,e^- \rightleftharpoons Zn \qquad \varphi^0_A = -0.76\,V$$
$$\text{Cathode}: \quad 2\,Br^- + Cl^- \rightleftharpoons ClBr_2^- + 2\,e^- \qquad \varphi^0_C = +1.40\,V$$
$$\text{Cell}: \quad Zn^{2+} 2\,Br^- + Cl^- \rightleftharpoons Zn + ClBr_2^- \qquad \varphi^0_Z = 1.80\,V$$

The results achieved were similar to those of a Zn/Br-RFB, but slightly higher efficiencies and energy densities were achieved.

3.2.1.4. $Zn^{2+}/Zn//VO_2^+/VO^{2+}$

Another variant was to use VO_2^+/VO^{2+} as a catholyte and Zn^{2+}/Zn in methanesulfonic acid (MSA) as an anolyte as an alternative for toxic and corrosive bromine or chlorine, despite the lower redox potential of the VO_2^+/VO^{2+} couple.[102]

$$\text{Anode}: \quad Zn^{2+} + 2\,e^- \rightleftharpoons Zn \qquad \varphi^0_A = -0.76\,V$$
$$\text{Cathode}: \quad VO^{2+} + H_2O \rightleftharpoons VO_2^+ + e^- + 2\,H^+ \qquad \varphi^0_C = +1.00\,V$$
$$\text{Cell}: \quad 2\,VO^{2+} + 2\,H_2O + Zn^{2+} \rightleftharpoons 2\,VO_2^+ + Zn + 4\,H^+ \qquad \varphi^0_Z = 1.76\,V$$

The concentration of VO^{2+} can reach up to 3–4 M in 3 M MSA solutions, which is significantly higher than the solubility of VO^{2+} salts in H_2SO_4 (see Section 3.2.3.1). A battery with 3 M VO^{2+} in 2.8 M MSA and 1.5 M Zn^{2+} in 0.5 M MSA achieved continuously decreasing efficiencies of 70–58 % in charge–discharge tests after 16 cycles. This was attributed to the production of hydrogen in the negative half-cell and the consequent electrolyte imbalance during charge and discharge. The diffusion coefficients of vanadium species in MSA as estimated by cyclic voltammetry were similar to that in aqueous sulfuric acid solution.

3.2.1.5. $Zn^{2+}/Zn//Ce^{4+}/Ce^{3+}$

The Zn/Ce hybrid RFB was patented by Clarke et al. in 2004[103–106] and is primarily characterized by its high open-circuit voltage of approximately 2.4 V. During the charging process, solid zinc is deposited from the solution and Ce^{III} is oxidized to Ce^{IV}. The electrolytes are based on methanesulfonic acid (MSA) to slow down the thermodynamically preferred oxygen-evolution reaction and at the same time to also ensure a relatively high solubility of the redox active materials (up to 0.8 M).[107]

$$\text{Anode}: \quad Zn^{2+} + 2\,e^- \rightleftharpoons Zn \qquad \varphi^0_A = -0.76\,V$$
$$\text{Cathode}: \quad 2\,Ce^{3+} \rightleftharpoons 2\,Ce^{4+} + 2\,e^- \qquad \varphi^0_C = +1.28\,V \text{ to } +1.72\,V$$
$$\text{Cell}: \quad 2\,Ce^{3+} + Zn^{2+} \rightleftharpoons Zn + 2\,Ce^{4+} \qquad \varphi^0_Z = 2.04\,V \text{ to } 2.48\,V$$

The biggest challenge is the cerium half-cell, which limits the performance of a battery.[34] Despite the high catalytic activity of platinum and platinum/iridium-based electrodes towards the oxygen-evolution reaction, these electrodes are, however, suitable for the positive half-cell,[108] because carbon-based materials are easily oxidized at high half-cell potentials[109] and the reaction is significantly faster.[35] The diffusion coefficient of Ce^{III} in MSA is approximately one order of magnitude lower than in aqueous acids[114] and decreases with increasing MSA concentration, which is probably caused by the complexing of cerium ions. The oxygen evolution reaction also becomes slower at higher MSA concentrations. The Ce^{IV}/Ce^{III} redox reactions are, therefore, electrochemically quasireversible and relatively slow. Solutions with 0.8 M cerium in 4 M MSA is optimal and is a compromise between the solubility of Ce^{III} and Ce^{IV} and the strong oxidative nature of the cerium ions. Complexation of cerium ions to diethylenetriaminepentaacetic acid (DTPA)

result in the rate and the electrochemical reversibility of the redox reactions being enhanced.[110] Previous research showed that the solubility and the rate of the Ce^{IV}/Ce^{III} reaction in aqueous H_2SO_4 is very limited.[111] The reaction rate is high in aqueous HNO_3, and 1M cerium solutions can be prepared;[112,113] however, nitrate is slightly reduced, which causes irreversible side reactions in the electrolyte. A battery setup without a membrane has an efficiency of up to 76% at 20 mA cm^{-2} and a current efficiency of 90%.[114] The cerium concentration was, however, only 0.2M, hence more side reactions and therefore lower efficiency can be expected at high concentrations. With a NAFION-based RFB, an efficiency of 39% was achieved with 0.8M Ce^{III} in 4M MSA at 50 mA cm^{-2} after 57 charge/discharge cycles.[115]

3.2.2. Cr^{3+}/Cr^{2+}

3.2.2.1. $Cr^{3+}/Cr^{2+}//Fe^{3+}/Fe^{2+}$

The first oil crisis in the early 1970s led to studies being carried out at the NASA Lewis Research Center to find an affordable stationary electrochemical energy storage concept which could store energy over hours or days at low cost.[116–119]

The battery system in the ideal case should fulfill the following requirements.[116]

- Simple electrode reactions
- High exchange current densities
- No high working temperatures
- Electrochemically reversible reactions

Further properties should include:

- Oxidized and reduced species should be present in solution
- The potentials of the redox couples should be in a range within which the solvent does not decompose during either charging or storage
- Ions with a high affinity for or containing oxygen (e.g. MnO_4^-, Cr^{3+}) should be avoided to simplify hydrogen management
- Complex ions (e.g. $Fe(CN)_6^{4-}$) should be avoided to obtain energy densities that are as high as possible.

The first studies have been performed with a system using Fe^{3+}/Fe^{2+} and TiO^{2+}/Ti^{3+} (see Section 3.2.5.6).[120] Other redox couples were also tested for their properties at carbon electrodes, where the redox transfers of Fe^{3+}/Fe^{2+} and Br_3^-/Br^- were reversible, while Cr^{3+}/Cr^{2+} V^V/V^{IV}, V^{IV}/V^{III}, and V^{III}/V^{II} were irreversible.[121] Vanadium was positively evaluated because of its high number of available oxidation states; however, it was not considered further because of its kinetics and reversibility as well as the high cost. There were indications of good reversibility for the Br_2/Br^- redox couple at boron carbide electrodes. Despite the low standard potential of Cr^{3+}/Cr^{2+} and the related risk of side reactions, that is, hydrogen evolution, development was focused on Fe/Cr because of the low costs and higher cell potential.

$$\text{Anode}: \quad Cr^{3+} + e^- \rightleftharpoons Cr^{2+} \qquad \varphi_A^0 = -0.42\,V$$
$$\text{Cathode}: \quad Fe^{2+} \rightleftharpoons Fe^{3+} + e^- \qquad \varphi_C^0 = +0.77\,V$$
$$\text{Cell}: \quad Cr^{3+} + Fe^{2+} \rightleftharpoons Cr^{2+} + Fe^{3+} \qquad \varphi_Z^0 = 1.19\,V$$

As a consequence of the almost unavoidably slow formation of hydrogen at the anode, a permanent imbalance in the charge carriers occurs, which leads to a decrease in capacity, because more Fe^{3+} than Cr^{2+} ions are formed during charging. To avoid this problem, a rebalancing can be carried out, whereby the hydrogen formed is transferred to another electrochemical cell and is oxidized at the anode there:

$$\text{Anode}: \quad 2H^+ + 2e^- \rightleftharpoons H_2 \qquad \varphi_A^0 = 0.02\,V$$
$$\text{Cathode}: \quad Fe^{2+} \rightleftharpoons Fe^{3+} + e^- \qquad \varphi_C^0 = +0.77\,V$$

In the cathode half-cell, the iron-containing catholyte is conducted and reduced in the same stoichiometric proportion as protons are formed at the anode. At the same time, the loss of protons is compensated through diffusion.[122–125] Higher current densities for the reduction of iron were achieved with a further developed cell, and attempts at reducing Cu^{2+}, Cr^{3+}, Ti^{4+}, and V^{4+} were also successful.[123]

In 1981, a prototype system with a nominal power of 1 kW and 12 kWh at a current density of 32 mA cm^{-2} was developed.[125] The system consisted of 4 stacks with a total of 156 cells.

A five-cell stack with an active area of 307 cm^2 per cell achieved energy efficiencies of 70–80% and a power density of 54 mW cm^{-2} at 81 mA cm^{-2} with an Au/Pb-catalyzed anode.[124] The manufacture of an Au/Pb-modified electrode was done by thermal reduction of a carbon felt impregnated with a gold loading of 20 μg cm^{-2} from a gold solution at 250°C and in situ deposition of lead from a 10^{-4}M $PbCl_2$ solution.[126] It revealed that the used felts varied according to their hydrophilic properties, pH value, gold loading capacity, and hydrogen overpotential. It was believed that reduced groups on the surface of the felt were the cause of the irreproducible and non-uniform deposition. The groups became oxidized on treatment with HNO_3. Differences in the hydrogen overpotential were also found, which can also be attributed to the groups on the surface. Oxidized surfaces had a higher overvoltage than reduced ones. The gold loading process can be made reproducible at higher hydrogen overpotential by pretreatment in 1M HNO_3. A corresponding cell reached a current efficiency of 98% at a 0–80% state of charge and current densities up to 108 mA cm^{-2}.[127]

Catalysts such as Pb, Bi/Pb, Bi, ZrC, Au/Pb, Cu/Pb, and Ag/Pb can not only accelerate the anode reactions, but also cause a higher hydrogen overpotential.[125,128–131]

Ion-exchange chromatography and visible spectroscopy allowed a variety of chromium complexes to be identified during the charge and discharge process.[132–134] In a discharged state, $[Cr(H_2O)_5Cl]^{2+}$ is the predominant species, and it is in a temperature-dependent equilibrium with $[Cr(H_2O)_6]^{3+}$. When the charge state is changed, the concentration of $[Cr(H_2O)_5Cl]^{2+}$ rapidly decreases while the concentration of $[Cr(H_2O)_6]^{3+}$ hardly changes, which indicates that the equilibrium between the two only emerges slowly. The equilibrium emerges more quickly in the presence of Cr^{II}. Oxidation occurs through a chloride-bridge-mediated inner-sphere redox reaction between $[Cr(H_2O)_5Cl]^+$ and $[Cr(H_2O)_5Cl]^{2+}$.

The performance can be improved considerably by using mixed electrolytes (1M $CrCl_3$, 1M $FeCl_2$, 2M HCl), a micro-

porous membrane, and higher temperatures of 65 °C with a bismuth/lead catalyzed anode reaction.[131,135–138]

The advantages of mixed electrolytes are:

- The use of microporous membranes, instead of highly selective and more expensive ion-exchange membranes is possible.
- Osmotically caused differences in volumes of anolyte and catholyte can be compensated for by mixing.
- Electrolyte production can be carried out more simply and therefore cheaply, because expensive separation of the iron or chromium is not necessary.
- Low cell resistance (separator) and consequent higher power densities result in power-related costs being reduced.

Disadvantages:

- Lower current efficiency because of a microporous separator.
- Reduced solubility of the redox couples and associated lower energy densities.
- Lower cell voltage.

However, the apparent loss in power because of the lower cell voltage can be compensated for by the anode reaction being faster at higher working temperatures.[135] The basic mechanism in this case is not only the reduced internal resistance of the cell, but a shift in the equilibrium from the inactive species $[Cr(H_2O)_6]^{3+}$ to the faster redox-active species $[Cr(H_2O)_5Cl]^{2+}$.[133,134] This results in significantly higher current densities up to 129 mA cm^{-2}, as well as at higher states of charge. The energy efficiencies obtained are between 75–85 % at a maximum of 1 % hydrogen evolution at the anode.

An efficiency of 75 % was achieved with a Bi/Pb-catalyzed anode, an 867 cm^2 cell stack at a temperature of 65 °C, and a current density of 60 mA cm^{-2} with mixed electrolytes and a cation exchange membrane with low selectivity.[139] A similarly constructed 14.5 cm^2 cell reached an energy efficiency of over 80 % at 80 mA cm^{-2} over 500 cycles.

A 1 kW Fe/Cr RFB with 6 cells achieved an energy efficiency of 83 % at 60 mA cm^{-2} and 0.24 % H_2 formation.[140]

3.2.2.2. $Cr^{3+}/Cr^{2+}//Br_2/Br^-$

A Cr/Br RFB was reported by Heintz and Illenberger in 1996[141] and Swartbooi in 2006.[142] In the first study, the diffusion of Br_2 through a cation exchange membrane was investigated, while in the second case a cell was developed with a cell voltage of 1.44 V at a standard potential difference of 1.49 V. The theoretical energy density was 57 Wh kg^{-1}.

3.2.2.3. $Cr^{3+}/Cr^{2+}///CrO_4^{2-}/Cr^{3+}$

The system patented by Kangro in the 1940s uses three different oxidation states of chromium in a sulfuric acid solution.[7] Compared to other RFBs, the difference in the standard potentials is relatively high at 1.77 V, which means as well as potentially high energy densities, problems occur with hydrogen formation in the anode half-cell and oxygen generation in the cathode half-cell.

$$\text{Anode}: \quad Cr^{3+} + e^- \rightleftharpoons Cr^{2+} \qquad \varphi_A^0 = -0.42\,V$$
$$\text{Cathode}: \quad Cr^{3+} \rightleftharpoons CrO_4^{2-} + e^- \qquad \varphi_C^0 = +1.35\,V$$
$$\text{Cell}: \quad 2\,Cr^{3+} \rightleftharpoons Cr^{2+} + CrO_4^{2-} \qquad \varphi_Z^0 = 1.77\,V$$

Kangro used 25 % $Cr_2(SO_4)_3$ in 2 M H_2SO_4 and lead, amalgamated lead, or mercury electrodes. A discharge voltage of 1.8 V was achieved with freshly amalgamated lead. Problems included the high overpotential of the reduction of Cr^{3+} and the question of a suitable cathode material which has high oxygen overpotential along with favorable reaction kinetics.[8] Nowadays the extremely poisonous and carcinogenic chromate and dichromate ions are not considered suitable for use in a battery.

3.2.3. V^{3+}/V^{2+}

Divalent vanadium ions form metastable solutions, and as a result of their negative potentials and the simple isostructural redox reactions to form V^{3+} as well as the possibility of combining with the two higher oxidation states of vanadium, V^{3+}/V^{2+} is one of the most studied redox couples for RFBs. Solubility in acids and material costs are moderate. As a consequence of its negative standard electrode potential, there are many possible combinations with other redox couples; however, carbon-based electrodes are used in aqueous media, at which the reaction kinetics are only moderate.

3.2.3.1. $V^{3+}/V^{2+}//VO_2^+/VO^{2+}$

The vanadium redox-flow battery (VRFB) is the most studied redox-flow battery system to date, although the suitability of acid-soluble di- to pentavalent vanadium was first discovered in 1986.[143] Before this, basic electrochemical research had been done on vanadium, mostly at platinum and mercury electrodes.[144–146] The formation of a film on the platinum electrodes, slow VO_2^+/VO^{2+} reactions, irreversible V^{3+}/V^{2+} reactions at carbon felt electrodes, and high costs resulted in further research in the frame of the NASA redox-flow batteries project being ruled out.[9] However, Sum et al. were later able to show that the rate and reversibility of the relevant redox reactions are highly dependent on the pretreatment of the electrodes, especially the oxidation state of the electrode surface,[147,148] which means the reactions can proceed reversibly or irreversibly.[149]

$$\text{Anode}: \quad V^{3+} + e^- \rightleftharpoons V^{2+} \qquad \varphi_A^0 = -0.25\,V$$
$$\text{Cathode}: \quad VO^{2+} + H_2O \rightleftharpoons VO_2^+ + 2\,H^+ + e^- \qquad \varphi_C^0 = +1.00\,V$$
$$\text{Cell}: \quad VO^{2+} + V^{3+} + H_2O \rightleftharpoons VO_2^+ + V^{2+} + 2\,H^+ \qquad \varphi_Z^0 = 1.25\,V$$

The advantage of the vanadium/vanadium system is in the use of ions of the same element at various oxidation states in both half-cells, which minimizes the change in the concentrations of the electrolyte by diffusion through the membrane in the other half-cell compartment, and achieves potentially higher energy densities and efficiencies. Other systems with redox couples with three or more oxidation states are only

known for Cr-RFB (see Section 3.2.2.3), U-RFB (see Section 3.5.1.2), Np-RFB (see Section 3.2.5.9), and as Pb-RFB hybrid systems (see Section 3.2.5.4). The two electrolytes are usually 1.5–2 M V solutions in 2 M H_2SO_4, which corresponds to theoretical maximum energy densities of 19–38 Wh L^{-1}. To attain the highest possible volumetric and gravimetric energy densities, high vanadium concentrations are necessary, which approach the saturation and solubility limits. A distinctive feature is the complex chemistry of the pentavalent vanadium, which tends towards irreversible condensation to vanadium pentoxide at temperatures above about 40 °C. Dilute V^V exists in strongly acidic solutions as yellow VO_2^+ dioxovanadium ions in its hydrated form of $[VO_2(H_2O)_4]^+$.[150–152] In more highly concentrated solutions ($[V^V] > 100$ mM, $[H_2SO_4] > 2$ M), $[VO_2(H_2O)_4]^+$ provides the basis for dimerization and formation of complexes with sulfate and hydrogen sulfate ions in the second coordination sphere (Figure 8). Subsequent deprotonation and decomposition of the dimer leads to the formation of V_2O_5, which precipitates at concentrations of about 0.25 M because of its limited solubility.

Another explanation for the thermal instability of V^V solutions is the possible existence of complex $[VO_2(H_2O)_3]^+$,

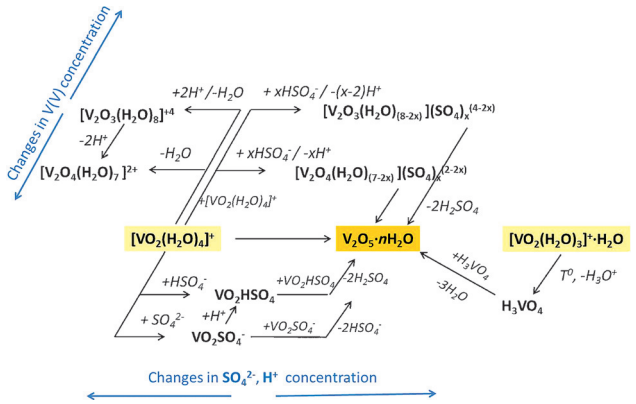

Figure 8. Reaction pathways for V^V ions depending on vanadium and sulfuric acid concentration.[6]

which is more stable at low temperatures than $[VO_2(H_2O)_4]^+$, and dehydrates at increasing temperatures with formation of neutral $VO(OH)_3$ and finally to V_2O_5 through deprotonation (Figure 8).[153] V^{IV} species appear as an octahedral, blue-colored $[VO(H_2O)_5]^{2+}$ complex,[154] which can undergo ion pairing with sulfate at high H_2SO_4 concentrations (> 5 M). It is presumed that SO_4^{2-} ions enter the inner coordination sphere of the V^{IV} complexes and that V^{IV} dimers may also be formed.[155] In mixtures of V^{IV} with V^V, which correspond to partially charged VRFBs, the formation of mixed-valence complexes at vanadium concentrations over 0.8 M and H_2SO_4 concentrations over 3 M has been observed:[156]

$$VO^{2+} + VO_2^{+} \rightleftharpoons V_2O_3^{3+}$$

This complex also influences the stability of the catholyte, as well as the electrochemical behavior of the V^V/V^{IV} redox couple in the positive half-cell. The following solutions are suggested to avoid precipitation of V^V:

1) Deprotonation can be prevented by raising the concentration of the acid in the electrolyte. However, this also leads to a decreasing solubility of vanadium species in other oxidation states at the same temperature, and precipitation/crystallization.[157]
2) Saturated vanadium solutions can be stabilized with additives (e.g. 5 % w/w potassium sulfate, 3 % w/w sodium hexametaphosphate, polyacrylic acid) which inhibit precipitation.[158] Organic (gelatine, xanthan, starch etc.) and inorganic (3 % w/w Aerosil 200, Aerosil 300) substances which cause gelatinization of the electrolyte can be used as stabilizers in vanadium solutions. Inorganic salts, organic tensides, and chemical compounds with hydroxy or amino groups have previously been studied as additives.[159,160] However, the practical application of such additives in the VRFB is disadvantaged by the fact that they are easily oxidized chemically by V^V ions, which can lead to capacity loss. The exact mechanism of the effects of these additives is not yet known. The stability of the electrolytes is usually estimated only ex situ, whereas the electrode material (carbon-based), being in contact with the electrolyte solution, can catalyze the coagulation of the V^V particles.
3) Solutions can be stabilized by changing the chemical structure of the vanadium ions in an electrolyte solution. Mixed acids (hydrochloric acid, phosphoric acid, sulfuric acid, oxalic acid, methanesulfonic acid, and their mixtures) are currently used as electrolytes for this purpose.[161,162] A chloride-containing electrolyte enables the dissolution of vanadium salts up to a concentration of 2.5 M and also has a high thermal stability up to 50 °C. The stability is based on the formation of $[VO_2Cl(H_2O)_2]$.[163] In mixed acid electrolytes (Cl^- and SO_4^{2-}), V^{III} species form a gelatinous precipitate (after ca. 10 days or at low temperatures), which dissolves again when the temperature is raised. A reason for this is the formation of neutral V^{III} species $[VSO_4(OH)(H_2O)_5]$ complexed by anions and $[V(SO_4)_2(H_2O)_4]^-[H_5O_2]^+$ ion pairs.[164] However, the use of hydrochloric acid can lead to undesirable evolution of chlorine as a side process.

To prepare the highly concentrated vanadium electrolyte, a $VOSO_4$ solution can be electrolyzed to V^V and V^{III}, where the V^{3+} solution formed can serve as the initial electrolyte for the anodic half-cell in a VRFB, together with a fresh portion of $VOSO_4$ solution for the cathodic one.[165] A suspension of V_2O_5 can also be electrolyzed, where a mixture of 50 % V^{3+} and 50 % VO^{2+} is obtained as an anolyte, which can also be used as the initial solution in both half-cells.[166] The dissolution of V_2O_5 in sulfuric acid, which is limited by its low solubility, is avoided with these methods.[167] VRFB systems are equipped with a heat management system to avoid irreversible precipitation of V_2O_5 at high temperatures.

Carbon-based materials are usually used for the electrodes because of the negative standard potential of the anolyte (−0.26 V).[168] Typical power densities are 50–100 mW cm^{-2}, which is 10 times lower than a PEMFC. It is known that both

redox couples undergo inner-sphere reactions with a strong sensitivity to the electrode surfaces. With negative V^{III}/V^{II} redox couples, however, the inner-sphere route dominates only at low coverage of the electrode with carbonyl groups.[169] The presence of *o*-benzoquinone-type groups suppresses the reaction rates, which are recovered, however, if the groups are reduced to the catechol form.[170] The rate of the positive half-cell reactions and the power density and efficiency of the battery can be strongly enhanced through functionalization of the electrode surface by various oxidation methods.[24,25] This results in the formation of C–OH, C=O, and COOH groups, which enable simplified electron transfer through the accumulation of vanadyl or divanadyl cations. It is believed that the oxidation of V^{IV} with glassy carbon electrodes occurs in three basic steps: a chemical-electrochemical-chemical (CEC) mechanism at low overpotential, which becomes an electrochemical-chemical-chemical (ECC) mechanism at higher anode or cathode overpotentials.[170] Electron transfer occurs via an adsorbed layer of an electrically neutral intermediate product $VO_2{\cdot}4H_2O$, which may precipitate, and finally adsorption ($VO_2^+ \rightleftharpoons VO_{2,ads}^+$) as a rate-determining step. A further CEC mechanism was recently suggested for the V^V/V^{IV} reactions, which considers the dimerization and formation of a mixed-valence V^{IV}/V^V complex, where the electrochemical polarization determines the rate.[171]

$$2\,[VO^{2+}\cdot 5\,H_2O] \underset{k_{-23}}{\overset{k_{23}}{\rightleftharpoons}} HV_2O_3^{3+}\cdot 9\,H_2O + H^+$$

$$HV_2O_3^{3+}\cdot 9\,H_2O \underset{k_{-24}}{\overset{k_{24}}{\rightleftharpoons}} HVO_2^{2+}\cdot 4\,H_2O + VO^{2+}\cdot 5\,H_2O + e^-$$

$$HVO_2^{2+}\cdot 4\,H_2O \underset{k_{-25}}{\overset{k_{25}}{\rightleftharpoons}} VO_2^+\cdot 4\,H_2O + H^+$$

A recently published study on the corrosion of graphite electrodes in vanadium electrolytes using on-line mass spectrometry revealed a preferred formation of CO_2 and CO instead of oxygen generation at the anode electrode.[172] In the absence of V^{IV}, for example, in 2 M H_2SO_4, the electrode corrosion is more pronounced, because the carbon oxidation is hindered by the oxidation of V^{IV}.

3.2.3.2. $V^{3+}/V^{2+}//Fe^{3+}/Fe^{2+}$

The V/Fe system represents a mixture of the Cr/Fe (Section 3.2.2.1) and VRFB systems. The use of vanadium species avoids the disadvantages of a chromium anode, for example, slow electrochemical reactions of Cr^{3+}/Cr^{2+} and the necessary catalysts, a higher reaction temperature of approximately 60 °C, and the problem of hydrogen evolution. An advantage of V/Fe is that the range of thermal stability can be extended by using iron species. This means that the otherwise necessary temperature management system and the associated costs are no longer required.

Anode :	$V^{3+} + e^-$	$\rightleftharpoons V^{2+}$	$\varphi_A^0 = -0.25\,V$
Cathode :	Fe^{2+}	$\rightleftharpoons Fe^{3+} + e^-$	$\varphi_C^0 = +0.77\,V$
Cell :	$V^{3+} + Fe^{2+}$	$\rightleftharpoons V^{2+} + Fe^{3+}$	$\varphi_Z = 1.02\,V$

The lower cathode potential results in the corrosion of carbon-based electrodes through intercalations or oxidation by chlorine formed from the chloride-based electrolyte by being reduced. Only mixed electrolytes can be used in practice because of diffusion of ions through the membrane. A battery with a mixture of 1.25 M V^{3+}, 1.25 M Fe^{2+}, and 2.3 M HCl achieved an energy efficiency of 70–83 % over a temperature range of 0–50 °C at 50 mA cm^{-2} and constant discharge capacities over 50 cycles.[173] Low energy density is a challenge associated with this system. However, the energy density can be improved by using a higher concentration of active redox couples. V^{3+}/V^{2+} dissolves to produce solutions up to 4 M in HCl, while Fe^{3+}/Fe^{2+} is barely soluble in HCl. With a mixed electrolyte, in which some of the chloride ions were replaced by sulfate ions, the solubility (and thus the energy density) was raised by 25 % to 1.5 M V^{3+} and 1.5 M Fe^{2+}, where an energy efficiency of over 80 % was demonstrated over 100 cycles. The energy efficiency was 70 % with a polyethylene microporous separator.[174] Similar values were also achieved with other microporous separators.[37] In a matrix study on the optimization of the electrolyte, taking into account temperature, composition, and conductivity, a battery with a solution of 1.5 M V^{3+} and 1.5 M Fe^{2+} in 3 M HCl gave the best performance values.[175] To further increase the power density, the anolyte volumes can be doubled, whereby the otherwise unused portion of vanadium in the catholyte can also be used as VO_2^+/VO^{2+}.[176] The end-of-charge voltage is thereby increased to that of a conventional VRFB and two plateaus are formed in the current–voltage curves for the reactions of V^{3+}/V^{2+} and VO_2^+/VO^{2+} or at lower potential for V^{3+}/V^{2+} and Fe^{3+}/Fe^{2+}, respectively. However, this arrangement also has the disadvantages of the reactions of VO_2^+/VO^{2+} (see Section 3.2.3.1). On the other hand, these batteries have a higher energy density than a VRFB because of the addition of Fe^{3+}/Fe^{2+}.

3.2.3.3. $V^{3+}/V^{2+}//ClBr_2^-/Br^-$

The vanadium/bromine (polyhalide) battery developed by Skyllas-Kazacos in 2003 enhances the advantages of the VRFB and represents what is known as the 2nd generation of VRFBs:[177,178]

1) The same electrolyte composition is used in both half-cells.
2) The concentration of vanadium in solution can be raised to 3—4 M , which means that energy densities of up to 30–50 Wh kg^{-1} can be achieved.
3) The temperature stability is not limited by the V^{IV}/V^V redox couple.

Anode :	$V^{3+} + e^-$	$\rightleftharpoons V^{2+}$	$\varphi_A^0 = -0.25\,V$
Cathode :	$2\,Br^- + Cl^-$	$\rightleftharpoons ClBr_2^- + 2\,e^-$	$\varphi_C^0 = +1.04\,V$
Cell :	$2\,V^{3+} + 2\,Br^- + Cl^-$	$\rightleftharpoons 2\,V^{2+} + ClBr_2^-$	$\varphi_Z^0 = 1.29\,V$

Typical electrolytes consist of 2 M $V^{3.5+}$ in a mixture of 6.4 M HBr and 2 M HCl.[179] The effect of quarternary ammonium bromides (MEM-Br, MEP-Br, TBA-Br) on the half-cell reactions of V^{III}/V^{II} has been studied.[180] The kinetics of Br_2/Br^- is controlled by mass transport, and neither the

kinetics nor the mechanism are affected by the complexing agents. MEM and MEP can reduce Br_2 vapors effectively, but increase membrane resistance.

3.2.3.4. $V^{3+}/V^{2+}//O_2/O^{2-}$

The development of galvanic cells based on the reaction of vanadium and oxygen goes back to Kaneko et al. in 1992.[181] In a patent, Kaneko et al. describe a system called a redox battery, in which divalent vanadium ions are oxidized at the anode to trivalent ions. Oxygen or air is reduced at the cathode with the aid of a catalyst (Figure 9). The theoretical

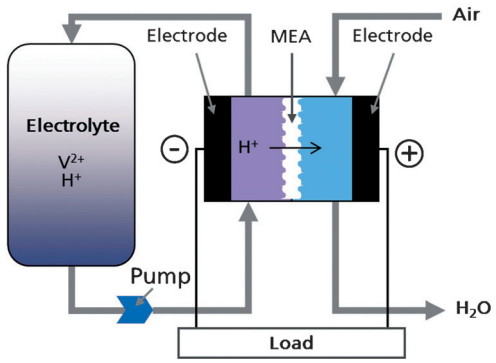

Figure 9. Operating principle of a vanadium/oxygen fuel cell.[6]

energy density compared to that of a VRFB is more than doubled as a result, since the weight of the catholyte when using atmospheric oxygen needs not be taken into account.

$$\text{Anode}: \quad V^{3+} + e^- \rightleftharpoons V^{2+} \qquad \varphi^0_A = -0.25\,V$$

$$\text{Cathode}: \quad O_2 + 4\,e^- + Cl^- \rightleftharpoons 2\,O_2^{2-} \qquad \varphi^0_C = +1.20\,V$$

$$\text{Cell}: \quad 2\,V^{3+} + O_2 + 4\,H^+ \rightleftharpoons 2\,V^{2+} + 2\,H_2O \qquad \varphi^0_Z = 1.45\,V$$

The preparation of a V^{2+} solution was carried out by electrolysis in a conventional RFB cell. Discharge current densities of up to 10 mA cm^{-2} with a 1 M VSO_4 in 4 M H_2SO_4 solution were achieved. Menictas and Skyllas-Kazacos examined the system at different temperatures as well as with different membranes and membrane electrode assemblies (MEAs).[182] The concentration of V^{2+} ions in 5 M H_2SO_4 was 1.8 M. The oxidizing agent used was gaseous oxygen. The biggest challenge was to prevent the dissolution of the catalyst layer of the MEA by swelling. A reduction of swelling enabled the operation of a five-cell stack over a period of 100 h.[183]

In 2010 Noack et al. reported on an experimental comparison of a VOFC with a VRFB.[184] The maximum discharge power density of the VOFC was 30 mW cm^{-2}. A 1.6 M VSO_4 solution was used in 2 M H_2SO_4.

Hosseiny et al. reported a VOFC designated as a vanadium–air redox-flow battery (VARFB), in which one MEA was exchanged for another with a different catalyst between charging and discharging. A platinum/carbon-based catalyst was used for discharging, and a titanium/iridium-based catalyst was used to reverse the reaction.[185] The concentration of the VSO_4 solution was 2 M in 3 M H_2SO_4. The charge and discharge current densities were 2.4 mA cm^{-2}. In 2011 Palminteri observed strong evolution of hydrogen in the Pt-based MEA, which was caused by diffusion of the V^{2+} solution into the cathode compartment. He explained the detachment of the catalyst layer and the resulting considerable decrease of battery power density by hydrogen evolution.[186] To avoid this problem, a cell was developed with an intermediate compartment separated by another membrane,[187] to oxidize diffusing V^{2+} ions to V^{3+} ions, and thus to prevent the formation of hydrogen at the Pt particles of the MEA. Although this type of galvanic cell is often called an RFB, strictly speaking, the lack of electrochemical reversibility of the cathode reactions makes it a fuel cell which "burns ions". A reversal of the reactions can currently only be achieved by an electrolysis cell equipped with special catalysts, which is identical to the conventional H_2/O_2 fuel cells. The challenges of the system are long-term stable cells, V^{III}/V^{II} solutions with high concentrations, and efficient water management at the cathode to be able to achieve higher energy and power densities.

3.2.3.5. $V^{3+}/V^{2+}//Ce^{4+}/Ce^{3+}$

Cerium readily undergoes complexation in highly concentrated sulfuric acid solutions. In solutions with concentrations below 0.5 M or 0.15 M, it is mainly present as solvated Ce^{3+} and Ce^{4+} ions, respectively,[188] with Ce^{4+} hydrolyzed at H_2SO_4 concentrations below 0.5 M. At higher concentrations of sulfate, Ce^{III} forms more $CeSO_4^+$ and $Ce(SO_4)_2^-$; in contrast, Ce^{IV} forms more $CeSO_4^{2+}$, $Ce(SO_4)_2$, and $Ce(SO_4)_3^{2-}$, whereas Ce^{IV} has stronger interactions with SO_4^{2-}. These characteristics make the electrochemical behavior complicated at the electrode. An RFB with 0.5 M Ce^{3+} and 0.5 M V^{3+} in 1 M H_2SO_4 achieved 68 % efficiency at 22 mA cm^{-2} with an energy density of 15 Wh L^{-1}. At carbon electrodes, the redox reaction of Ce^{IV}/Ce^{III} is electrochemically irreversible. As a result of the complexation of cerium ions with SO_4^{2-} and the decrease in the solubility of Ce species, low H_2SO_4 concentrations are more appropriate as well as higher temperatures to increase the rate of cerium redox reactions. It is difficult to find a suitable solvent for cerium salts because Ce^{IV}/Ce^{III}, which has a standard electrode potential above oxygen evolution, is not stable in HNO_3 and $HClO_4$, while ClO_4^- and NO_3^- cannot form stable complexes. Ce^{IV} oxidizes chloride ions from HCl to Cl_2, while H_2SO_4 solutions form stable complexes with Ce^{IV}.[189] Investigation of the electrochemical properties of Ce^{IV}/Ce^{III} has shown that reversibility of its redox reactions at platinum electrodes is affected by Pt oxides on the electrode surfaces. A reduction in the amount of surface oxides enhanced the charge transfer. An obstacle to the development of aqueous V/Ce RFBs is the high oxidative potential of the cathode in conjunction with the slow reactions of the cerium redox couple at carbon-based electrodes, so the choice of suitable electrodes with simultaneous slow evolution of oxygen is limited.

3.2.4. H^+/H_2

Hydrogen-based systems are not classic RFBs, but when a hydrogen-based anode is combined with a suitable cathodic redox couple such as Br_2/Br^- and continuous process management is performed with electrolyte circulation, these systems can be referred to RFBs. The H^+/H_2 reactions proceed reversibly on platinum electrodes and at high rates, but the inhibition and ageing of the catalyst can also lead to performance problems. The required storage of hydrogen and electrolyte cross-over from the cathodic half-cell result in the need for highly complex process engineering compared to all-liquid-based RFBs. Despite the technical complexity of battery construction, their power densities could be profitable.

3.2.4.1. $H^+/H_2//Br_2/Br^-$

H/Br systems were already proposed for large-scale stationary energy storage in the 1960–1970s.[190–192] They were presumed to have the following advantages compared to other energy storage devices:[193]

- Rapid electrode kinetics and thus high energy efficiencies.
- Same cell for charging and discharging processes.
- Tolerance to overcharging and deep discharging.
- Possibility of using solid polymer electrolyte membranes and hence different pressures to store hydrogen directly as a hydride.
- High current efficiency and hence a low self-discharge rate.
- No mass-transfer limitation because of the high solubility of bromine in HBr.
- Bromine storage and bromine electrode can work through the low vapor pressure at close to ambient pressure
- Products and reactants are flowing media which minimize imbalances between the cells

The high reaction rate and related high power density and energy efficiency were key reasons for the development of H/Br systems. The bromine-associated redox reactions proceed quickly and efficiently on activated carbon electrodes, whereby there was no need for catalysts. However, the kinetics can be increased significantly through the use of, for example, Pt.

$$\begin{aligned}
&\text{Anode :} && 2\,H^+ + 2\,e^- \rightleftharpoons H_2 && \varphi^0_A = 0.00\,V\\
&\text{Cathode :} && 2\,Br^- \rightleftharpoons Br_2 + 2\,e^- && \varphi^0_C = +1.06\,V\\
&\text{Cell :} && 2\,HBr \rightleftharpoons H_2 + Br_2 && \varphi^0_Z = 1.09\,V
\end{aligned}$$

By using NAFION as a membrane, the current densities obtained were up to 180 $mA\,cm^{-2}$ with an efficiency of 70 %.[193] An advantage over chlorine-based systems is the formation of complex Br_3^- and Br_5^- ions in the catholyte, which hinders diffusion through the separator and thus can lead to high current efficiencies. After a systematic optimization of the cell structure at a current density of 0.3 $A\,cm^{-2}$, more than 10000 h of operation could be achieved in discharge mode, with limited signs of ageing.[194] A loss of Pt catalyst at the anode was often evident, which was assigned to the high potentials under the open-circuit mode and the diffusion of Br_2 to the anode. Additionally, there were significant problems of water outflow at the anode at operating temperatures of 25–50 °C, which resulted in loss of power. In addition, poisoning of the Pt-based anode catalyst by halide ions driven by diffusion was found, which also leads to a loss of power.[195] Thermally treated and untreated platinum alloys had a higher tolerance to bromide ions than platinum black. Tungsten carbide electrodes, in contrast, had a lower activity for the anode reaction, but no detectable activity in terms of bromine reduction.[196] In addition, no change was observed in their activity towards the oxidation of hydrogen, which makes this type of electrodes interesting for polymer electrolyte free cell design. A new cell design, with a nanoporous proton-conducting membrane, allowed discharge power densities of up to 1.5 $W\,cm^{-2}$ at 80 °C to be achieved.[197] The energy efficiency during discharging was almost 90 %, which is approximately double the efficiency of a fuel cell. The same catalyst was used at the anode and cathode at a loading of 1.5 $mg\,cm^{-2}$ Pt. To avoid the corrosion and contamination, the voltage of the anode was kept constant at about 0 V versus NHE. For this purpose, a constant flow of dry hydrogen was maintained. The bromine solution consisted of 0.9 M Br_2 in 1 M HBr. The authors found no degradation in the performance of the cell during their investigations. To overcome the corrosion problems of Pt on the bromine cathode, a cell with an activated carbon cathode has been developed and examined,[198] which could also achieve high power densities of 1.4 $W\,cm^{-2}$ at 55 °C. The cell consisted of a conventional MEA with a Pt catalyst as the anode and three carbon papers activated in concentrated H_2SO_4, which were stacked and used as a flow-through cathode. In a direct comparison of an HBr cell with an H_2/O_2 cell, the HBr cell with 0.3 $W\,cm^{-2}$ achieved power densities almost twice as high as the fuel cell at room temperature.[199] In a comparison of cells with an interdigitated channel structure versus those that are serpentine-shaped, the ones with the interdigitated structure achieved higher power densities.

To reduce the cost of the system, tests were performed on a membrane-free cell with a laminar fluid flow.[75] Power densities up to 795 $mW\,cm^{-2}$ were achieved with 5 M Br_2 in 3 M HBr solution. The voltage efficiency was 92 % at 25 % maximum power density. The open fluid structure meant that no charge and discharge cycles could be completed, and thus it is only possible to speculate about the current efficiency, which at optimal flow should be 72 %, thereby giving an efficiency of 66 %.[200] The high reaction kinetics and the potentially high energy densities make this system extremely interesting for energy storage. However, the handling of toxic and corrosive bromine is a major challenge in regard to suitable materials for the battery components as well as in regard to safety, especially at elevated temperatures. The diffusion of bromine in the anode compartment requires a complicated approach for its separation and recycling, since otherwise capacity loss will occur and hydrogen storage or its components can be difficult. It is these challenges that explain why up to now no complete system has been tested for hydrogen storage and circulation, but only with hydrogen feeding from an external hydrogen source.

3.2.4.2. $H^+/H_2//Cl_2/Cl^-$

In addition to Br_2/Br^- the redox couple Cl_2/Cl^- in combination with H^+/H_2 was also proposed in the 1970s for stationary energy storage.[201] As with the bromine-based system, NAFION can be used as a polymer electrolyte membrane. Hydrogen can be stored as a metal hydride ($FeTiH_z$) and at low temperatures chlorine can be kept in liquid form in a separate tank.

$$\text{Anode}: \quad 2H^+ + 2e^- \rightleftharpoons H_2 \qquad \varphi_A^0 = 0.00\,V$$
$$\text{Cathode}: \quad 2Cl^- \rightleftharpoons Cl_2 + 2e^- \qquad \varphi_C^0 = +1.36\,V$$
$$\text{Cell}: \quad 2HCl \rightleftharpoons H_2 + Cl_2 \qquad \varphi_Z^0 = 1.36\,V$$

The hydrochloric acid concentration should not exceed 35%, otherwise carbon corrosion is increased and membrane resistance as well as the HCl vapor pressure will be higher. Under these conditions, and because of the rapid reactions, it is possible to achieve an energy efficiency of over 70%,[202] whereby only a small portion of Cl_2 is lost by diffusion to the anode.[203] With the use of polymer electrolyte membranes, the water content in the membrane determines the transport properties of ions, which leads to a dependence on the acid concentration.[204] Another side effect is the transport of low-concentration acid through the membrane, which leads to self-humidification of the anode during electrolysis. With 3 M HCl and an operating temperature of 50 °C, a cell achieved a maximum power density of 0.51 $W\,cm^{-2}$ at 0.5 V. A Pt-based catalyst had significantly higher performance values than a Rh-based catalyst, such that the performance capabilities of the Pt-catalyzed cell dropped to 45% after 120 h through the formation of H_2PtCl_6, while the performance of the Rh-based cell remained stable over extended periods of time.[205] According to Thomassen et al.[206] the chlorine reduction takes place on platinum in accordance with the Heyrovsky mechanism:

$$Cl_{2(aq)} + e^- \rightleftharpoons Cl_{(ads)} + Cl^-{}_{(aq)}$$

In general, it was found that both the mechanism and kinetics of the reduction of Cl_2 at Pt and Ru are highly dependent on the oxide layer on the electrode surface.[206] With a cathode mixed metal oxide catalyst with low precious metal content $(Ru_{0,09}Co_{0,91})_3O_4$ for the Cl_2/Cl^- redox reaction, power densities of over 1 $W\,cm^{-2}$ were achieved during discharging and over 0.3 $W\,cm^{-2}$ for charging.[207] A comparison of three different cell designs led to the identification of the different advantages and disadvantages of the system.[208] In a conventional PEM fuel-cell design, high HCl concentrations and associated dehydration of the membrane lead to higher cell resistance and power losses. Corrosion problems were increasingly found with the use of a cell with a low concentration of HCl. A cell with a membrane of polybenzimidazole modified by phosphoric acid achieved long-term stability, but lower performance values, which was probably due to the formation of higher phosphoric acid polymers in the membrane:

$$H_3PO_4 \rightarrow H_4P_2O_7 \rightarrow H\text{-}(HPO_3)_n\text{-}OH$$

H_2/Cl_2 systems have been proposed as an energy source for space missions because of their higher energy density compared to H_2/O_2 systems.[209]

3.2.4.3. $H^+/H_2//Fe^{3+}/Fe^{2+}$

Another approach for the replacement of the slow O_2/O^{2-} reaction in a fuel cell is the use of Fe^{3+}/Fe^{2+} with a standard electrode potential of +0.77 V. The exchange current density is several factors of ten greater than that of the O_2/O^{2-} reaction, while the mass transport to the electrode is also greatly increased because of the higher solubility of the iron compound compared to O_2. Compared to Cl_2- and Br_2-based systems, the iron compounds used have low toxicity and are much cheaper than vanadium. Discharge trials on a 4 cm^2 cell with a conventional anode structure and a catalyst-free cathode achieved power densities of up to 170 $mW\,cm^{-2}$ at 70 °C with a 0.9 M Fe^{2+} solution.[210]

$$\text{Anode}: \quad 2H^+ + 2e^- \rightleftharpoons H_2 \qquad \varphi_A^0 = 0.00\,V$$
$$\text{Cathode}: \quad Fe^{2+} \rightleftharpoons Fe^{3+} + e^- \qquad \varphi_C^0 = +0.77\,V$$
$$\text{Cell}: \quad 2H^+ + 2Fe^{2+} \rightleftharpoons H_2 + 2Fe^{3+} \qquad \varphi_Z^0 = 0.77\,V$$

To investigate the charge and discharge behaviour, a similar cell was used and operated with 0.7 M $Fe_2(SO_4)$ in 0.8 M H_2SO_4, 0.9 M $FeCl_3$ in 0.8 M HCl, or 0.9 M $Fe(NO_3)_3$ in 0.8 M HNO_3 at room temperature.[211] The nitrate-based cell achieved maximum discharge power densities of 234 $mW\,cm^{-2}$, followed by the chloride-based one with 207 $mW\,cm^{-2}$ and the sulfate-based one with 148 $mW\,cm^{-2}$. The nitrate-based cell was only stable for a few cycles, which was probably caused by the formation of NO_2 and thus a reduced amount of reactive Fe^{3+}. The chloride-based system successfully completed over 50 cycles at 25 $mA\,cm^{-2}$ with only a small loss in capacity. The sulfate-based system also demonstrated low capacity losses over several cycles. The charging overvoltage for all three systems was substantially greater than the discharge overvoltage, and accordingly they could only be charged with relatively low current densities. This strongly asymmetric behavior was attributed to the low reaction rate of Fe^{3+}/Fe^{2+}, but no more detailed reasons were given. Cells with a Pt/Ir catalyst for iron reduction achieved up to 270 $mW\,cm^{-2}$ power density for 1 M $FeSO_4$ in 2 M H_2SO_4 at 40 °C.[212] A cell with a 1.5 M $FeSO_4$ solution, however, only achieved 110 $mW\,cm^{-2}$. A system with 1.5 M $FeCl_3$ in 2 M HCl achieved 240 $mW\,cm^{-2}$, and a system with 1.4 M $FeBr_3$ in 2 M HBr 190 $mW\,cm^{-2}$. Measurements of the half-cell voltage at the cathode revealed 5–20 mV overvoltage, which was an insignificant contribution to the total overvoltage of 300 mV at 0.64 $A\,cm^{-2}$. Accordingly, the iron reduction proceeded very quickly with all electrolytes, while the hydrogen oxidation probably strongly depended on the electrolyte anions. The active sites of the Pt catalyst were blocked by the adsorption of anions migrating into the anodic compartment, thereby causing the performance of the Cl^-- and Br^--based systems to be lower than that of SO_4^{2-}. This effect is common for H/Cl and H/Br cells, such that sulfate does not cause passivation of the Pt catalyst. However, the efficiency in the

case of a 1.5 M $FeSO_4$ electrolyte solution decreased, because the iron species diffusing into the anodic half-cell precipitated. In an investigation of different cathode materials, a cell with untreated carbon paper showed the highest performance values.[213] When reduced iron is oxidized by oxygen in the discharging process, the system is a mediated fuel cell, since this process is not reversible (see Section 3.7).

3.2.4.4. $H^+/H_2//VO_2^+/VO^{2+}$

An H/V cell with a conventional Pt-based MEA as an anode, a catalyst-free cathode with a serpentine-shaped flow field, and 1 M VO_2^+/VO^{2+} electrolyte in 5 M H_2SO_4 achieved power densities of over 54 mW cm^{-2}. Charge and discharge tests performed with 11 mA cm^{-2} and a 0.2 M VO^{2+} solution achieved a current efficiency of 84 % and an energy efficiency of 43 %.[214] To optimize the system, the commercial PEMFC-MEA used was replaced with one that was coated with catalyst only on the anode side and contained two untreated carbon papers as a cathode. Without impregnation with PTFE, the usability was higher and thus the mass transport to the electrode was facilitated, whereby a maximum power density of 114 mW cm^{-2} could be achieved and the charging–discharging energy efficiency was increased to 60 %.

3.2.5. Other Systems

3.2.5.1. $Fe^{2+}/Fe//Fe^{3+}/Fe^{2+}$

Batteries based exclusively on iron present an interesting alternative because of the ready availability of the storage material. However, deposition and dissolution are very slow, while at the same time there is a relatively low hydrogen overvoltage, so that emerging hydrogen leads to energy and charge-carrier losses.[215] A current efficiency of 90 % and an energy efficiency of 50 % were achieved at 60 °C with 60 mA cm^{-2}. Studies on the optimization of the metallic deposition in RFBs led to an optimized structure of the anode, such that a nonconductive felt was used as a spacer between the porous electrode and membrane.[216]

3.2.5.2. $S/S^{2-}//Br_2/Br^-$

Battery systems based on polysulfide/sulfide ions as the anolyte and bromine/bromide, chlorine/chloride, or iodine/iodide as catholyte were first mentioned in 1984 by Remick and Ang.[217] In these batteries during discharge, sulfides and low-molecular-weight polysulfides are oxidized to higher polysulfides at the anode. At the same time, bromine is reduced to bromide at the cathode:

$$\text{Anode:}\quad 2\,Na^+ + x\,Na_2S_{x+1} + 2\,e^- \rightleftharpoons (x+1)\,Na_2S_x \qquad \varphi^0_A = -0.27\,V \qquad x = 1-4$$

$$\text{Cathode:}\quad 2\,NaBr \rightleftharpoons Br_2 + 2\,Na^+ + 2\,e^- \qquad \varphi^0_C = +1.06\,V$$

$$\text{Cell:}\quad 2\,Na^+ + x\,Na_2S_{x+1} + 2\,NaBr \rightleftharpoons (x+1)\,Na_2S_x + 2\,Na^+ + Br_2 \qquad \varphi^0_Z = 1.33\,V$$

Typically, the anolyte consists of sodium sulfide (Na_2S_2) and the catholyte of NaBr, to which Br_2 is added to saturation. NAFION can be used for separation of the two half-cells, this also enables charge compensation by transport of Na ions. The slow sulfide/polysulfide reactions on carbon electrodes mean that metal electrodes of cobalt or nickel can be used.[218–220] In a comparison of carbon felt electrodes with electrodes made of activated carbon, which were each coated with cobalt, the carbon felt electrodes achieved better performance than those with activated carbon.[220] The authors found the cause to be an accumulation of elemental sulfur in the cobalt-coated activated carbon electrode, which led to transport problems and a consequent loss of performance. The cobalt-coated carbon felt electrodes achieved energy efficiencies as high as 81 % at 40 mA cm^{-2} over 50 cycles, while the other electrode deteriorated in performance after just a few cycles. From this background, a 100 MWh RFB was constructed in the late 1990s, but not completed.[221–223] In addition to the challenges of the bromine and the relatively slow reactions of sulfur, further considerable challenges are caused by the diffusion of sulfide in the cathode compartment, which leads to irreversible oxidation of sulfite and thus continuously decreases the capacity during operation.

3.2.5.3. $Cd^{2+}/Cd//Fe^{3+}/Fe^{2+}$

The Cd/Fe system is an attempt to minimize the cost and the diffusion of ions through the membrane. Cd^{2+} is relatively cheap, does not react with Fe^{2+} or Fe^{3+}, and can be separated efficiently from 0.5 M H_2SO_4 solutions because of the fast electrochemical reactions and hydrogen overvoltage.[224] The electrolytes consist of 0.5 M $FeSO_4$ and 0.25 M $Fe_2(SO_4)_3$ in 1 M H_2SO_4 for the positive half-cell and 1.5 M $CdSO_4$ in 1 M H_2SO_4 for the negative one. The separator used is NAFION. The discharge voltage of the battery was 10 mA cm^{-2} at 0.99 V with a current efficiency of 91 % and an energy efficiency of 71 %. The efficiency decreases, however, during the first 50 charge/discharge cycles.

3.2.5.4. $Pb^{2+}/Pb//PbO_2/Pb^{2+}$

An RFB based only on lead was first proposed in 2004 by Hazza et al.[225] In conventional sulfuric acid based lead–acid batteries, there is a reaction of solid $PbSO_4$ to solid Pb at the anode and to solid PbO_2 at the cathode during charging. By using methanesulfonic acid, Pb^{2+} is in solution and reacts during charging to form solid deposits at the electrodes:

$$\text{Anode:}\quad Pb^{2+} + 2\,e^- \rightleftharpoons Pb$$

$$\text{Cathode:}\quad Pb^{2+} + 2\,H_2O \rightleftharpoons PbO_2 + 4\,H^+ + 2\,e^-$$

$$\text{Cell:}\quad 2\,Pb^{2+} + 2\,H_2O \rightleftharpoons Pb + PbO_2 + 4\,H^+$$

As a result, a membrane-free RFB can be built, in which the same electrolyte is used in both half cells. The deposition and dissolution of lead on glassy carbon electrodes in 2 M CH_3SO_3H is a fast process with a low overvoltage that runs without disturbance. The hydrogen overvoltage of lead is

high, so high power densities can be expected. The diffusion coefficient of Pb^{2+} in 2 M CH_3SO_3H is 6.1×10^{-6} $cm^2 s^{-1}$. The cathode reaction of Pb^{2+} and PbO_2, however, is much slower and has a higher overvoltage. This affects the formation of PbO_2 in particular. As a result of the high voltage, the formation of oxygen as a side reaction also cannot be ruled out. The reduction of PbO_2 to Pb^{2+} is likely to proceed through an insoluble intermediate which can be more easily oxidized than Pb^{2+}. Pb^{2+} has a maximum solubility of about 2 M Pb^{2+} in 1 M CH_3SO_3H. The solubility decreases significantly at higher acid concentrations. The conductivity of the solution increases with the acid concentration, but decreases with the concentration of Pb^{2+}, which has been attributed both to higher viscosity and also to the formation of ion pairs with $CH_3SO_3^-$. The properties are contradictory and change in the operation of an RFB, since protons are involved in the reaction. A 1.5 M $Pb(CH_3SO_3)_2$ solution in 0.9 M CH_3SO_3H was proposed as a favored electrolyte composition. An RFB was investigated with this electrolyte composition, whereby a cell voltage of 1.78 V and current efficiency of $>85\,\%$ at 20–100 mA cm^{-2} were obtained.[226] The negative electrode was made of glassy carbon or nickel foam and the positive one was made of planar and brushed glassy carbon. Lead dendrite formation during the charging process, particularly at the negative electrode, can cause a problem for the system, which can result in a short circuit of the cell. For a uniform deposition of Pb, sodium lignin sulfonate and polyethylene glycol were investigated as additives, whereby the former produced significantly improved deposits with inert character at a concentration of 1 g L^{-1}, and the latter achieved hardly any changes, even at high concentrations.[227] Another possibility is a complete discharge and the oxidation of Pb residues by oxygen, such that finally an oxygen excess is removed, and a pH change has to be considered:[228]

$$2\,Pb + 4\,H^+ + O_2 \rightarrow 2\,Pb^{2+} + 2\,H_2O$$

The ability of different metal ion additives to increase the reaction rate of PbO_2/Pb^{2+} was investigated. Additives of Fe^{3+} and Bi^{3+} produced no changes, while an addition of Ni^{2+} achieved a slightly lower overvoltage, but at the same time lower current efficiency. The effects of the Ni^{2+} additive become inconsiderable with time. In discharges with 100 mA cm^{-2}, a layer was left on the positive electrode, which probably consisted of poorly soluble PbO.[227] In another study, lower rates of PbO_2 formation and slower oxygen evolution were found on addition of Bi^{3+}, but also finer and more firmly fixed PbO_2 deposits.[229] The addition of 5 mM hexadecyltrimethylammonium cation ($C_{16}H_{33}(CH_3)_3N^+$) particularly to low concentrated Pb and CH_3SO_3H solutions led to uniform metal deposition, with the acid concentration having the greatest influence. The concentration of the MSA should not exceed 2 M for the dendrite formation to remain moderate.[230] The $C_{16}H_{33}(CH_3)_3N^+$ had little influence on the deposition of PbO_2, but the high current densities and high acid concentrations caused a tendency for increased detachment of PbO_2 from the carbon substrate.[231] In CH_3SO_3H, PbO_2 separates preferably as the α-PbO_2 columbite with an orthorhombic structure that forms dense and free-standing films. At elevated temperatures, the tetragonal rutile structures of β-PbO_2 are more prevalent, which also forms dense films. Mixtures of the two modifications generally lead to loose deposits. Furthermore, thicker PbO_2 films have a particularly high overvoltage during the reduction compared to a rapid formation of PbO_2.[232] A Pb-RFB with an active surface area of 100 cm^2 could successfully complete over 100 charge and discharge cycles, although solid PbO_2 collected at the bottom of the cell. Lead dendrites and oxygen evolution also led to problems, which increased with the lower concentration of Pb^{2+}.[233] Similar effects limited the life of an RFB in a bipolar two-cell configuration.[234] H_2O_2 can be added periodically to clean the surfaces of the electrode substrates of residues of Pb and PbO_2. The H_2O_2 oxidizes Pb to Pb^{2+} or reduces PbO_2 to Pb^{2+}, and thus prolongs the cycle life.[235]

3.2.5.5. *Polyoxometalates*

RFBs based on two polyoxometalates (POMs) with three redox transitions were reported on in 2013.[236] A current efficiency of over 95 % was achieved with 20 mM POM in 0.5 M H_2SO_4 and in an organic electrolyte with graphite felt electrodes and a NAFION membrane.

$$\text{Anode}: \quad [SiV^{IV}_3W^{VI}_9O_{40}]^{10-} + 3\,e^- \rightleftharpoons [SiV^{IV}_3W^{V}_3W^{VI}_6O_{40}]^{13-}$$

$$\text{Cathode}: \quad [SiV^{IV}_3W^{VI}_9O_{40}]^{10-} \rightleftharpoons [SiV^{V}_3W^{VI}_3O_{40}]^{7-} + 3\,e^-$$

$$\text{Cell}: \quad [SiV^{IV}_3W^{VI}_9O_{40}]^{13-} + [SiV^{IV}_3W^{VI}_9O_{40}]^{10-} \rightleftharpoons [SiV^{IV}_3W^{V}_3W^{VI}_6O_{40}]^{13-} + [SiV^{V}_3W^{VI}_9O_{40}]^{7-}$$

The redox-active compound A-α-$K_6HSiV_3W_{12}O_{40}$ was made of a tungstate-based Keggin structure and formed both the anode and cathode substance. It is stable over a wide pH and temperature range, and its electrochemical behavior is based on V^V and W^{VI} centers, which have a potential difference of about 1 V. A similar idea of the adaptation of redox-active centers in POMs is reported in Ref. [237]. In the modified Keggin structure $[Mn^{III}_3(OH)_3SiW_9O_{34}]^{4-}$, transitions of Mn^{II}-Mn^{III}-Mn^{IV} are used to act as a cathode, and the W centers with a lower redox potential are used as the anode. POMs have better kinetics than the V^V electrode reactions and a good pH dependence of the redox transitions at pH 4–6. POMs have great research potential because they have different redox-active centers (or redox transitions) and are stable at neutral pH. However, the tendency to strong adsorption of the POMs on carbon electrode surfaces, which influences the kinetics, as well as the possible complexity and high costs of the synthesis of POMs mean that they have been neglected until now.

3.2.5.6. *$TiO^{2+}/Ti^{3+}//Fe^{3+}/Fe^{2+}$*

Titanium species are of interest as redox couples in RFBs because of their low cost and the large number of oxidation states. Unlike V^{II}, Ti^{II} is not stable in aqueous media and oxidizes to Ti^{3+} with the formation of hydrogen. TiO^{2+} in turn undergoes hydrolysis to $TiO_2 \cdot 4\,H_2O$. However, Ti^{IV} can be

stabilized in solution through complexation with Cl^-, thereby forming hexachlorotitanate $[TiCl_6]^{2-}$.

Anode : $TiO^{2+} + 2H^+ + e^- \rightleftharpoons Ti^{3+} + H_2O$ $\varphi^0_A = 0.04\,V$
Cathode : $Fe^{2+} \rightleftharpoons Fe^{3+} + e^-$ $\varphi^0_C = +0.77\,V$
Cell : $TiO^{2+} + Fe^{2+} + 2H^+ \rightleftharpoons Ti^{3+} + Fe^{3+} + H_2O$ $\varphi^0_Z = 0.73\,V$

Experiments were already performed with chloride- and sulfate-based Ti/Fe RFBs in the 1950s.[8,9] The same electrolyte compositions were used for both half-cells. An RFB based on 1 M $TiCl_4$, 1 M $FeCl_2$, and 1.5 M HCl achieved up to 55 % energy efficiency at low current densities. An RFB based on 1 M $Ti(SO_4)_2$, 1 M $FeSO_4$, and 0.75 M H_2SO_4 achieved 50 % energy efficiency. In the 1970s, 1 M solutions of metal ions were used at NASA in 0.5–6 M HCl.[120] The open-circuit voltage decreased with the higher acid concentrations, and the efficiency of the cells increased through the higher conductivity. The highest performance values were achieved with a cell having 6 M HCl as an anolyte and 0.5 M HCl as a catholyte. However, the anion-exchange membrane used had a low selectivity relative to cations, so that the acid concentration, in particular, levelled off with the number of cycles and the open circuit voltage dropped.[238] For TiO^{2+}/Ti^{3+}, an alloy of 97 % tungsten with 3 % rhenium was found on which the reaction was significantly faster than on graphite.

3.2.5.7. $TiO^{2+}/Ti^{3+}//ClBr_2^-/Br^-$

Skyllas-Kazacos and Milne studied the complexation of $TiCl_4$ with HBr, thereby obtaining a solution of $TiBr_4Cl_2^{2-}$.[244] In combination with a bromine-based catholyte, which also contains chloride, a Ti/Br-RFB with mixed halogen complexes is produced:

Anode : $TiBr_4Cl_2^{2-} + e^- \rightleftharpoons TiBr_2Cl_2^- + 2Cl^-$
Cathode : $2Br^- + Cl^- \rightleftharpoons ClBr_2^- + 2e^-$

Or simplified with uncomplexed ions:

Anode : $TiO^{2+} + 2H^+ + e^- \rightleftharpoons Ti^{3+} + H_2O$ $\varphi^0_A = 0.04\,V$
Cathode : $2Br^- \rightleftharpoons Br_2 + 2e^-$ $\varphi^0_C = +1.06\,V$
Cell : $TiO^{2+} + 2Br^- + 2H^+ \rightleftharpoons Ti^{3+} + Br_2 + H_2O$ $\varphi^0_Z = 1.10\,V$

An RFB with 4 M HBr, 3 M HCl, and 0.56 M $TiCl_4$ achieved a current efficiency of 97–98 % at 40 mA cm^{-2}. The largest cell voltage reached was 0.93 V.

3.2.5.8. $CuCl/Cu//Cu^{2+}/CuCl$

An all-copper RFB was proposed in 2014 by Sanz et al.[239] The authors explain the advantages of the system to be fast electrochemical processes and simplicity, since no catalysts or expensive ion-exchange membranes are needed. Other advantages include: copper chloride complexes are highly soluble in aqueous media; the relatively low cell voltage results in no hydrogen, chlorine, or oxygen evolving; simple electrolytic production by reaction of Cu^{2+} with Cu; high energy efficiency; low power-specific costs because of the relatively low price and the availability of high-purity copper; and a wide temperature range of 5–70 °C that obviates expensive heat management. The electrolyte consisted of up to 3 M Cu^I in 4 M HCl and 2 M $CaCl_2$. Cyclovoltammetric (CV) studies of Cu^+/Cu resulted in the suggestion that the dissolution process of Cu through adsorbed CuCl with subsequent complex formation of $[CuCl_2]^-$ could take place and thus would affect the rate of copper oxidation. Furthermore, the formation of hydrogen at low voltages was possible during the deposition, which led to lower energy efficiency and electrolyte imbalances or an incomplete dissolution of Cu during the CV measurement. The redox couple Cu^{2+}/CuCl had an electrochemically reversible behavior. The diffusion coefficient of Cu^I was, however, at 1.47×10^{-6} cm^2 s^{-1} about a factor of ten lower than in other aqueous solutions, which could lead to transport limitations. One battery achieved an energy efficiency of 60 % at 40 °C at 20 mA cm^{-2}. The average discharge voltage at this current density was about 0.4 V. However, the battery only charged and discharged at about one tenth of the theoretical maximum capacity. The redox couples are presumed to be Cu^{2+}/Cu^+ and Cu^+/Cu, but Cu^I and Cu^{II} ions are complexed in the presence of Cl^-, which leads to a shift of the standard potentials. Stabilization the Cu^I species by complexing with Cl^- enabled a stepwise reduction of Cu^{II} to Cu^I and then to Cu metal. Here, different Cu^I and Cu^{II} complexes can form in the system described: for example, $CuCl_3^-$, $CuCl_4^{2-}$, $CuCl_2^-$, $CuCl_3^-$. Without complexing counterions a direct two-electron reduction of Cu^{II} to Cu metal takes place.[78]

Anode : $Cu^{2+} + e^- \rightleftharpoons Cu^+$ $\varphi^0_A = +0.153\,V$
Cathode : $Cu \rightleftharpoons Cu^+ + e^-$ $\varphi^0_C = +0.521\,V$
Cell : $2Cu^+ \rightleftharpoons Cu + Cu^{2+}$ $\varphi^0_Z = 0.368\,V$

As with all other hybrid systems, disadvantageous formation of dendrites or the dissolution of metal copper are again to be expected. In addition, the deposition of Cu limits the maximum possible capacity of the battery. Furthermore, only a very low energy density can be expected due to the very low potential difference.

3.2.5.9. $Np^{4+}/Np^{3+}//NpO_2^{2+}/NpO_2^+$

Theoretical considerations have been undertaken on the use of minor actinides (An) neptunium (Np) and americium (Am), as well as uranium (U) and plutonium (Pu) from spent fuel rods, as redox couples for RFBs. They can exist in oxidation states from An^{III} to An^{VI} and their reduced and oxidized forms are isostructural, that is, An^{4+}/An^{3+} and dioxoactinoidyl cations AnO_2^{2+}/AnO_2^+, respectively. Accordingly, high electron transfer rates can be expected.[240]

Anode : $Np^{4+} + e^- \rightleftharpoons Np^{3+}$ $\varphi^0_A = 0.15\,V$
Cathode : $NpO_2^+ \rightleftharpoons NpO_2^{2+} + e^-$ $\varphi^0_C = +1.14\,V$
Cell : $Np^{3+} + NpO_2^{2+} \rightleftharpoons Np^{4+} + NpO_2^{2+}$ $\varphi^0_Z = 1.29\,V$

Np in the form of Np^{4+}/Np^{3+} and NpO_2^{2+}/NpO_2^{+} was identified from Pourbaix and redox potential diagrams as the most promising candidate. Since U^{V}, Pu^{V}, and Am^{IV} tend to disproportionate and thus slow reactions are to be expected, these compounds were not considered further for aqueous electrolytes. However, U^{V} is stable in the form of acetylacetonate complexes in aprotic solutions. The voltage difference between the two redox transitions of UO_2^{2+}/UO_2^{+} and U^{VI}/U^{III} is about 2.18 V (see Section 3.5.1.2).[241] An average annual quantity of 630 kg ^{237}Np is generated by 40 Japanese nuclear power plants and thus 36 kWh storage capacity can be estimated theoretically. A battery based on 0.05 M Np in 1 M HNO_3 could be charged and discharged.[242] It was shown by calculations that a Np-based battery could achieve very high efficiencies up to 99.1 % at 70 mA cm^{-2} because of the much higher rate constants ($k_0(Np^{4+}/Np^{3+}) = 1.4 \times 10^{-2}$ cm s^{-1} and $k_0(Np^{V}/Np^{IV}) = 2.1 \times 10^{-2}$ cm s^{-1}) compared to a VRFB ($k_0(V^{3+}/V^{2+}) = 1.75 \times 10^{-5}$ cm s^{-1} and $k_0(V^{V}/V^{IV}) = 7.5 \times 10^{-4}$ cm s^{-1}).

3.2.5.10. $Cu^{2+}/Cu//PbO_2/Pb^{2+}$

Pan et al. published a study on a Cu/Pb-based RFB in 2008.[243] In this battery, elemental copper deposited at the anode and PbO_2 at the cathode from a sulfuric acid solution during the charging process. The concentration of dissolved $CuSO_4$ was 0.6 M, which corresponds to a capacity of 32 Ah L^{-1}. The anode consisted of graphite, the cathode of $PbO_2/PbSO_4$. The metallic copper become detached during the deposition from the graphite-based anode and appeared as a suspension in the electrolyte circuit where it was reoxidized at the graphite electrode during discharging. In general, solids become detached from both electrodes. The charge/discharge cycles were performed at 20.8 mA cm^{-2}, and the Cu^{2+}/Cu reaction was found to contribute most to the losses of overvoltage. Only 16 % of the theoretical capacity has been used.

Anode : $Cu^{2+} + 2e^- \rightleftharpoons Cu$ $\quad \varphi_A^0 = +0.34$ V

Cathode : $PbSO_4 + 2H_2O \rightleftharpoons PbO_2 + 4H^+ + SO_4^{2-} + 2e^-$ $\quad \varphi_C^0 = +1.69$ V

Cell : $CuSO_4 + PbSO_4 + 2H_2O \rightleftharpoons Cu + PbO_2 + 2H_2SO_4$ $\quad \varphi_Z^0 = 1.35$ V

Galvanostatic charging for 2 h and then discharging to 1.1 V has been performed. Two main points are to be regarded as critical for the practical use of the battery. The formation of a suspension of metallic copper causes difficulties for the technical implementation of the system (pumps, reactor) and also causes losses from mass transport to the electrode. Furthermore, the overvoltage of hydrogen evolution on copper should be considered as a side reaction, which limits the power density.

3.2.5.11. $I_2/I^-//IO_3^-/I_2$

A single iodine-based battery was investigated by Skyllas-Kazacos and Milne:[244]

Anode : $I_2 + 2e^- \rightleftharpoons 2I^-$ $\quad \varphi_A^0 = +0.54$ V

Cathode : $\frac{1}{2} I_2 + 3H_2O \rightleftharpoons IO_3^- + 6H^+ + 5e^-$ $\quad \varphi_C^0 = +1.20$ V

Cell : $6I_2 + 6H_2O \rightleftharpoons 2IO_3^- + 12H^+ + 10I^-$ $\quad \varphi_Z^0 = 0.66$ V

Cyclovoltammetric studies and cell tests with a solution of 0.5 M I_2, 1.25 M KI, and 6 M HCl resulted in extensive formation of I_2, which led to blockage of the cell during the first charging process. The dissolution of I_2 as I_3^- requires a sufficient amount of I^-. However, I^- can undergo symproportionation with IO_3^- to recover I_2 in the positive half-cell. Iodine can then no longer be complexed as I_3^- in solution at the decreased content of I^-.

3.3. Inorganic Metal–Ligand Complexes/Protic Electrolytes

3.3.1. $Fe^{II/III}$-EDTA, Oxalates, Citrates, Triethanolamines

3.3.1.1. Br_2/Br^-

To shift the standard redox potential of Fe^{3+}/Fe^{2+} to more negative values, iron ions have been complexed with ethylenediaminetetraacetic acid (EDTA), oxalate, and citrate ligands.[245] This should also improve the charge transfer and minimize the diffusion of ions (cross-over) through the membrane. The Fe^{III}/Fe^{II}-EDTA complexes had a lower pH-dependent potential, improved reversibility, and better kinetics than the iron-citrate complex, but a low solubility of a maximum of 0.2 M in 1 M sodium acetate solution. The Fe-EDTA complexes were evaluated in the negative half-cell of an RFB combined with Br_2/Br^- in the positive half-cell at pH 6, the optimal pH value for the iron complex. The open-circuit voltage was 1.1 V, and the energy efficiency 80 % at 10 mA cm^{-2}. Lower voltage efficiencies were obtained in the case of Fe-citrate and Fe-oxalate.[246] An Fe-triethanolamine complex had a solubility of 0.4 M in 3 M NaOH with 2 M triethanolamine. As the proportion of organic complex rose, the overvoltage for hydrogen evolution at the carbon electrodes increased significantly. To study the behavior of a battery, the iron-based anode reaction has also been combined in a flow cell having a cathode reaction of Br_2/Br^- in 2 M NaBr. The cell voltage was about 2 V and the energy efficiency reached up to 70 % at 20 mA cm^{-2}, while the cycles were non-uniform. The disadvantage of this half-cell combination is that the neutral or basic medium is less suitable for the bromine reaction due to bromine hydrolysis.[246] Electrolytes in which the iron complexes have a higher solubility as well as optimum pH ranges for the Br_2/Br^- redox reaction are one of the challenges for future research on this type of RFB.[246]

3.3.2. Cr^{III}/Cr^{II}-EDTA//Cr^{V}/Cr^{III}-EDTA

A Cr-Cr-RFB (all-chromium RFB) based on 0.2 M Cr-(EDTA) at pH 4—7 has been reported.[247] The current efficiency was 100 % at a current density of 30 mA cm^{-2} and

at a 48% state of charge. However, the energy efficiency for a full charge/discharge process was only 7%. The same research group investigated the redox couples Cr^{III}/Cr^{II}-EDTA and Cr^{V}/Cr^{III}-EDTA in an electrochemical hydrogen cell (for the hydrogen cell see, for example, Ref. [261]).[248] The kinetics of the Cr^{III}/Cr^{II}-EDTA redox reactions at pH 4–7 was fast, with an outer-sphere reaction mechanism being suggested. However, the kinetics of Cr^{V}/Cr^{III}-EDTA was relatively unfavorable. The advantage of this system is the mildness of the media used, which may be important for the long-term stability of RFBs.

3.4. Inorganic–Organic Hybrid systems/Protic Electrolytes

3.4.1. Zinc/Polyaniline

A flow battery with a suspension of 150 $g\,L^{-1}$ polyaniline in 2 M $ZnCl_2$ and 2 M NH_4Cl was tested, whereby 32 cycles with 20 $mA\,cm^{-2}$ could be completed and a current efficiency of 97% could be achieved.[249] Zn^{2+}/Zn was used as an anodic redox couple and the pH value of the electrolyte solution was adjusted to 4.5. A microporous membrane was used as the separator. The advantage of a flow-through cell design with a polyaniline suspension is the higher reaction rate and capacity, since polyaniline reacts only on contact with the electrode surface. The cathode reaction was significantly slower than that of the anode reaction.

3.4.2. Bifunctional Systems V/Glyoxal and V/L-Cysteine

A bifunctional redox-flow battery composed of a combination of a VOFC with a cell for the electrosynthesis of organic materials with simultaneous energy storage was investigated for the oxidation of glyoxal to glyoxylic acid and L-cysteine to L-cysteic acid.[250,251] The systems consisted of a conventional VOFC, which used oxygen to oxidize V^{2+} to V^{3+} and water, and a second cell, where glyoxal was oxidized with water by V^{3+}. The vanadium solution was circulated through both cells. The electrosynthesis was proposed to act as the energy storage, while the energy consumption was to be performed by the VOFC. The use of Fe^{3+}/Fe^{2+} with separate oxidation by oxygen as the oxidant in the VOFC for bypassing the ORR has also been proposed.[251]

3.4.3. Quinone Derivatives as Redox Couples

3.4.3.1. Cd^{2+}/Cd//Chloranil

The combination of cadmium deposition with the electrochemical reaction of tetrachloro-*p*-benzoquinone (chloranil) in acidic medium (0.5 M H_2SO_4) was described in Ref. [252]. This is a hybrid RFB with a discharge voltage of about 1 V, 99% current efficiency, and 82% energy efficiency. However, the performance was stable for only about 100 cycles. The environmental acceptability of chlorinated aromatic compounds and the lower chemical stability of organic compounds compared to inorganic ones are obstacles to further work.

3.4.3.2. Pb^{2+}/Pb//Tiron

A similar idea to the Cd/chloranil-RFB was described in the investigation of a Pb/tiron-RFB.[253] Tiron (1,2-dihydroxybenzene-3,5-disulfonic acid) is a catechol derivative that undergoes rapid and reversible electrochemical redox reactions in acid. However, it also has a pH-dependent and complicated three-step reaction mechanism with proton transfer and structural changes, which may lead to unstable long-term behavior of the half cell. The Pb/tiron electrolyte consisted of 0.25 M tiron in 3 M H_2SO_4. The tiron half-cell was separated from the lead half-cell by NAFION. A battery with a low self-discharge achieved 82% energy efficiency, with the capacity decreasing continuously with the increasing number of cycles.

3.4.3.3. Anthraquinone/Bromine

A metal-free RFB based on 9,10-anthraquinone-2,7-disulfonic acid (AQDS) and Br_2/Br^- in H_2SO_4 or HBr was presented by Huskinson et al. in 2014.[254] Cyclovoltammetric studies revealed a high rate constant of 7.2×10^{-3} $cm\,s^{-1}$ for the reduction of AQDS with a diffusion coefficient of 3.8×10^{-6} $cm^2\,s^{-1}$. The electrochemical reversibility was at a theoretical value of 59 $mV\,n^{-1}$, with a peak difference of 34 mV, whereby the redox reaction proceeds in a two-electron step to $AQDSH_2$. The measured standard potential was around +0.213 V. DFT calculations showed a strong dependence of the standard potential on the position and number of additional hydroxy groups; for example, 1,8-dihydroxy-9,10-anthraquinone-2,7-disulfonic acid (DHAQDS) had an experimentally evaluated formal potential of +0.118 V. The electrochemical properties could be modified through targeted functionalization, so that higher cell voltages, higher solubility, and thus higher energy densities could be achieved. A cell with AQDS achieved a maximum power density of 3.3 $W\,cm^{-2}$ at a catalyst-free carbon electrode. Quinone derivatives seem to be attractive due to their availability from biological processes. However, they have relatively low temperature stability and solubility in aqueous media, as well as low chemical and electrochemical stability, which can result in low cycle lifetimes.

3.5. Dipolar Aprotic Electrolytes

Dipolar aprotic solvents have a wider electrochemical working potential range than protic electrolytes and can furthermore dissolve redox couples that are unstable in aqueous or protic media. It is, therefore, possible in principle to realize higher cell voltages by using an RFB with aprotic electrolyte solutions.[255] As metal ions in such a solution usually dissolve poorly and are mostly incompletely solvated, either redox-active organic molecules or metal–ligand complexes of the metals from the d and f series of the periodic table of elements are used. In principle, the general reaction scheme for the RFBs based on metal complexes does not differ significantly between the various metal complexes provided that no change in the metal coordination number

occurs. A change in the coordination sphere during a redox conversion in the battery cannot, however, be completely excluded.

$$\text{Anode}: \quad [ML_k]^x \rightleftharpoons [ML_k]^{x+z} + z\,e^-$$
$$\text{Cathode}: \quad [ML_k]^y + z\,e^- \rightleftharpoons [ML_k]^{y-z}$$

Here M is the central atom (metals such as Ru, Fe, V, etc.), L is the ligand (2,2′-bipyridine, β-diketonate etc.), k is the number of the ligands, z is the number of transferred electrons, and x and y are the charges of the complexes under consideration. Polar solvents, which have a high donor number and usually a high dielectric constant, are used as the solvent.[256] Acetonitrile is usually used as the solvent because of the high dissolution ability of salts and supporting electrolytes, the low viscosity at room temperature, and therefore increased conductivity. A few non-aqueous RFBs have been investigated with dimethyl sulfoxide, propylene carbonate, or dioxolane-based electrolytes. Supporting electrolyte salts are often added in the form of tetrafluoroborates or hexafluorophosphates to the aprotic solvents to provide ionic transport and conductivity.[16]

Microporous membranes were used as separators in the first studies. A few anion-exchange membranes (Neosepta AHA, Astom Japan, or Fumasep FAP4, Fumatech GmbH, Germany) have sufficient chemical resistance to the electrolyte solutions used. A review on separators for non-aqueous RFBs from previously published studies is given by Shin et al.[16]

For aprotic solvents, there is no common classification of the different redox couples in the electrochemical series because of a lack of definition of standard conditions and corresponding reference electrodes for non-aqueous electrolytes. In publications to date, however, the Ag/Ag^+ electrode has been widely used as a reference electrode in an appropriate solvent for organic electrolytes. The Li/Li^+ electrode is also frequently used as a reference for the evaluation of cathode materials for lithium-flow batteries. Both electrodes are, strictly speaking, pseudoreference electrodes.[257]

The previously published RFB systems with aprotic electrolyte solutions are usually presented only as half-cell studies. Most of these studies are carried out in so-called electrochemical hydrogen cells.[261] Different separators can be used in these experimental cells, and the electrochemical characteristics of the cell can be evaluated under stationary conditions. In a few tests, RFB cells with convective mass transport were used.

3.5.1. Metal–Ligand Complexes

3.5.1.1. 2,2′-Bipyridine Complexes

The first study of a redox-flow battery with ligand complexes was performed by Matsuda et al. on ruthenium–bipyridyl complexes.[258] A solution of tris(2,2′-bipyridyl)ruthenium(II) tetrafluoroborate ($[Ru(bpy)_3](BF_4)_2$) in acetonitrile was used as the electrolyte solution. Tetraethylammonium tetrafluoroborate (Et_4NBF_4) was added as a supporting electrolyte.

$$\text{Anode}: \quad [Ru(bpy)_3]^{2+} + e^- \rightleftharpoons [Ru(bpy)_3]^+ \qquad \phi_A = -1.60\,V \text{ versus } Ag/Ag^+$$
$$\text{Cathode}: \quad [Ru(bpy)_3]^{2+} \rightleftharpoons [Ru(bpy)_3]^{3+} + e^- \qquad \phi_C = +1.00\,V \text{ versus } Ag/Ag^+$$
$$\text{Cell}: \quad 2\,[Ru(bpy)_3]^{2+} \rightleftharpoons [Ru(bpy)_3]^{3+} + [Ru(bpy)_3]^+ \qquad \phi_Z = 2.60\,V$$

For this system, depending on the pore size of the separator used, overall current efficiencies of 50–80% have been demonstrated in the electrochemical hydrogen cell. A flow-through cell with an anion-exchange membrane (Neosepta ACH-45T) and a flow rate of about $0.18\,mL\,s^{-1}$ had an efficiency of approximately 40%. The maximum concentration of the $[Ru(bpy)_3](BF_4)_2$ complex in acetonitrile is about 0.2 M. However, an influence of the concentration on the efficiency of the cell could be detected. The maximum efficiency of the battery with Ru electrolytes was found at a concentration of 0.02–0.05 M. The cause for the low current efficiency was presumed to be the chemical instability of the Ru^+ complex.

The more-stable iron– and nickel–bipyridyl complexes were investigated by Kim et al.[259] Iron– and nickel–bipyridyl solutions in acetonitrile were combined in a cell to achieve a cell voltage of 2 V. A combination of $[Fe(bpy)_3](BF_4)_2$ as anolyte and $[Ni(bpy)_3](BF_4)_2$ as the catholyte had a higher efficiency than the $[Ru(bpy)_3](BF_4)_2$ system studied by Matsuda et al. Copper or molybdenum foils were used as cathodes.

$$\text{Anode}: \quad [Ni(bpy)_3]^{2+} + 2\,e^- \rightleftharpoons [Ni(bpy)_3] \qquad \phi_A = -1.70\,V \text{ versus } Ag/Ag^+$$
$$\text{Cathode}: \quad [Fe(bpy)_3]^{2+} \rightleftharpoons [Fe(bpy)_3]^{3+} + e^- \qquad \phi_C = +0.60\,V \text{ versus } Ag/Ag^+$$
$$\text{Cell}: \quad 2\,[Fe(bpy)_3]^{2+} + [Ni(bpy)_3]^{2+} \rightleftharpoons 2\,[Fe(bpy)_3]^{3+} + [Ni(bpy)_3] \qquad \phi_Z = 2.30\,V$$

The same system was examined by Mun et al. in a flow cell.[260] A carbon felt was used as the electrode and a FAP4 anion-exchange membrane (Fumatech GmbH, Germany) was used as the separator. The flow rate in this study was $65\,mL\,min^{-1}$. With a cell voltage of 2.2 V, the current efficiency and the energy efficiency amounted to 90.4% and 81.8%, respectively, in the first cycle. However, the capacity decreased to almost 40% after the fifth cycle because of diffusion of ions through the membrane.

3.5.1.2. Acetylacetonate Complexes

Ruthenium–acetylacetonate complexes ($Ru(acac)_3$) are, in contrast to bipyridyl complexes, chemically stable and have a higher solubility in acetonitrile,[261] as well as favorable reaction kinetics.[262] Morita et al.[263] determined the rate constants for the electrode reaction to be in the following order: $[Ru(bpy)_3]^{2+} < [Fe(bpy)_3]^{2+} < [Ru(acac)_3]$.

The ruthenium complex is neutral in its initial state, that is, uncharged. The central atom has the formal oxidation state of +3. During the charging process, the ruthenium changes its

oxidation state to +4 at the positive electrode or to +2 at the negative one.

Anode : $[Ru(acac)_3] + e^- \rightleftharpoons [Ru(acac)_3]^-$

Cathode : $[Ru(acac)_3] \rightleftharpoons [Ru(acac)_3]^+ + e^-$

Cell : $2\,[Ru(acac)_3] \rightleftharpoons [Ru(acac)_3]^+ + [Ru(bpy)_3]^-$

$\phi_Z = 1.77\,V$

For measurements in an electrochemical hydrogen cell, energy efficiencies were evaluated from the second charging cycle to be approximately 57%. Chakrabarti et al. studied the same system in a flow cell.[264] Porous graphite felts with an active surface of 5 cm × 5 cm were used as the electrodes. The flow rate was $0.36\,mL\,s^{-1}$. Two different concentrations of $[Ru(acac)_3]$ were chosen (0.02 M and 0.1 M). The applied current densities were $11.6\,mA\,cm^{-2}$ at charging and $2.1\,mA\,cm^{-2}$ at discharging (0.02 M); $58.1\,mA\,cm^{-2}$ at charging and $10.2\,mA\,cm^{-2}$ at discharging (0.1 M). The maximum discharge densities achieved were $1.4\,mW\,cm^{-2}$ or $7.2\,mW\,cm^{-2}$.

A uranium redox-flow battery based on uranyl acetylacetonate was proposed by Yamamura et al.[265] The solubilities in acetonitrile (ACN), propylene carbonate (PC), dimethylformamide (DMF), and dimethyl sulfoxide (DMSO) were determined for uranium complexes with differently substituted β-diketonate ligands. The highest solubility of more than 0.8 M was achieved for the complex with the fully fluorinated hexafluoro derivative $[UO_2(hfa)_2]$. The causes for the higher solubility of hexafluoroacetylacetonate complexes were presumed to be structural changes of the complex during solvation. The solvent molecules are pentacoordinated in the hexafluoro ligands. Depending on the polarity of the solvent, this coordination is stabilized by dipole–dipole interactions. Accordingly, the strongest interactions are to be expected with DMSO and DMF as solvent, since these solvents have a high donor number (DN) and a high dipole moment. Cyclovoltammetric measurements showed a dependence of the potential differences of U^V/U^{VI} and U^{III}/U^{IV} on the solvent. The potentials shifted to more negative potentials if the basicity of the ligand increased. The open-circuit voltage of batteries with acetylacetonate ligands ($[UO_2(acac)_2]$) was estimated to be more than 1.0 V and should increase further when the ligands are more basic. A uranyl RFB, however, has not yet been built, since the uranyl complex tends to dissociate. Yamamura et al. undertook further investigations to find more-stable ligands for the system.[266–268]

As with the uranium system, a high efficiency in the use of neptunium compounds is expected.[241,242,269] An efficiency of about 99% has been estimated by means of electrochemical calculations. In such a cell, a neptunium complex would be present in the anolyte and a dineptunyl complex with the transitions of Np^{3+} to Np^{4+} and NpO_2^{2+} to NpO_2^+ in the catholyte. As a result of the high radioactivity of Np, no attempts have been made under electrolyte convection mode.

The best characterized RFB system based on the organic solvent is the vanadium(III)-acetylacetonate system ([V(acac)$_3$] system).[270–274] The vanadium complex has three different oxidation states and thus two redox transitions which, depending on the solvent used, would make batteries with open-circuit voltages between 2.18 and 2.61 V possible.

Anode : $[V(acac)_3] + e^- \rightleftharpoons [V(acac)_3]^-$

$\phi_A = -1.72\,V$ versus Ag/Ag^+

Cathode : $[V(acac)_3] \rightleftharpoons [V(acac)_3]^+ + e^-$

$\phi_C = +0.46\,V$ versus Ag/Ag^+

Cell : $2\,[V(acac)_3] \rightleftharpoons [V(acac)_3]^+ + [V(acac)_3]^-$

$\phi_Z = 2.18\,V$

Shinkle et al. investigated $[V(acac)_3]$ in acetonitrile with tetraethylammonium tetrafluoroborate ($TEABF_4$) as a supporting electrolyte in a hydrogen cell.[272] A current efficiency of 70% and an energy efficiency of 35% were found for this system. The low current efficiency was obtained as a result of a side reaction of $[V(acac)_3]$, which takes place in the presence of small amounts of water remaining in the solutions:

$$[V(acac)_3] + H_2O \rightarrow [VO(acac)_2] + Hacac + H^+ + e^-$$

Oxidation of the vanadyl complex could also be detected by small amounts of residual oxygen in the solutions. The oxidation to a vanadyl complex could be partially reversed through addition of an excess of the acetylacetone ligand (Hacac) to the solvent, if the voltage was set to −2 V versus SCE (SCE: saturated calomel electrode).[275–277] Herr et al.[273] were able to confirm this experimentally. A mechanism for ligand exchange was described by Watanabe et al.[278] There are two different routes in this mechanism (Figure 10). In one, a ligand exchange can take place in $[V(acac)_3]$ (I*) and, in the other, in $[VO(acac)_2]$ (IV*). It is also assumed that the exchange of water in $[VO(acac)_2]$ is faster with Hacac and accordingly occurs preferentially.

Herr et al. investigated $[V(acac)_3]$ in other solvents in a flow cell, with and without convection of the electrolytes.[273,274] Therein different solvent mixtures, amongst other things, were investigated. A mixture of acetonitrile, 1,3-dioxolane, and dimethyl sulfoxide (ADD) resulted in a higher solubility of the $[V(acac)_3]$, whereby a theoretical maximum energy density equivalent to that in a VRFB could be achieved.

Zhang et al. investigated the effect of conducting salts. Tetrabutylammonium hexafluorophosphate ($TBAPF_6$) and the ionic liquid (IL) 1-ethyl-3-methylimidazolium hexafluorophosphate were used as additives to achieve a higher power in a hydrogen cell.[279] However, no higher current efficiency was achieved than when using $TBAPF_6$.

Chromium(III)-acetylacetonate [($Cr(acac)_3$)], with four redox transitions, offers a maximum voltage difference of 4.1 V.[280] Only two transitions have been realized experimentally in both half-cells, however:

Anode : $[Cr(acac)_3] + e^- \rightleftharpoons [Cr(acac)_3]^-$

$\phi_A = -2.20\,V$ versus Ag/Ag^+

Cathode : $[Cr(acac)_3] \rightleftharpoons [Cr(acac)_3]^+ + e^-$

$\phi_C = +1.20\,V$ versus Ag/Ag^+

Cell : $2\,[Cr(acac)_3] \rightleftharpoons [Cr(acac)_3]^+ + [Cr(acac)_3]^-$

$\phi_Z = 3.40\,V$

The current efficiency and the energy efficiency ranged from 53 to 58% and from 21 to 22% at 50% state of charge. The maximum solubility of $[Cr(acac)_3]$ was 0.4 M.

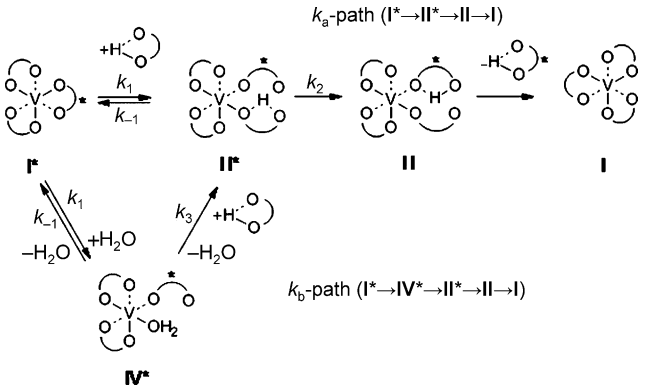

Figure 10. Possible mechanism for ligand exchange at $[V(acac)_3]$.[278]

$[Mn(acac)_3]$ has also been characterized in a hydrogen cell.[281] The two partial reactions offer a voltage difference of 1.1 V, which is the lowest value of all β-diketonate complexes.

$$\text{Anode}: \quad [Mn(acac)_3] + e^- \rightleftharpoons [Mn(acac)_3]^- \qquad \phi_A = -0.40\,\text{V versus Ag/Ag}^+$$

$$\text{Cathode}: \quad [Mn(acac)_3] \rightleftharpoons [Mn(acac)_3]^+ + e^- \qquad \phi_C = +0.70\,\text{V versus Ag/Ag}^+$$

$$\text{Cell}: \quad 2\,[Mn(acac)_3] \rightleftharpoons [Mn(acac)_3]^+ + [Mn(acac)_3]^- \qquad \phi_Z = 1.10\,\text{V}$$

The energetic efficiency of the cell was 21% and the maximum solubility in acetonitrile was approximately 0.6 M.

3.5.1.3. *N,N′-Ethane-1,2-diyldinitrilo–Co^{II} Complexes*

N,N′-Ethane-1,2-diyldinitrilo ligands have better complexing ability than the acetylacetonates for cobalt. Zhang et al. investigated (4*E*,4′*E*)-4,4′-(1,2-ethandiyldinitrilo)di(2-pentanonyl) complexes (acacen complexes) of cobalt in acetonitrile with $TBAPF_6$ as the conducting salt.[282] Both partial reactions showed quasireversible electron transitions in the cyclic voltammogram.

$$\text{Anode}: \quad [Co(acacen)] + e^- \rightleftharpoons [Co(acacen)]^- \qquad \phi_A = -2.20\,\text{V versus Ag/Ag}^+$$

$$\text{Cathode}: \quad [Co(acacen)] \rightleftharpoons [Co(acacen)]^+ + e^- \qquad \phi_C = -0.20\,\text{V versus Ag/Ag}^+$$

$$\text{Cell}: \quad 2\,[Co(acacen)] \rightleftharpoons [Co(acacen)]^+ + [Co(acacen)]^- \qquad \phi_Z = 2.00\,\text{V}$$

Current efficiency and energy efficiencies of up to 90% were achieved in a battery test in a hydrogen cell. As with the $[V(acac)_3]$ system, water and oxygen have a negative impact on the current efficiency.

3.5.1.4. *Other Ligands*

Cappillino et al. performed studies on vanadium complexes with so-called "non-innocent" ligands.[283] The term "non-innocent" refers to ligands that allow redox transitions of the ligand in addition to the usual transitions of the central atom, whereby higher energy densities are possible because of the additional electron transfers. Cappillino et al. examined the vanadium(IV) complex $[TEA]_2[V(mnt)_3]$ (mnt = $(NC)_2C_2S_2^{2-}$, Figure 11) in acetonitrile, and found different

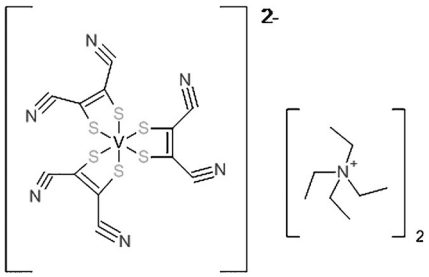

Figure 11. Structure of $[TEA]_2[V(mnt)_3]$.

electron transitions. For example, an electron is transferred to the central atom during the reduction of this complex, while an electron is removed from the ligand in the oxidation, however. Cyclovoltammetric studies revealed three redox transitions corresponding to the complex charges 4−/3−, 3−/2−, 2−/1−. The voltage difference (ΔE) between the external redox transitions was about 2.3 V. If the hydrocarbon chain of the ligand is extended from C_1 to C_8, the 4−/3− redox peak shifts to negative potentials, so that the voltage difference increases by 140 mV. Only the 3−/2− and 2−/1− transitions with an open-circuit voltage of 1.1 V were examined in a battery test. Compared to a battery without electrolyte convection, the efficiency fell from 45% to about 20–25% during the first 16 cycles. The current efficiency after the 5th cycle was approximately 90%. The theoretical maximum volumetric energy density in this case was 13 $Wh\,L^{-1}$. If, however, it is reduced to $[V(mnt)_3]^{4-}$, it can be doubled. The maximum solubility of the compound was about 0.9 $mol\,L^{-1}$.

3.5.2. *Redox-Active Organic Compounds*

Many natural redox reactions involve neat organic molecules that could theoretically be available in virtually unlimited quantities.[284] A first purely organic RFB has been built following this biomimetic principle.[285] The redox-active substance used for the cathode was 2,2,6,6-tetramethyl-1-piperidinyloxy (TEMPO) and for the anolyte *N*-methylphthalimide in acetonitrile. $NaClO_4$ was added as the conducting salt. Figure 12 shows the reaction equations of

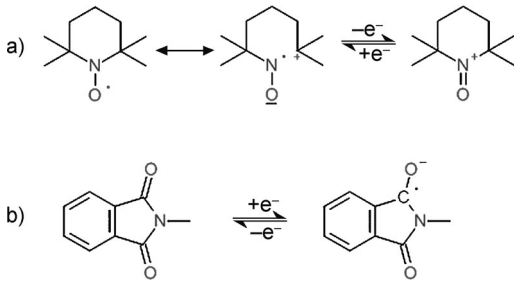

Figure 12. Redox mechanism of a) TEMPO and b) *N*-methylphthalimide.

the two compounds. Both redox transitions are reversible. The voltage difference is about 1.6 V. A current efficiency of about 90 % was achieved for the first 20 cycles in a battery test without electrolyte convection.

3.5.3. Li-Based RFBs

Two approaches are usually followed to combine the high power density of a lithium metal or lithium-ion battery with the advantages of a flow battery in terms of scalable capacity. In one of these approaches, electrolytes are generated on the base of suspensions of conventional lithium anodes and cathode materials. In the other, there are lithium systems with a metallic lithium anode, an ion-permeable protective layer, and an organic catholyte, in which the redox-active substance is dissolved. In the approach whereby suspensions are used, the challenge lies in the incorporation of electrically conductive additives, so that the percolation threshold of the electrolyte is exceeded. The addition of large amounts of electrically conductive carbon blacks, such as Ketjen Black, frequently results in the suspensions being viscous and difficult to pump. A bare lithium anode, however, like all lithium metal anodes, tends to undergo dendrite formation during metal deposition. Wang et al.[286] provide an extensive overview of the previously published lithium-flow batteries.

The first lithium-flow battery was investigated by Duduta et al.[287] The catholyte used was a suspension of $LiCoO_2$ (20 vol %; 10.2 M) with 1.5 % Ketjen Black. The anolyte used was a suspension of $Li_4Ti_5O_{12}$ (10 vol %; 2.3 M) with 2 % Ketjen Black. The battery was tested without electrolyte convection and achieved a current efficiency of 73 % and 80 % for the first two cycles. Suspension batteries, because of their solid content, usually have a higher theoretical energy density than those based on solutions. The authors expect energy densities of about 130–250 $Wh\,kg^{-1}$ in an optimized system.

Another organic lithium-ion RFB is based on two organic redox-active compounds: 2,5-di-*tert*-butyl-1,4-bis(2-methoxyethoxy)benzene (DBBB) and 2,3,6-trimethylquinoxaline. Both substances were dissolved together with $LiPF_6$ or $LiBF_4$ in propylene carbonate (PC).[288] DBBB is a stable air-insensitive compound and quinoxaline is soluble in PC up to 7 M, has a low mass, and two-electron transitions. Substitution of 2,3,6-trimethylquinoxaline, however, decreases the solubility and the theoretical energy density can be calculated to be around 12 $Wh\,L^{-1}$. The current efficiency and the energy efficiency amounted to 70 % and 37 %, respectively, for 30 cycles.

A hybrid organometallic RFB was studied by Wang et al.[289] The anthraquinone derivative 1,5-bis{2-[2-(2-methoxyethoxy)ethoxy]ethoxy}anthracene-9,10-dione (15D3GAQ) was used in polycarbonate as the catholyte. $LiPF_6$ was added as a conducting salt. The anode consisted of bare lithium. A microporous membrane was used as the separator (Celgard 3401, Celgard Inc. USA). Figure 13 shows the redox mechanism of 15D3GAQ.

Cyclovoltammetric investigations revealed two redox transitions, which are about 0.27 V apart. The battery operating without electrolyte convection was galvanostatically

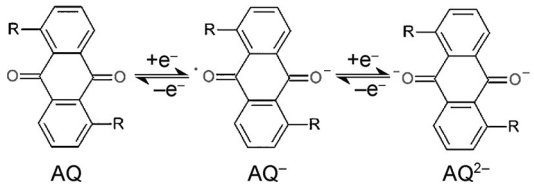

Figure 13. Redox mechanism of 15D3GAQ.[289]

charged and discharged between 1.8 and 2.8 V. Energetic efficiencies of 82 % were achieved over 9 cycles. The volumetric energy density was approximately 25 $Wh\,L^{-1}$.

To avoid the pumping of suspensions, Huang et al. proposed the concept of a lithium battery which is chemically charged and discharged with a redox mediator.[290] In contrast to a conventional RFB, the energy-storage material in this redox-flow lithium-ion battery (RFLB) is in a solid form in the tank and is circulated by an electrolyte with a dissolved mediator. For the cathode, a catholyte consisting of a mixture of ferrocene (Fc) and 1,1′-dibromoferrocene ($FcBr_2$) was investigated for the lithiation and delithiation, respectively. The two ferrocene species had a difference in redox potentials of about 400 mV. The value of the redox potentials of the two mediators is sufficient to function as a mediator for the lithiation and delithiation reaction of lithium iron phosphate ($LiFePO_4$). The feasibility of such a flow battery was investigated by the lithiation reaction of the catholyte in a half-cell. Metallic lithium was used as the counter electrode and lithium-conductive ceramic (Ohara Inc.) was used as the separator. The electrolyte consisted of a mixture of dimethyl carbonate (DMC) and ethylene carbonate (EC) with the addition of $LiPF_6$ as a conducting salt. $LiFePO_4$ has been proposed as a cathode material and lithium titanate ($Li_4Ti_5O_{12}$, LTO) as an anode material for a possible battery system. A mediator corresponding to the ferrocene for the anolyte is currently not known. A fixed lithium conductor should also be used as a separator in the overall system. A redox-mediated flow battery with a fixed energy-storage tank, in principle, offers the possibility of high theoretical energy densities that are, however, likely to be rarely achieved in practice. The differences in the redox potentials of these two cathode materials is about 1.65 V, in the vicinity of aqueous systems. The terminal voltage of the entire system will be significantly lower in the discharge case. The theoretical energy density of the solid lithium intercalation materials was decreased by using a liquid mediator. Other challenges are suitable ion conductors which have sufficient conductivity at room temperature and sufficiently stable organic redox couples as a mediator for the LTO.

A semi-aqueous semi-organic Li-RFB was described by Lu and Goodenough.[74,291] The battery contained an aqueous $[Fe(CN)_6]/[Fe(CN)_6]^{4-}$ solution as catholyte and $LiPF_6$ in an equal mixture of ethyl carbonate and diethyl carbonate as anolyte. The half-cells were separated by a $Li_{1+x+y}Al_xTi_{2-x}Si_yP_{3-y}O_{12}$ membrane from OHARA Inc. Four different flow rates were tested. The highest flow rate (0.41 $mL\,min^{-1}$) delivered a power density of 17 $mW\,cm^{-2}$. In the stationary test operation, this was only 58 % of the

maximum value. The current efficiency achieved was 99% after 20 cycles with an open circuit voltage of about 3.4 V.

In the second study by Lu and Goodenough, a Li/Fe^{3+} battery was initially tested[74] with $Fe(NO_3)_3$. Fe^{3+}/Fe^{2+} was excluded from further investigation because of the hydrolysis of Fe^{3+}, in which either FeO(OH) or $Fe(OH)_3$ are formed, depending on the pH value. Further studies were carried out with the already mentioned $K_3[Fe(CN)_6]$. When the concentration of $K_3[Fe(CN)_6]$ was increased from 0.01 M to 0.1 M, the charging and discharging curves shifted by a total of 50 mV to higher voltage values of 0.3 mAh. The capacity, however, increased to about 2.3 mAh. The capacity remained constant for at least 25 cycles at both concentrations. The battery with the lower concentration was able to complete 1000 charge/discharge cycles with no noticeable change in capacity. The current efficiency for 0.01 M $K_3[Fe(CN)_6]$ was 98.6% and for 0.1 M $K_3[Fe(CN)_6]$ it was 97.6%. A maximum discharge power density of 12.53 mW cm^{-2} was achieved with a 1 M iron solution.

Despite the Fe^{3+} hydrolysis observed by Lu and Goodenough, this electrolyte was used in the studies of Wang et al.[292] In these, the stability of the electrolyte was increased by additives, which kept the pH value constant and thus should inhibit hydrolysis. The addition of HCl enabled the battery to complete 20 charge/discharge cycles without significant changes. Furthermore, $(NH_4)_2S_2O_8$ was administered to the electrolyte as a strong oxidizing agent when, after discharging, Fe^{3+} was converted completely into Fe^{2+}. Thus, the cell could be repeatedly discharged by the addition of a stoichiometric amount of oxidant.

3.6. Ionic Liquids, Deep Eutectics, and Strong Eutectic Solvents

Despite the high electrochemical stability of dipolar aprotic solvents, and the resulting possibility of stabilizing large voltage differences in an electrolytic system, sufficient energy densities cannot usually be achieved in such systems. This is due to the low solubility of the redox-active substance. The necessary addition of conducting salt further restricts the maximum solubility,[293] such that the actually achievable energy density of such electrolyte systems is lower in the given temperature range than that expected from the solubility. The ionic conductivity of such electrolyte systems is dependent on the dissociation of the conducting salt as well as on the solubility. This is usually a few orders of magnitude lower in the dipolar solutions than in aqueous systems.

So-called "deep eutectics" of molten salts or "strongly eutectic solvents" or "ionic liquids" possess high ionic conductivity at room temperature and have, as long as they are water-free, high electrochemical stability over a wide potential range.[294] "Deep eutectics" are frequently referred to as "ionic liquids" of the first generation. They are usually formed by the trans-halogenation of a metal halide of the main III or I groups as well as V to VIII groups (usually aluminum chloride) with a halide salt of a voluminous and asymmetrically substituted organic cation (usually alkyl pyridinium or 1,3-dialkylimidazolium). "Deep eutectics" are usually hygroscopic and decompose in the presence of water.[295] A summary of redox reactions in "deep eutectics" can be found in Ref. [296].

"Strongly eutectic solvents" are also called "deep eutectic solvents" (DESs), but are mixtures of voluminous asymmetrically substituted organic cations with polyhydric alcohols.[297] These solvents are, therefore, a mixture of a solvent with an organic salt. The melting point of this mixture is lower than that of the salt due to a eutectic. An advantage of DESs is the low cost at which they can be produced. In addition, they are usually soluble in water and in some cases even biodegradable. According to Nkuku and LeSuer, oxygen has an undetectable effect on their electrochemical stability.[298] Therefore, inert conditions are not required for their practical application when used in the RFB. High concentrations of metal oxides of vanadium, chromium, iron, and zinc can be achieved in DES.[299]

Ionic liquids consist of a voluminous and asymmetrical substituted cation or anion usually also with an organic counterion. However, there are also ionic liquids, which include chlorides, bromides, or fluoroborates. A summary of the physical properties of ionic liquids can be found in Zhang et al.[300]

The first systems based on "deep eutectics" were produced by Katayama et al. on the basis of iron chlorides.[301] They investigated a "deep eutectic" of 1-ethyl-3-methylimidazolium chloride (EMICl) and $FeCl_3/FeCl_2$ by means of cyclic voltammetry. At 130 °C, the iron compounds undergo a reversible one-electron transition at about 0.1 V. A sodium chloride/sodium electrode has been proposed as a negative electrode, so that a cell voltage of around 2.15 V can be obtained.

Wen et al. built a similar system on a bromine cathode.[246] The anolyte consisted of 2 M NaBr and the catholyte of 0.2–0.5 M Fe^{III}-triethanolamine (TEA) in 3 M NaOH in a 0.4 M solution of NaCl. The studies showed that the redox transition Fe^{3+}-TEA/Fe^{2+}-TEA is electrochemically reversible, which requires high concentrations of TEA. The solubility of Fe^{3+}-TEA and Fe^{2+}-TEA was 0.6 M and 0.4 M, respectively. The concentration of NaOH also affects the cyclic voltammogram curves. Side reactions could be suppressed when the ratio of the NaOH and TEA concentrations is in the range of 1:6. The battery test showed a concentration of 0.4 M Fe^{3+}-TEA to be suitable. The energy efficiency was approximately 70% at a current density of 20 mA cm^{-2}.

"Deep eutectics" with redox centers that are liquid at room temperature have been described by Anderson et al.[302–304] $Cu(DEA)_6(EHN)_2$ (DEA = diethanolamine; EHN = 2-ethylhexanoate) was mentioned as an example. This deep eutectic showed a quasireversible redox transition in the ionic liquid 1-butyl-3-methylimidazolium hexafluorophosphate, and thus might be suitable for use in an RFB.

A copper-hybrid RFB based on a "deep eutectic" of copper(I) chloride was presented by Porterfield and Yoke.[305] A similar battery using a DES was investigated by Lloyd et al.[306] The eutectic solvent used, which has the common name ethaline, was produced from choline chloride and ethylene glycol in the proportion 1:2. The negative half-cell contained only ethaline and a bare copper electrode, and in

the positive half-cell anhydrous $CuCl_2$ was used in ethaline. The reaction took place at a Pt electrode.

$$\text{Anode}: \quad CuCl_4^{2-} + e^- \rightleftharpoons CuCl_3^{2-} + Cl^-$$
$$\text{Cathode}: \quad Cu + 3\,Cl^- \rightleftharpoons CuCl_3^{2-} + e^-$$
$$\text{Cell}: \quad Cu + CuCl_4^{2-} + 2\,Cl^- \rightleftharpoons 2\,CuCl_3^-$$

A current efficiency of 94.3% and an energy efficiency of 52.1% were achieved on charging/discharging with 10 mA cm^{-2}.

A variety of studies in ILs and DES for half-cell reactions have been carried out.[307–326] An RFB cell with an "ionic liquid" as the electrolyte was, however, first described by Noack et al. in his patent.[327] An example was given of a battery with 0.5 M VCl_3 in 2-hydroxyethylformiate without electrolyte convection. The battery was charged and discharged at 5 mA cm^{-2} between 0.5 V and 1.65 V over 9000 cycles, and a capacity of 20% was found after 5000 cycles.

3.7. Mediated Fuel Cells

These are H_2/O_2 fuel cells operated by means of mediated redox reactions. Two electrolyte solutions are fed in circulation through a cell, such that the redox couples are chemically regenerated externally by hydrogen and oxygen. In a chemical balance, hydrogen reacts with oxygen. Often, a focus is put on the slow reduction reaction of oxygen. The confusion with redox-flow batteries is easy to make with these systems. However, since such systems can only supply electrical energy, these are fuel cells. Such fuel-cell mediators are based, for example, on ions of Sn/Br, Sn/Fe Sn/V, Fe/Cu V V^{-1}, Ti/V, polyoxometalates, or biologically catalyzed systems.[328–334]

3.8. Photocatalytic Redox-Flow Batteries

The photolysis of water into hydrogen and oxygen is of particularly interest for the direct conversion of light into chemical energy.[335,336] However, the gaseous products can only be stored at relatively high expense, which is why Liu et al. studied the photo-electrochemical properties of V^V/V^{IV} in 2012, to save energy directly by reversible redox reactions in liquids.[337] Significant photocatalytic effects were observed in TiO_2 and TiO_2/WO_3 electrodes.

A cell (Figure 14) with a TiO_2 photoanode for the photocatalytic oxidation of VO^{2+} to VO_2^+ achieved a photocurrent yield of 12% at 350 nm, albeit at a very low V concentration of 0.01 M.[338] A TiO_2/WO_3 electrode at the same V concentration achieved slightly higher photocurrents.[339] Such systems are not strictly speaking batteries/accumulators, since it is not electrical energy that is converted into chemical energy, but rather radiant energy. However, the energy extraction is purely electrochemical and can be assisted by photolysis for energy storage, which produces photocatalytic RFBs.

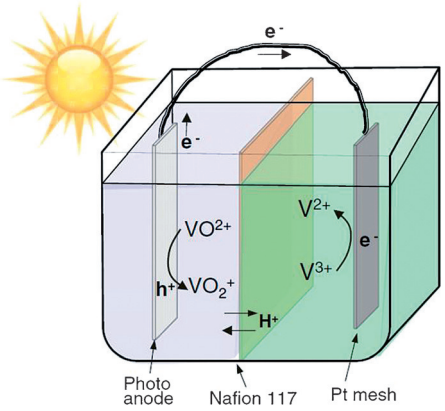

Figure 14. Schematic illustration of a photoelectrochemical vanadium cell (from Ref. [338]).

4. Battery Systems

For the safe and efficient operation of RFB storage, systems are needed which must meet the specific requirements of the battery chemistry and, where necessary, also the location of the battery and different procedural technical components (pumps, sensors and actuators, heat transfers, control and feedback control technology). The energy to operate the plant affects the energy efficiency of the battery, although a distinction is made between cell and system energy efficiency. The optimized and safe operation is guaranteed by a battery management system that can be based on different models.

The electrode surfaces and number of cells are adjusted in an RFB system to implement the desired power. As with fuel cells, individual cells are combined into a cell stack for this purpose, which is generally constructed from the conductive electrolytes in a different way from a fuel-cell stack and, for example, electrical shunt currents and local voltage differences must be taken into account. In accordance with the basic principle, the redox couples have to be pumped through cells, and this is usually done in parallel through all the individual cells of the plant.

The adjustment of the amount of energy is made by the choice of the volumes of electrolyte solutions, and this strongly depends on the concentration and potential of the redox couples, as well as the possible range of the charge state. For each system, a power to energy ratio can be chosen, a choice which is relatively open and limited downwards only by the dead volume of the cell stack. Free scaling is not possible in hybrid RFBs. The deposition of solids during the reaction, for example, with zinc-based RFBs, results in the amount of energy depending on the possibility of forming similar-scale layers and is limited by the half-cell structure of the deposition electrode. Normally, the energy storage devices are relatively inexpensive, in the €50–300 Wh^{-1} range, whereas the cost of the energy converter can be €1000–3500 kW^{-1}. As a result, systems with a highest possible energy/power ratio can be of interest to achieve low storage costs.

The state of charge in RFBs can be determined at any time during operation. Various methods are possible for this.

The method most often used is the measurement of the open-circuit voltage of a reference cell, which like all other cells is placed in parallel in the electrolyte circuits. From the Nernst Equation, the open-circuit voltage correlates with the concentration of the various oxidation states of the redox couples, whereby the state of charge can also be determined in the battery when the current is flowing. Other methods are redox-potential measurements in each circuit or spectrometric methods.

The temperature dependence of the reaction kinetics and the possibility of side reactions at elevated temperatures mean that more or less extensive heat management is often necessary. In addition, the electrolytes must not freeze, to prevent damage to the fluid-leading components. The loss of efficiency caused by the internal resistance of the cell stack occurs as a temperature increase first in the electrolyte and can be removed by heat exchangers.

A rebalancing of the electrolyte composition after a certain operating time is necessary due to the incomplete selectivity of membranes, pressure differentials, side reactions, and electromigration. In almost all battery types, the amount and concentration of the individual electrolytes change, which leads to a steadily increasing loss of capacity and can be restored by a mixing of the anolyte and catholyte. However, this is only possible with batteries in which the same electrolyte composition can be used in both half cells. Substantially more complex is the inversion of side reactions such as the formation of oxygen and hydrogen, or the reaction of the electrolyte with the diffusing atmospheric oxygen.

5. Summary

It is mainly V-, ZnBr-, and FeCr-RFBs that have so far been commercialized. These are also relatively familiar battery systems. These types of RFBs are currently in a phase of upscaling and market testing, although no real conclusions about the long-term stability of the batteries are yet possible. The reasons for the commercialization are, on the one hand, low storage costs (Zn, Br, Fe, Cr) and, on the other hand, the potentially long life (VRFB). Storage and conversion costs and shelf life largely determine the cost per unit of stored energy, which should be minimized through the use of RFBs.

The reactors, similar to fuel cells, are built almost identically for all different battery types, in some cases have catalysts, and therefore have similar costs. The conversion costs can be reduced by alternative materials and manufacturing methods or by better reaction kinetics. In this context, understanding the mechanisms of electrode reactions in various electrolytes and electrocatalysis will become more important in future research to obtain permanent high-capacity batteries. The overwhelming number of studies on redox couples has taken place in the past mainly on Hg, Pt, Au, and C electrodes. In almost all RFBs, corrosion problems with carbon-based electrodes caused by the use of strong negative or positive redox couples must be expected, and this is one of the greatest challenges.

The current high-performance polymer electrolyte membranes are a high cost factor, so that cheaper alternatives of ion-exchange membranes or microporous separators for VRFBs which have a high selectivity and high ion conductivity are being sought. Innovative low-temperature ceramic separators would allow completely new battery systems in which, for example, alkaline and alkaline earth metals could be used as the anode and, therefore, much higher energy densities could be achieved.

A factor which is often underestimated is the elastomers for seals, which need to be stable at high and low electrochemical potentials. Although there are fluoropolymers which have a high stability, at more than €1000 kW^{-1} they are far too expensive for RFBs. Ethylene-propylene-diene rubber-based materials are much cheaper, in the range of €10–50 kW^{-1}, but are not suitable for all systems and are difficult to use for the production of cell stacks because they can only be viably implemented by special manufacturing techniques such as multicomponent injection moulding. Applicable and cured-in-place sealing materials offer the potential for low development times and costs in virtually any cell sizes. However, the current material selection is very limited.

Except for organic RFBs, the energy-related costs are mainly dominated by the redox couples used. Although the elements can often be easily recycled, the electrolyte, in addition to its production cost, generally involves high capital and operating costs. Accordingly, the redox couples should be based on elements that are as abundant as possible so that the production costs for the entire energy storage medium are as low as possible. Inorganic solutions of light elements offer the largest potential for this, whereby solvent-free systems are conceivable, for example based on liquid alkali metals, which at the same time allow high energy densities. Bromine-based batteries have the great advantage of extremely rapid cathode reactions and high energy densities, but because of the toxicity of bromine are not regarded as acceptable.

How to cite: *Angew. Chem. Int. Ed.* **2015**, *54*, 9776–9809
Angew. Chem. **2015**, *127*, 9912–9947

[1] C. Bussar, M. Moos, R. Alvarez, P. Wolf, T. Thien, H. Chen, Z. Cai, M. Leuthold, D. U. Sauer, A. Moser, *8th International Renewable Energy Storage Conference and Exhibition (IRES 2013)* **2014**, *46*, 40–47.
[2] G. Pleßmann, M. Erdmann, M. Hlusiak, C. Breyer, *8th International Renewable Energy Storage Conference and Exhibition (IRES 2013)* **2014**, 46, 22–31.
[3] B. Dunn, H. Kamath, J.-M. Tarascon, *Science* **2011**, *334*, 928–935.
[4] T. M. I. Mahlia, T. J. Saktisahdan, A. Jannifar, M. H. Hasan, H. S. C. Matseelar, *Renewable Sustainable Energy Rev.* **2014**, *33*, 532–545.
[5] C. Budischak, D. Sewell, H. Thomson, L. Mach, D. E. Veron, W. Kempton, *J. Power Sources* **2013**, *225*, 60–74.
[6] Fraunhofer-Institut für Chemische Technologie, Pfinztal, Germany, 2014.
[7] W. Kangro, DE Patent 914264, **1949**.
[8] H. Pieper, Dissertation, Braunschweig, **1958**.
[9] W. Kangro, H. Pieper, *Electrochim. Acta* **1962**, *7*, 435–448.

[10] M. H. Chakrabarti, N. P. Brandon, S. A. Hajimolana, F. Tariq, V. Yufit, M. A. Hashim, M. A. Hussain, C. T. J. Low, P. V. Aravind, *J. Power Sources* **2014**, *253*, 150 – 166.
[11] X. Li, H. Zhang, Z. Mai, H. Zhang, I. Vankelecom, *Energy Environ. Sci.* **2011**, *4*, 1147 – 1160.
[12] B. Schwenzer, J. Zhang, S. Kim, L. Li, J. Liu, Z. Yang, *ChemSusChem* **2011**, *4*, 1388 – 1406.
[13] G. Kear, A. A. Shah, F. C. Walsh, *Int. J. Energy Res.* **2012**, *36*, 1105 – 1120.
[14] A. Parasuraman, T. M. Lim, C. Menictas, M. Skyllas-Kazacos, *Electrochim. Acta* **2013**, *101*, 27 – 40.
[15] P. Leung, X. Li, C. Ponce de León, L. Berlouis, C. T. J. Low, F. C. Walsh, *RSC Adv.* **2012**, *2*, 10125 – 10156.
[16] S.-H. Shin, S.-H. Yun, S.-H. Moon, *RSC Adv.* **2013**, *3*, 9095 – 9116.
[17] M. Skyllas-Kazacos, M. H. Chakrabarti, S. A. Hajimolana, F. S. Mjalli, M. Saleem, *J. Electrochem. Soc.* **2011**, *158*, R55 – R79.
[18] G. L. Soloveichik, *Annu. Rev. Chem. Biomol. Eng.* **2011**, *2*, 503 – 527.
[19] W. Wang, Q. Luo, B. Li, X. Wei, L. Li, Z. Yang, *Adv. Funct. Mater.* **2013**, *23*, 970 – 986.
[20] International Electrotechnical Commission (IEC) TC 21/TC 105 Joint Working Group 7 "Flow Batteries", 2014.
[21] T. Reddy, *Linden's Handbook of Batteries*, 4th ed., McGraw Hill Professional, New York, **2010**.
[22] M.-A. Goulet, E. Kjeang, *J. Power Sources* **2014**, *260*, 186 – 196.
[23] B. Sun, M. Skyllas-Kazakos, *Electrochim. Acta* **1991**, *36*, 513 – 517.
[24] B. Sun, M. Skyllas-Kazacos, *Electrochim. Acta* **1992**, *37*, 2459 – 2465.
[25] B. Sun, M. Skyllas-Kazacos, *Electrochim. Acta* **1992**, *37*, 1253 – 1260.
[26] C. Ponce-de-León, G. W. Reade, I. Whyte, S. E. Male, F. C. Walsh, *Electrochim. Acta* **2007**, *52*, 5815 – 5823.
[27] A. Z. Weber, M. M. Mench, J. P. Meyers, P. N. Ross, J. T. Gostick, Q. Liu, *J. Appl. Electrochem.* **2011**, *41*, 1137 – 1164.
[28] Y. Shao, X. Wang, M. Engelhard, C. Wang, S. Dai, J. Liu, Z. Yang, Y. Lin, *J. Power Sources* **2010**, *195*, 4375 – 4379.
[29] H. Q. Zhu, Y. M. Zhang, L. Yue, W. S. Li, G. L. Li, D. Shu, H. Y. Chen, *J. Power Sources* **2008**, *184*, 637 – 640.
[30] B. Caglar, P. Fischer, P. Kauranen, M. Karttunen, P. Elsner, *J. Power Sources* **2014**, *256*, 88 – 95.
[31] M. Park, Y.-J. Jung, J. Ryu, J. Cho, *J. Mater. Chem. A* **2014**, *2*, 15808 – 15815.
[32] Q. H. Liu, G. M. Grim, A. B. Papandrew, A. Turhan, T. A. Zawodzinski, M. M. Mench, *J. Electrochem. Soc.* **2012**, *159*, A1246 – A1252.
[33] Q. Xu, T. S. Zhao, P. K. Leung, *Appl. Energy* **2013**, *105*, 47 – 56.
[34] P. K. Leung, C. Ponce-de-León, C. T. J. Low, A. A. Shah, F. C. Walsh, *J. Power Sources* **2011**, *196*, 5174 – 5185.
[35] P. K. Leung, C. Ponce de León, C. T. J. Low, F. C. Walsh, *Electrochim. Acta* **2011**, *56*, 2145 – 2153.
[36] M. Rychcik, M. Skyllas-Kazacos, *J. Power Sources* **1987**, *19*, 45 – 54.
[37] X. L. Wei, L. Y. Li, Q. T. Luo, Z. M. Nie, W. Wang, B. Li, G. G. Xia, E. Miller, J. Chambers, Z. G. Yang, *J. Power Sources* **2012**, *218*, 39 – 45.
[38] T. Mohammadi, M. Skylla-Kazacoz, *J. Power Sources* **1995**, *56*, 91 – 96.
[39] T. Mohammadi, M. Skyllas-Kazacos, *J. Membr. Sci.* **1995**, *98*, 77 – 87.
[40] B. Tian, C. W. Yan, F. H. Wang, *J. Membr. Sci.* **2004**, *234*, 51 – 54.
[41] X. Teng, J. Dai, J. Su, Y. Zhu, H. Liu, Z. Song, *J. Power Sources* **2013**, *240*, 131 – 139.
[42] W. Wei, H. Zhang, X. Li, Z. Mai, H. Zhang, *J. Power Sources* **2012**, *208*, 421 – 425.
[43] S. Loeb, S. Sourirajan, Report No. 6060, University of California **1960**.
[44] H. Zhang, H. Zhang, X. Li, Z. Mai, J. Zhang, *Energy Environ. Sci.* **2011**, *4*, 1676 – 1679.
[45] W. Xu, X. Li, J. Cao, Z. Yuan, H. Zhang, *RSC Adv.* **2014**, *4*, 40400 – 40406.
[46] W. P. Wei, H. M. Zhang, X. F. Li, H. Z. Zhang, Y. Li, I. Vankelecom, *Phys. Chem. Chem. Phys.* **2013**, *15*, 1766 – 1771.
[47] H. Zhang, H. Zhang, X. Li, Z. Mai, W. Wei, *Energy Environ. Sci.* **2012**, *5*, 6299 – 6303.
[48] H. L. Yeager, A. Steck, *J. Electrochem. Soc.* **1981**, *128*, 1880 – 1884.
[49] M. Vijayakumar, M. S. Bhuvaneswari, P. Nichimuthu, B. Schwenzer, S. Kim, Z. Yang, J. Liu, G. L. Graff, S. Thevuthasan, J. Hu, *J. Membr. Sci.* **2011**, *366*, 325 – 334.
[50] H. Z. Zhang, C. Ding, J. Y. Cao, W. Xu, X. F. Li, H. M. Zhang, *J. Mater. Chem. A* **2014**, *2*, 9524 – 9531.
[51] S. Kim, J. Yan, B. Schwenzer, J. Zhang, L. Li, J. Liu, Z. Yang, M. A. Hickner, *Electrochem. Commun.* **2010**, *12*, 1650 – 1653.
[52] J. Li, Y. Zhang, S. Zhang, X. Huang, L. Wang, *Polym. Adv. Technol.* **2014**, ***25***, 1610 – 1615.
[53] D. Düerkop, H. Widdecke, T. Turek, U. Kunz, A. R. dos Santos, *Conference Proceedings of the International Flow Battery Forum* **2014**.
[54] S. Kim, T. B. Tighe, B. Schwenzer, J. Yan, J. Zhang, J. Liu, Z. Yang, M. A. Hickner, *J. Appl. Electrochem.* **2011**, *41*, 1201 – 1213.
[55] D. Chen, M. A. Hickner, *Phys. Chem. Chem. Phys.* **2013**, *15*, 11299 – 11305.
[56] S.-G. Park, N.-S. Kwak, C. W. Hwang, H.-M. Park, T. S. Hwang, *J. Membr. Sci* **2014**, *468*, 98 – 106.
[57] D. Chen, M. A. Hickner, E. Agar, C. Kumbur, *Electrochem. Commun.* **2013**, *26*, 37 – 40.
[58] D. Xing, S. Zhang, C. Yin, B. Zhang, X. Jian, *J. Membr. Sci.* **2010**, *354*, 68 – 73.
[59] S. Zhang, C. Yin, D. Xing, D. Yang, X. Jian, *J. Membr. Sci.* **2010**, *363*, 243 – 249.
[60] B. Zhang, S. Zhang, D. Xing, R. Han, C. Yin, X. Jian, *J. Power Sources* **2012**, *217*, 296 – 302.
[61] S. Zhang, B. Zhang, G. Zhao, X. Jian, *J. Mater. Chem. A* **2014**, *2*, 3083 – 3091.
[62] B. Zhang, S. Zhang, D. Xiang, C. Yin, R. Han, X. Jian, *Acta Chim. Sin. (Engl. Ed.)* **2011**, *69*, 2583 – 2588.
[63] J. Ma, Y. Wang, J. Peng, J. Qiu, L. Xu, J. Li, M. Zhai, *J. Membr. Sci.* **2012**, *419*, 1 – 8.
[64] J. Yuan, C. Yu, J. Peng, Y. Wang, J. Ma, J. Qiu, J. Li, M. Zhai, *J. Polym. Sci. Part A* **2013**, *51*, 5194 – 5202.
[65] G. Hu, Y. Wang, J. Ma, J. Qiu, J. Peng, J. Li, M. Zhai, *J. Membr. Sci.* **2012**, *407*, 184 – 192.
[66] J. Qiu, J. Zhang, J. Chen, J. Peng, L. Xu, M. Zhai, J. Li, G. Wie, *J. Membr. Sci.* **2009**, *334*, 9 – 15.
[67] J. Qiu, M. Zhai, J. Chen, Y. Wang, J. Peng, L. Xu, J. Li, G. Wei, *J. Membr. Sci.* **2009**, *342*, 215 – 220.
[68] X. Teng, Y. Zhao, J. Xi, Z. Wu, X. Qiu, L. Chen, *J. Power Sources* **2009**, *189*, 1240 – 1246.
[69] J. Xi, Z. Wu, X. Qiu, L. Chen, *J. Power Sources* **2007**, *166*, 531 – 536.
[70] J. Kim, J.-D. Jeon, S.-Y. Kwak, *Electrochem. Commun.* **2014**, *38*, 68 – 70.
[71] D. Chen, S. Wang, M. Xiao, D. Han, Y. Meng, *J. Power Sources* **2010**, *195*, 7701 – 7708.
[72] J. Pan, S. Wang, M. Xiao, M. Hickner, Y. Meng, *J. Membr. Sci.* **2013**, *443*, 19 – 27.
[73] J.-G. Kim, S.-H. Lee, S.-I. Choi, C.-S. Jin, J.-C. Kim, C.-H. Ryu, G.-J. Hwang, *J. Ind. Eng. Chem.* **2010**, *16*, 756 – 762.
[74] Y. Lu, J. B. Goodenough, Y. Kim, *J. Am. Chem. Soc.* **2011**, *133*, 5756 – 5759.

[75] W. A. Braff, M. Z. Bazant, C. R. Buie, *Nat. Commun.* **2013**, *4*, 2346.
[76] R. Ferrigno, A. D. Stroock, T. D. Clark, M. Mayer, G. M. Whitesides, *J. Am. Chem. Soc.* **2002**, *124*, 12930 – 12931.
[77] R. Ferrigno, A. D. Stroock, T. D. Clark, M. Mayer, G. M. Whitesides, *J. Am. Chem. Soc.* **2003**, *125*, 2014 – 2014.
[78] A. J. Bard, R. Parsons, J. Jordan, *Standard Potentials in Aqueous Solution*, CRC, New York, **1985**.
[79] C. S. Bradley, US-Patent 312802, **1885**.
[80] H. S. Lim, *J. Electrochem. Soc.* **1977**, *124*, 1154 – 1157.
[81] S. Barnartt, D. A. Forejt, *J. Electrochem. Soc.* **1964**, *111*, 1201 – 1204.
[82] R. Rich, *Inorganic Reactions in Water*, Springer, Berlin, Heidelberg, **2007**.
[83] P. Singh, K. White, A. J. Parker, *J. Power Sources* **1983**, *10*, 309 – 318.
[84] K. J. Cathro, *J. Power Sources* **1988**, *23*, 365 – 383.
[85] S. V. M. Mastragostinos, *Electrochim. Acta* **1983**, *28*, 501 – 505.
[86] K. J. Cathro, K. Cedzynska, D. C. Constable, P. M. Hoobin, *J. Power Sources* **1986**, *18*, 349 – 370.
[87] P. M. Hoobin, K. J. Cathro, J. O. Niere, *J. Appl. Electrochem.* **1989**, *19*, 943 – 945.
[88] G. Bauer, J. Drobits, C. Fabjan, H. Mikosch, P. Schuster, *J. Electroanal. Chem.* **1997**, *427*, 123 – 128.
[89] W. Kautek, A. Conradi, C. Fabjan, G. Bauer, *Electrochim. Acta* **2001**, *47*, 815 – 823.
[90] D. J. Eustace, *J. Electrochem. Soc.* **1980**, *127*, 528 – 532.
[91] B. E. Conway, Y. Phillips, S. Y. Qian, *J. Chem. Soc. Faraday Trans.* **1995**, *91*, 283 – 293.
[92] S. Ferro, C. Orsan, A. de Battisti, *J. Appl. Electrochem.* **2005**, *35*, 273 – 278.
[93] M. Mastragostino, C. Gramellini, *Electrochim. Acta* **1985**, *30*, 373 – 380.
[94] I. Vogel, A. Möbius, *Electrochim. Acta* **1991**, *36*, 1403 – 1408.
[95] X. Rui, A. Parasuraman, W. Liu, D. H. Sim, H. H. Hng, Q. Yan, T. M. Lim, M. Skyllas-Kazacos, *Carbon* **2013**, *64*, 464 – 471.
[96] X. Rui, M. O. Oo, D. H. Sim, S. c. Raghu, Q. Yan, T. M. Lim, M. Skyllas-Kazacos, *Electrochim. Acta* **2012**, *85*, 175 – 181.
[97] "On the Kinetics and Mechanism of Bromine/Bromide Redox Electrodes": C. Fabjan, G. Hirss, *DECHEMA Monogr.* **1986**, *102*, 149 – 161.
[98] J.-D. Jeon, H. S. Yang, J. Shim, H. S. Kim, J. H. Yang, *Electrochim. Acta* **2014**, *127*, 397 – 402.
[99] F. Beck, P. Rüetschi, *Electrochim. Acta* **2000**, *45*, 2467 – 2482.
[100] J. Jorné, J. T. Kim, D. Kralik, *J. Appl. Electrochem.* **1979**, *9*, 573 – 579.
[101] L. Zhang, Q. Lai, J. Zhang, H. Zhang, *ChemSusChem* **2012**, *5*, 867 – 869.
[102] C. Tang, D. Zhou, *Electrochim. Acta* **2012**, *65*, 179 – 184.
[103] R. L. Clarke, B. Dougherty, S. Harrison, P. J. Millington, S. Mohanta, US-Patent 2004/0202925A1, **2004**.
[104] R. L. Clarke, B. J. Dougherty, S. Harrison, J. P. Millington, S. Mohanta, US-Patent 2006/0063065A1, **2006**.
[105] R. L. Clarke, B. Dougherty, S. Harrison, P. J. Millington, S. Mohanta, US-Patent 2004/0197651A1, **2004**.
[106] R. L. Clarke, B. Dougherty, S. Harrison, P. J. Millington, S. Mohanta, US-Patent 2004/0197649A1, **2004**.
[107] G. Nikiforidis, L. Berlouis, D. Hall, D. Hodgson, *Electrochim. Acta* **2014**, *125*, 176 – 182.
[108] G. Nikiforidis, L. Berlouis, D. Hall, D. Hodgson, *Electrochim. Acta* **2014**, *115*, 621 – 629.
[109] G. Nikiforidis, L. Berlouis, D. Hall, D. Hodgson, *J. Power Sources* **2013**, *243*, 691 – 698.
[110] P. Modiba, A. M. Crouch, *J. Appl. Electrochem.* **2008**, *38*, 1293 – 1299.
[111] A. Paulenova, S. E. Creager, J. D. Navratil, Y. Wei, *J. Power Sources* **2002**, *109*, 431 – 438.
[112] Y. Wei, B. Fang, T. Arai, M. Kumagai, *J. Appl. Electrochem.* **2005**, *35*, 561 – 566.
[113] L. Jelinek, Y. Wei, K. Mikio, *J. Rare Earths* **2006**, *24*, 257 – 263.
[114] P. K. Leung, C. Ponce de León, F. C. Walsh, *Electrochem. Commun.* **2011**, *13*, 770 – 773.
[115] See Ref. [34].
[116] L. H. Thaller, *Proc. 9th Intersoc. Energy Conv. Eng. Conf.*, San Francisco, CA **1974**; NASA TM X-71540, p. 924 **1974**.
[117] L. H. Thaller, US 3,996,064, **1975**.
[118] *Redox flow cell development and demonstration project*, calendar year 1976, NASA TM-73873, **1977**.
[119] N. H. Hagedorn, *NASA Redox Storage System Development Project—Final Report*, NASA TM-83677 **1984**.
[120] M. A. Reid, R. F. Gahn, *Factors affecting the open-circuit voltage and electrode kinetics of some iron/titanium redox flow cells*, NASA TMX-73669 **1977**.
[121] *Redox flow cell development and demonstration project*, calendar year 1977, NASA TM-79067, **1979**.
[122] L. H. Thaller, *Redox Flow Cell Energy Storage Systems*, NASA TM-79143 **1979**.
[123] D. K. Stalnaker, J. C. Acevedo, *An electrochemical rebalance cell for Redox systems*, NASA TM-83363 **1983**.
[124] L. H. Thaller, *Recent advances in redox flow cell storage systems*, NASA TM-79186 **1979**.
[125] A. W. Nice, *NASA Redox system development project status*, NASA TM-82665 **1981**.
[126] V. Jalan, H. Stark, J. Giner, *Requirements for optimization of electrodes and electrolyte for the iron/chromium Redox flow cell*, NASA CR-165218 **1981**.
[127] R. F. Gahn, J. Charleston, J. S. Ling, M. A. Reid, *Performance of advanced chromium electrodes for the NASA Redox Energy Storage System*, NASA TM-82724 **1981**.
[128] J. D. Giner, K. Cahill, *Advanced screening of electrode couples*, NASA CR-159738 **1980**.
[129] J. D. Giner, K. Cahill, US 4,270,984, **1979**.
[130] C. Y. Yang, *J. Appl. Electrochem.* **1982**, *12*, 425 – 434.
[131] *NASA redox storage system development project*, calendar year 1982, NASA TM-83469, **1983**.
[132] M. A. Reid, D. A. Johnson, *Chemical and electrochemical behavior of the Cr^{III}/Cr(II) half cell in the NASA Redox Energy Storage System*, NASA TM-82913 **1982**.
[133] G. Stevens, *Spectrophotometric analysis of aqueous mixtures of some chromium (III) complexes*, NASA CR-172999 **1983**.
[134] D. A. Johnson, M. A. Reid, *J. Electrochem. Soc.* **1985**, *132*, 1058 – 1062.
[135] R. F. Gahn, N. H. Hagedorn, J. S. Ling, *Single cell performance studies on the Fe/Cr Redox Energy Storage System using mixed reactant solutions at elevated temperature*, NASA TM-83385 **1983**.
[136] Ext. Abstr. No. 19, Fall Meeting, N. H. Hagedorn, *Electrochem. Soc.* **1983**, 30.
[137] N. H. Hagedorn, *NASA Redox Project status summary*, NASA TM-83401, **1983**.
[138] *NASA redox storage system development project* - Calendar Year 1981, NASA TM-83087, **1983**.
[139] R. F. Gahn, N. H. Hagedorn, J. A. Johnson, *Cycling Performance of the Iron-Chromium Redox Energy Storage System*, NASA TM-87034, **1985**.
[140] A. Wakabayashi, Y. Umehara, Y. Okada, T. Ichimura, *3rd Int. Conf. On Batteries For Utility Energy Storage*, NEDO, Kobe, Japan **1991**.
[141] A. Heintz, C. Illenberger, *Int. Symposium Progress Membr. Sci. Technol.* **1996**, *113*, 175 – 181.
[142] A. Swartbooi, 2nd CSIR Biennial Conference, Pretoria, South Africa, **2008**, pp. 4.
[143] M. Skyllas-Kazacos, M. Rychcik, R. G. Robins, A. G. Fane, M. A. Green, *J. Electrochem. Soc.* **1986**, *133*, 1057 – 1058.

[144] J. J. Lingane, *J. Am. Chem. Soc.* **1945**, *67*, 182 – 188.
[145] D. G. Davis, Jr., *Talanta* **1960**, *3*, 335 – 345.
[146] Y. Israel, L. Meites, *J. Electroanal. Chem.* **1964**, *8*, 99 – 119.
[147] E. Sum, M. Skyllas-Kazacos, *J. Power Sources* **1985**, *15*, 179 – 190.
[148] E. Sum, M. Rychcik, M. Skyllas-Kazacos, *J. Power Sources* **1985**, *16*, 85 – 95.
[149] Z. González, A. Sánchez, C. Blanco, M. Granda, R. Menéndez, R. Santamaría, *Electrochem. Commun.* **2011**, *13*, 1379 – 1382.
[150] C. Madic, G. M. Begun, R. L. Hahn, J. P. Launay, W. E. Thiessen, *Inorg. Chem.* **1984**, *23(4)*, 469 – 476.
[151] N. Kausar, R. Howe, M. Skyllas-Kazacos, *J. Appl. Electrochem.* **2001**, *31*, 1327 – 1332.
[152] X. Lu, *Electrochim. Acta* **2001**, *46*, 4281 – 4287.
[153] M. Vijayakumar, L. Li, G. Graff, J. Liu, H. Zhang, Z. Yang, J. Z. Hu, *J. Power Sources* **2011**, *196*, 3669 – 3672.
[154] M. Vijayakumar, S. D. Burton, C. Huang, L. Li, Z. Yang, G. L. Graff, J. Liu, J. Hu, M. Skyllas-Kazacos, *J. Power Sources* **2010**, *195*, 7709 – 7717.
[155] X. Wu, J. Wang, S. Liu, X. Wu, S. Li, *Electrochim. Acta* **2011**, *56*, 10197 – 10203.
[156] D. N. Buckley, X. Gao, R. P. Lynch, N. Quill, M. J. Leahy, *J. Electrochem. Soc.* **2014**, *161*, A524 – A534.
[157] C. Ding, H. Zhang, X. Li, T. Liu, F. Xing, *J. Phys. Chem. Lett.* **2013**, *4*, 1281 – 1294.
[158] M. Skyllas-Kazacos, *Electrochem. Solid-State Lett.* **1999**, *2*, 121 – 122.
[159] G. Wang, J. Chen, X. Wang, J. Tian, H. Kang, X. Zhu, Y. Zhang, X. Liu, R. Wang, *J. Electroanal. Chem.* **2013**, *709*, 31 – 38.
[160] L. Zhang, H. Zhang, Q. Lai, X. Li, Y. Cheng, *J. Power Sources* **2013**, *227*, 41 – 47.
[161] M. Vijayakumar, W. Wang, Z. Nie, V. Sprenkle, J. Hu, *J. Power Sources* **2013**, *241*, 173 – 177.
[162] J. G. Lee, S. J. Park, Y. I. Cho, Y. G. Shul, *RSC Adv* **2013**, *3*, 21347 – 21351.
[163] L. Li, S. Kim, W. Wang, M. Vijayakumar, Z. Nie, B. Chen, J. Zhang, G. Xia, J. Hu, G. Graff, et al., *Adv. Energy Mater.* **2011**, *1*, 394 – 400.
[164] M. Vijayakumar, L. Li, Z. Nie, Z. Yang, J. Hu, *Phys. Chem. Chem. Phys.* **2012**, *14*, 10233 – 10242.
[165] M. Skyllas-Kazacos, F. Grossmith, *J. Electrochem. Soc.* **1987**, *134*, 2950 – 2953.
[166] M. Kazacos, R. J. C. Mcdermott, M. Skyllas-Kazacos, WO 1989005363A1, **1989**.
[167] M. Kazacos, M. Cheng, M. Skyllas-Kazacos, *J. Appl. Electrochem.* **1990**, *20*, 463 – 467.
[168] M. Kazacos, M. Skyllas-Kazacos, *J. Electrochem. Soc.* **1989**, *136*, 2759 – 2760.
[169] P. Chen, R. L. McCreery, *Anal. Chem.* **1996**, *68*, 3958 – 3965.
[170] M. Gattrell, J. Qian, C. Stewart, P. Graham, B. MacDougall, *Electrochim. Acta* **2005**, *51*, 395 – 407.
[171] W. Wang, X. Fan, J. Liu, C. Yan, C. Zeng, *J. Power Sources* **2014**, *261*, 212 – 220.
[172] H. Liu, Q. Xu, C. Yan, *Electrochem. Commun.* **2013**, *28*, 58 – 62.
[173] W. Wang, S. Kim, B. Chen, Z. Nie, J. Zhang, G.-G. Xia, L. Li, Z. Yang, *Energy Environ. Sci.* **2011**, *4*, 4068 – 4073.
[174] W. Wang, Z. Nie, B. Chen, F. Chen, Q. Luo, X. Wei, G.-G. Xia, M. Skyllas-Kazacos, L. Li, Z. Yang, *Adv. Energy Mater.* **2012**, *2*, 487 – 493.
[175] B. Li, L. Li, W. Wang, Z. Nie, B. Chen, X. Wei, Q. Luo, Z. Yang, V. Sprenkle, *J. Power Sources* **2013**, *229*, 1 – 5.
[176] W. Wang, L. Li, Z. Nie, B. Chen, Q. Luo, Y. Shao, X. Wei, F. Chen, G.-G. Xia, Z. Yang, *J. Power Sources* **2012**, *216*, 99 – 103.
[177] M. Skyllas-Kazacos, *J. Power Sources* **2003**, *124*, 299 – 302.
[178] M. Skyllas-Kazacos, *New vanadium bromide redox fuel cell*, presented at EuroPES2004, Greece. **2004**.
[179] H. Vafiadis, M. Skyllas-Kazacos, *J. Membr. Sci.* **2006**, *279*, 394 – 402.
[180] G. Poon, A. Parasuraman, T. M. Lim, M. Skyllas-Kazacos, *Electrochim. Acta* **2013**, *107*, 388 – 396.
[181] H. Kaneko, N. Akira, N. Ken, S. Kanji, N. Masato, US. US5318865, **1994**.
[182] C. Menictas, M. Skyllas-Kazacos, *Final Report, SERDF grant, New South Wales Office of Energy*, Australia, **1997**.
[183] C. Menictas, M. Skyllas-Kazacos, *J. Appl. Electrochem.* **2011**, *41*, 1223 – 1232.
[184] J. Noack, C. Cremers, K. Pinkwart, J. Tuebke, *218th The Electrochemical Society Meeting*, Las Vegas, **2010**.
[185] S. S. Hosseiny, M. Saakes, M. Wessling, *Electrochem. Commun.* **2011**, *13*, 751 – 754.
[186] D. Palminteri, Diplomarbeit, Hochschule für Technik und Wirtschaft Karlsruhe, **2011**.
[187] J. Noack, T. Berger, J. Tübke, K. Pinkwart, WO 2013007817A1, **2013**.
[188] B. Fang, S. Iwasa, Y. Wei, T. Arai, M. Kumagai, *Electrochim. Acta* **2002**, *47*, 3971 – 3976.
[189] Y. Liu, X. Xia, H. Liu, *J. Power Sources* **2004**, *130*, 299 – 305.
[190] C. Berger, R. M. Lurie, *The Electrochemical Society Meeting*, USA, **1961**.
[191] W. Glass, G. H. Boyle, *Fuel Cell Systems*, *Vol. 47*, Am. Chem. Soc. Washington, DC, **1969**, pp. 203 – 220.
[192] J. F. McElroy, *Hydrogen/Halogen Energy Storage Systems Development*, Phase one summary report, General Electric Company, Wilmington, USA, **1977**.
[193] R. S. Yeo, D.-T. Chin, *J. Electrochem. Soc.* **1980**, *127*, 549 – 555.
[194] G. G. Barna, S. N. Frank, T. H. Teherani, L. D. Weedon, *J. Electrochem. Soc.* **1984**, *131*, 1973 – 1980.
[195] J. A. Kosek, A. B. Laconti, *Proceedings of the Space Electrochemical Research and Technology Conference* **1988**, *22*, 293 – 300.
[196] C. F. H. Kronberger, *Monatsh. Chem.* **1990**, *121*, 979 – 989.
[197] V. Livshits, A. Ulus, E. Peled, *Electrochem. Commun.* **2006**, *8*, 1358 – 1362.
[198] K. T. Cho, P. Ridgway, A. Z. Weber, S. Haussener, V. Battaglia, V. Srinivasan, *J. Electrochem. Soc.* **2012**, *159*, A1806 – A1815.
[199] H. Kreutzer, V. Yarlagadda, T. van Nguyen, *J. Electrochem. Soc.* **2012**, *159*, F331 – F337.
[200] K. T. Cho, P. Albertus, V. Battaglia, A. Kojic, V. Srinivasan, A. Z. Weber, *Energy Technol.* **2013**, *1*, 596 – 608.
[201] E. Gileadi, S. Srinivasan, F. J. Salzano, C. Braun, A. Beaufrere, S. Gottesfeld, L. J. Nuttall, A. B. Laconti, *J. Power Sources* **1977**, *2*, 191 – 200.
[202] D.-T. Chin, *J. Electrochem. Soc.* **1979**, *126*, 713 – 720.
[203] R. S. Yeo, J. McBreen, *J. Electrochem. Soc.* **1979**, *126*, 1682 – 1687.
[204] E. N. Balko, J. F. McElroy, A. B. Laconti, *Int. J. Hydrogen Energy* **1981**, *6*, 577 – 587.
[205] M. Thomassen, B. Børresen, G. Hagen, R. Tunold, *J. Appl. Electrochem.* **2003**, *33*, 9 – 13.
[206] M. Thomassen, B. Børresen, G. Hagen, R. Tunold, *Electrochim. Acta* **2005**, *50*, 1157 – 1167.
[207] B. Huskinson, J. Rugolo, S. K. Mondal, M. J. Aziz, *Energy Environ. Sci.* **2012**, *5*, 8690 – 8698.
[208] M. Thomassen, E. Sandnes, B. Børresen, R. Tunold, *J. Appl. Electrochem.* **2006**, *36*, 813 – 819.
[209] E. B. Anderson, E. J. Taylor, G. Wilemski, A. Gelb, *Proceedings of the Fourth Space Electrochemical Research and Technology Conference*, **1994**, *47*, 321 – 328.
[210] K. Fatih, D. P. Wilkinson, F. Moraw, A. Ilicic, F. Girard, *Electrochem. Solid-State Lett.* **2008**, *11*, B11 – B15.
[211] M. C. Tucker, V. Srinivasan, P. N. Ross, A. Z. Weber, *J. Appl. Electrochem.* **2013**, *43*, 637 – 644.

[212] M. Alon, A. Blum, E. Peled, *J. Power Sources* **2013**, *240*, 417 – 420.
[213] M. C. Tucker, K. T. Cho, A. Z. Weber, *J. Power Sources* **2014**, *245*, 691 – 697.
[214] V. Yufit, B. Hale, M. Matian, P. Mazur, N. P. Brandon, *J. Electrochem. Soc.* **2013**, *160*, A856 – A861.
[215] L. W. Hruska, *J. Electrochem. Soc.* **1981**, *128*, 18 – 25.
[216] K. L. Hawthorne, J. S. Wainright, R. F. Savinell, *J. Power Sources* **2014**, *269*, 216 – 224.
[217] R. J. Remick, P. G. P. Ang, US 4485154, **1981**.
[218] S. Ge, B. Yi, H. Zhang, *J. Appl. Electrochem.* **2004**, *34*, 181 – 185.
[219] P. Zhao, H. Zhang, H. Zhou, B. Yi, *Electrochim. Acta* **2005**, *51*, 1091 – 1098.
[220] H. Zhou, H. Zhang, P. Zhao, B. Yi, *Electrochim. Acta* **2006**, *51*, 6304 – 6312.
[221] A. Price, S. Bartley, G. Cooley, S. Male, *Power Eng. J.* **1999**, *13*, 122 – 129.
[222] A. Price, *Power Eng. J.* **1999**, *13*, 179 – 186.
[223] A. Price, *Renewable Energy Storage* (ImechE. Seminar Publication) **2000**, *7*, 11.
[224] J. Cheng, H. M. Zhang, Y. H. Wen, G. P. Cao, Y. S. Yang, *Adv. Mater. Res.* **2012**, *399 – 401*, 1519 – 1523.
[225] A. Hazza, D. Pletcher, R. Wills, *Phys. Chem. Chem. Phys.* **2004**, *6*, 1773 – 1778.
[226] D. Pletcher, R. Wills, *Phys. Chem. Chem. Phys.* **2004**, *6*, 1779 – 1785.
[227] A. Hazza, D. Pletcher, R. Wills, *J. Power Sources* **2005**, *149*, 103 – 111.
[228] D. Pletcher, R. Wills, *J. Power Sources* **2005**, *149*, 96 – 102.
[229] O. Shmychkova, T. Luk′yanenko, A. Velichenko, L. Meda, R. Amadelli, *Electrochim. Acta* **2013**, *111*, 332 – 338.
[230] D. Pletcher, H. Zhou, G. Kear, C. T. J. Low, F. C. Walsh, R. G. A. Wills, *J. Power Sources* **2008**, *180*, 621 – 629.
[231] D. Pletcher, H. Zhou, G. Kear, C. T. J. Low, F. C. Walsh, R. G. A. Wills, *J. Power Sources* **2008**, *180*, 630 – 634.
[232] X. Li, D. Pletcher, F. C. Walsh, *Electrochim. Acta* **2009**, *54*, 4688 – 4695.
[233] J. Collins, G. Kear, X. Li, C. T. J. Low, D. Pletcher, R. Tangirala, D. Stratton-Campbell, F. C. Walsh, C. Zhang, *J. Power Sources* **2010**, *195*, 1731 – 1738.
[234] R. G. A. Wills, J. Collins, D. Stratton-Campbell, C. T. J. Low, D. Pletcher, F. C. Walsh, *J. Appl. Electrochem.* **2010**, *40*, 955 – 965.
[235] J. Collins, X. Li, D. Pletcher, R. Tangirala, D. Stratton-Campbell, F. C. Walsh, C. Zhang, *J. Power Sources* **2010**, *195*, 2975 – 2978.
[236] H. D. Pratt, N. S. Hudak, X. Fang, T. M. Anderson, *J. Power Sources* **2013**, *236*, 259 – 264.
[237] J. Friedl, C. Bauer, R. Al-Oweini, D. Yu, U. Kortz, H. Hoster, U. Stimming, *Meeting Abstracts* **2012**, *MA2012-02*, 3551.
[238] R. F. Gahn, *Supply of reactants for Redox bulk energy storage systems*, NASA TM-78995, **1978**.
[239] L. Sanz, D. Lloyd, E. Magdalena, J. Palma, K. Kontturi, *J. Power Sources* **2014**, *268*, 121 – 128.
[240] Y. Shiokawa, H. Yamana, H. Moriyama, *J. Nucl. Sci. Technol.* **2000**, *37*, 253 – 256.
[241] Y. Shiokawa, T. Yamamura, K. Shirasaki, *J. Phys. Soc. Jpn.* **2006**, *75*, 137 – 142.
[242] T. Yamamura, N. Watanabe, Y. Shiokawa, *J. Alloys Compd.* **2006**, *408 – 412*, 1260 – 1266.
[243] J. Pan, Y. Sun, J. Cheng, Y. Wen, Y. Yang, P. Wan, *Electrochem. Commun.* **2008**, *10*, 1226 – 1229.
[244] M. Skyllas-Kazacos, N. Milne, *J. Appl. Electrochem.* **2011**, *41*, 1233 – 1243.
[245] Y. H. Wen, H. M. Zhang, P. Qian, H. T. Zhou, P. Zhao, B. L. Yi, Y. S. Yang, *J. Electrochem. Soc.* **2006**, *153*, A929 – A934.
[246] Y. H. Wen, H. M. Zhang, P. Qian, H. T. Zhou, P. Zhao, B. L. Yi, Y. S. Yang, *Electrochim. Acta* **2006**, *51*, 3769 – 3775.
[247] C.-H. Bae, E. P. L. Roberts, M. H. Chakrabarti, M. Saleem, *Int. J. Green Energy* **2011**, *8*, 248 – 264.
[248] C.-H. Bae, E. P. L. Roberts, R. A. W. Dryfe, *Electrochim. Acta* **2002**, *48*, 279 – 287.
[249] Y. Zhao, S. Si, C. Liao, *J. Power Sources* **2013**, *241*, 449 – 453.
[250] Y. H. Wen, J. Cheng, P. H. Ma, Y. S. Yang, *Electrochim. Acta* **2008**, *53*, 3514 – 3522.
[251] Y. H. Wen, J. Cheng, Y. Xun, P. H. Ma, Y. S. Yang, *Electrochim. Acta* **2008**, *53*, 6018 – 6023.
[252] Y. Xu, Y. Wen, J. Cheng, G. Cao, Y. Yang, *Electrochem. Commun.* **2009**, *11*, 1422 – 1424.
[253] Y. Xu, Y.-H. Wen, J. Cheng, G.-P. Cao, Y.-S. Yang, *Electrochim. Acta* **2010**, *55*, 715 – 720.
[254] B. Huskinson, M. P. Marshak, S. Er, M. R. Gerhardt, C. J. Galvin, X. Chen, A. Aspuru-Guzik, R. G. Gordon, M. J. Aziz, C. Suh, *Nature* **2014**, *505*, 195 – 198.
[255] P. Singh, *J. Power Sources* **1984**, *11*, 135 – 142.
[256] C. Reichardt, *Solvent effects in organic chemistry*, Wiley-VCH, Weinheim, **2003**.
[257] K. Izutsu, *Electrochemistry in Nonaqueous Solutions*, Wiley-VCH, Weinheim, **2002**.
[258] Y. Matsuda, K. Tanaka, M. Okada, Y. Takasu, M. Morita, T. Matsumura-Inoue, *J. Appl. Electrochem.* **1988**, *18*, 909 – 914.
[259] J.-H. Kim, K. J. Kim, M.-S. Park, N. J. Lee, U. Hwang, H. Kim, Y.-J. Kim, *Electrochem. Commun.* **2011**, *13*, 997 – 1000.
[260] J. Mun, M.-J. Lee, J.-W. Park, D.-J. Oh, D.-Y. Lee, S.-G. Doo, *Electrochem. Solid-State Lett.* **2012**, *15*, A80 – A82.
[261] M. H. Chakrabarti, R. A. W. Dryfe, E. P. L. Roberts, *Electrochim. Acta* **2007**, *52*, 2189 – 2195.
[262] A. Endo, Y. Hoshino, K. Hirakata, Y. Takeuchi, K. Shimizu, Y. Furushima, H. Ikeuchi, G. P. Sato, *Bull. Chem. Soc. Jpn.* **1989**, *62*, 709 – 716.
[263] M. Morita, Y. Tanaka, K. Tanaka, Y. Matsuda, T. Matsumura-Inoue, *Bull. Chem. Soc. Jpn.* **1988**, *61*, 2711 – 2714.
[264] M. H. Chakrabarti, E. P. L. Roberts, C. Bae, M. Saleem, *Energy Convers. Manage.* **2011**, *52*, 2501 – 2508.
[265] T. Yamamura, Y. Shiokawa, H. Yamana, H. Moriyama, *Electrochim. Acta* **2002**, *48*, 43 – 50.
[266] T. Yamamura, K. Shirasaki, Y. Shiokawa, Y. Nakamura, S.-Y. Kim, *J. Alloys Compd.* **2004**, *374*, 349 – 353.
[267] T. Yamamura, K. Shirasaki, D. X. Li, Y. Shiokawa, *J. Alloys Compd.* **2006**, *418*, 139 – 144.
[268] K. Shirasaki, T. Yamamura, Y. Shiokawa, *J. Alloys Compd.* **2006**, *408 – 412*, 1296 – 1301.
[269] K. Hasegawa, A. Kimura, T. Yamamura, Y. Shiokawa, *J. Phys. Chem. Solids* **2005**, *66*, 593 – 595.
[270] Q. Liu, A. E. S. Sleightholme, A. A. Shinkle, Y. Li, L. T. Thompson, *Electrochem. Commun.* **2009**, *11*, 2312 – 2315.
[271] A. A. Shinkle, A. E. S. Sleightholme, L. T. Thompson, C. W. Monroe, *J. Appl. Electrochem.* **2011**, *41*, 1191 – 1199.
[272] A. A. Shinkle, A. E. S. Sleightholme, L. D. Griffith, L. T. Thompson, C. W. Monroe, *J. Power Sources* **2012**, *206*, 490 – 496.
[273] T. Herr, J. Noack, P. Fischer, J. Tübke, *Electrochim. Acta* **2013**, *113*, 127 – 133.
[274] T. Herr, P. Fischer, J. Tübke, K. Pinkwart, P. Elsner, *J. Power Sources* **2014**, *265*, 317 – 324.
[275] M. A. Nawi, T. L. Riechel, *Inorg. Chem.* **1981**, *20*, 1974 – 1978.
[276] M. A. Nawi, T. L. Riechel, *Inorg. Chem.* **1982**, *21*, 2268 – 2271.
[277] M. Kitamura, K. Sasaki, H. Imai, *Bull. Chem. Soc. Jpn.* **1977**, *50*, 3199 – 3201.
[278] A. Watanabe, H. Kido, K. Saito, *Inorg. Chem.* **1981**, *20*, 1107 – 1111.
[279] D. Zhang, Q. Liu, X. Shi, Y. Li, *J. Power Sources* **2012**, *203*, 201 – 205.

[280] Q. Liu, A. A. Shinkle, Y. Li, C. W. Monroe, L. T. Thompson, A. E. S. Sleightholme, *Electrochem. Commun.* **2010**, *12*, 1634 – 1637.
[281] A. E. S. Sleightholme, A. A. Shinkle, Q. Liu, Y. Li, C. W. Monroe, L. T. Thompson, *J. Power Sources* **2011**, *196*, 5742 – 5745.
[282] D. Zhang, H. Lan, Y. Li, *J. Power Sources* **2012**, *217*, 199 – 203.
[283] P. J. Cappillino, H. D. Pratt, N. S. Hudak, N. C. Tomson, T. M. Anderson, M. R. Anstey, *Adv. Energy Mater.* **2014**, *4*, 1300566.
[284] M. Armand, J.-M. Tarascon, *Nature* **2008**, *451*, 652 – 657.
[285] Z. Li, S. Li, S. Liu, K. Huang, D. Fang, F. Wang, S. Peng, *Electrochem. Solid-State Lett.* **2011**, *14*, A171 – A173.
[286] Y. Wang, P. He, H. Zhou, *Adv. Energy Mater.* **2012**, *2*, 770 – 779.
[287] M. Duduta, B. Ho, V. C. Wood, P. Limthongkul, V. E. Brunini, W. C. Carter, Y.-M. Chiang, *Adv. Energy Mater.* **2011**, *1*, 511 – 516.
[288] F. R. Brushett, J. T. Vaughey, A. N. Jansen, *Adv. Energy Mater.* **2012**, *2*, 1390 – 1396.
[289] W. Wang, W. Xu, L. Cosimbescu, D. Choi, L. Li, Z. Yang, *Chem. Commun.* **2012**, *48*, 6669 – 6671.
[290] Q. Huang, H. Li, M. Grätzel, Q. Wang, *Phys. Chem. Chem. Phys.* **2013**, *15*, 1793 – 1797.
[291] Y. Lu, J. B. Goodenough, *J. Mater. Chem.* **2011**, *21*, 10113 – 10117.
[292] Y. Wang, Y. Wang, H. Zhou, *ChemSusChem* **2011**, *4*, 1087 – 1090.
[293] A. A. Shinkle, T. J. Pomaville, A. E. S. Sleightholme, L. T. Thompson, C. W. Monroe, *J. Power Sources* **2014**, *248*, 1299 – 1305.
[294] A. Lewandowski, A. Świderska-Mocek, *J. Power Sources* **2009**, *194*, 601 – 609.
[295] H. Weingärtner, *Angew. Chem. Int. Ed.* **2008**, *47*, 654 – 670; *Angew. Chem.* **2008**, *120*, 664 – 682.
[296] "Room Temperature Molten Salt Systems": C. H. Hussey in *Advances in Molten Salt Chemistry*, Vol. 5 (Ed.: G. Mamantov), Elsevier, NY, **1983**.
[297] M. H. Chakrabarti, F. S. Mjalli, I. M. AlNashef, M. A. Hashim, M. A. Hussain, L. Bahadori, C. T. J. Low, *Renewable Sustainable Energy Rev.* **2014**, *30*, 254 – 270.
[298] C. A. Nkuku, R. J. LeSuer, *J. Phys. Chem. B* **2007**, *111*, 13271 – 13277.
[299] A. P. Abbott, G. Frisch, J. Hartley, K. S. Ryder, *Green Chem.* **2011**, *13*, 471 – 481.
[300] S. Zhang, N. Sun, X. He, X. Lu, X. Zhang, *J. Phys. Chem. Ref. Data* **2006**, *35*, 1475 – 1517.
[301] Y. Katayama, I. Konishiike, T. Miura, T. Kishi, *J. Power Sources* **2002**, *109*, 327 – 332.
[302] C. L. Staiger, H. D. Pratt III, J. C. Leonard, D. Ingersoll, T. M. Anderson, *Vortrag bei "Electrical Energy Storage Applications & Technologies (EESAT) Conference"*, **2011**.
[303] T. M. Anderson, D. Ingersoll, A. J. Rose, C. D. Staiger, J. C. Leonard, *Dalton Trans.* **2010**, *39*, 8609 – 8612.
[304] H. D. Pratt III, A. J. Rose, C. L. Staiger, D. Ingersoll, T. M. Anderson, *Dalton Trans.* **2011**, *40*, 11396 – 11401.
[305] W. W. Porterfield, J. T. Yoke, *Adv. Chem.* **1976**, *150*, 104 – 111.
[306] D. Lloyd, T. Vainikka, K. Kontturi, *Electrochim. Acta* **2013**, *100*, 18 – 23.
[307] C. J. Anderson, M. R. Deakin, G. R. Choppin, W. D'Olieslager, L. Heerman, D. J. Pruett, *Inorg. Chem.* **1991**, *30*, 4013 – 4016.
[308] W.-J. Gau, I.-W. Sun, *J. Electrochem. Soc.* **1996**, *143*, 170 – 174.
[309] W.-J. Gau, I.-W. Sun, *J. Electrochem. Soc.* **1996**, *143*, 914 – 919.
[310] J. S.-Y. Liu, P.-Y. Chen, I.-W. Sun, C. L. Hussey, *J. Electrochem. Soc.* **1997**, *144*, 2388 – 2392.
[311] T. B. Scheffler, C. L. Hussey, *Inorg. Chem.* **1984**, *23*, 1926 – 1932.
[312] S. K. D. Strubinger, I. W. Sun, W. E. Cleland, C. L. Hussey, *Inorg. Chem.* **1990**, *29*, 4246 – 4252.
[313] S. K. D. Strubinger, I. W. Sun, W. E. Cleland, C. L. Hussey, *Inorg. Chem.* **1990**, *29*, 993 – 999.
[314] I. W. Sun, C. L. Hussey, *Inorg. Chem.* **1989**, *28*, 2731 – 2737.
[315] P. A. Barnard, C. L. Hussey, *J. Electrochem. Soc.* **1990**, *137*, 913 – 918.
[316] K. R. Hanz, T. L. Riechel, *Inorg. Chem.* **1997**, *36*, 4024 – 4028.
[317] E. G.-S. Jeng, I.-W. Sun, *J. Electrochem. Soc.* **1998**, *145*, 1196 – 1201.
[318] T. M. Laher, C. L. Hussey, *Inorg. Chem.* **1982**, *21*, 4079 – 4083.
[319] F.-M. Lin, C. L. Hussey, *J. Electrochem. Soc.* **1993**, *140*, 3093 – 3096.
[320] M. Lipsztajn, R. A. Osteryoung, *Inorg. Chem.* **1985**, *24*, 716 – 719.
[321] I. W. Sun, E. H. Ward, C. L. Hussey, K. R. Seddon, J. E. Turp, *Inorg. Chem.* **1987**, *26*, 2140 – 2143.
[322] X.-H. Xu, C. L. Hussey, *J. Electrochem. Soc.* **1992**, *139*, 3103 – 3108.
[323] C. L. Hussey, L. A. King, J. S. Wilkes, *J. Electroanal. Chem. Interfacial Electrochem.* **1979**, *102*, 321 – 332.
[324] D. Lloyd, T. Vainikka, L. Murtomäki, K. Kontturi, E. Ahlberg, *Electrochim. Acta* **2011**, *56*, 4942 – 4948.
[325] D. Lloyd, T. Vainikka, M. Ronkainen, K. Kontturi, *Electrochim. Acta* **2013**, *109*, 843 – 851.
[326] M. Yamagata, N. Tachikawa, Y. Katayama, T. Miura, *Electrochim. Acta* **2007**, *52*, 3317 – 3322.
[327] J. Noack, J. Tübke, K. Pinkwart, DE 10 2009 009 357A1, **2010**.
[328] D. Karamanev, US 7572546 B2, **2009**.
[329] H. Hojjati, K. Penev, V. R. Pupkevich, D. G. Karamanev, *AIChE J.* **2013**, *59*, 1844 – 1854.
[330] A. M. Posner, *Fuel* **1955**, *34*, 330 – 338.
[331] D.-G. Oei, *J. Appl. Electrochem.* **1982**, *12*, 41 – 51.
[332] B. Folkesson, *J. Appl. Electrochem.* **1990**, *20*, 907 – 911.
[333] D.-G. Oei, J. T. Kummer, *J. Appl. Electrochem.* **1982**, *12*, 87 – 100.
[334] H. Hojjati, K. Penev, V. R. Pupkevich, D. G. Karamanev, *AIChE J.* **2013**, *59*, 1844 – 1854.
[335] K. Maeda, K. Domen, *J. Phys. Chem. Lett.* **2010**, *1*, 2655 – 2661.
[336] J. Luo, J.-H. Im, M. T. Mayer, M. Schreier, M. K. Nazeeruddin, N.-G. Park, S. D. Tilley, H. J. Fan, M. Gratzel, *Science* **2014**, *345*, 1593 – 1596.
[337] D. Liu, F. Liu, J. Liu, *J. Power Sources* **2012**, *213*, 78 – 82.
[338] Z. Wei, D. Liu, C. Hsu, F. Liu, *Electrochem. Commun.* **2014**, *45*, 79 – 82.
[339] D. Liu, Z. Wei, C.-j. Hsu, Y. Shen, F. Liu, *Electrochim. Acta* **2014**, *136*, 435 – 441.

Received: November 6, 2014
Published online: June 26, 2015

